

PARAMETRIC STUDY ON FATIGUE FAILURE USING  
CRACK INITIATION METHOD

MOHD FADZRUL HISYAM BIN BADARUDIN

BACHELOR OF MECHANICAL ENGINEERING  
UNIVERSITI MALAYSIA PAHANG

2012

## UNIVERSITI MALAYSIA PAHANG

### BORANG PENGESAHAN STATUS TESIS♦

JUDUL: **PARAMETRIC STUDY ON FATIGUE FAILURE USING  
CRACK INITIATION METHOD**

SESI PENGAJIAN: 2011/2012

Saya **MOHD FADZRUL HISYAM BIN BADARUDIN (890520-08-5229)**  
(HURUF BESAR)

Mengaku membenarkan tesis (Sarjana Muda/Sarjana/Doktor Falsafah)\* ini disimpan di Perpustakaan dengan syarat-syarat kegunaan seperti berikut:

1. Tesis adalah hak milik Universiti Malaysia Pahang (UMP).
2. Perpustakaan dibenarkan membuat salinan untuk tujuan pengajian sahaja.
3. Perpustakaan dibenarkan membuat salinan tesis ini sebagai bahan pertukaran antara institusi pengajian tinggi.
4. \*\*Sila tandakan ( ✓ )

☐

**SULIT**

(Mengandungi maklumat yang berdarjah keselamatan atau kepentingan Malaysia seperti yang termaktub di dalam AKTA RAHSIA RASMI 1972)

☐

**TERHAD**

(Mengandungi maklumat TERHAD yang telah ditentukan oleh organisasi/badan di mana penyelidikan dijalankan)

☒

**TIDAK TERHAD**

Disahkan oleh:

\_\_\_\_\_  
(TANDATANGAN PENULIS)

\_\_\_\_\_  
(TANDATANGAN PENYELIA)

Alamat Tetap:

**NO. 27, LORONG 12,  
PERKAMPUNGAN SUNGAI ISAP DAMAI,  
25150 KUANTAN,  
PAHANG DARUL MAKMUR**

**NASRUL AZUAN BIN ALANG**

(Nama Penyelia)

Tarikh: **25 JUN 2012**

Tarikh: **25 JUN 2012**

CATATAN: \* Potong yang tidak berkenaan.  
\*\* Jika tesis ini SULIT atau TERHAD, sila lampirkan surat daripada pihak berkuasa/organisasi berkenaan dengan menyatakan sekali tempoh tesis ini perlu dikelaskan sebagai atau TERHAD.  
♦ Tesis dimaksudkan sebagai tesis bagi Ijazah doktor Falsafah dan Sarjana secara Penyelidikan, atau disertai sebagai pengajian secara kerja kursus dan penyelidikan, atau Laporan Projek Sarjana Muda (PSM).

PARAMETRIC STUDY ON FATIGUE FAILURE USING CRACK INITIATION  
METHOD

MOHD FADZRUL HISYAM BIN BADARUDIN

Report submitted in partial fulfilment of the requirements  
for the award of the degree of  
Bachelor of Mechanical Engineering

Faculty of Mechanical Engineering  
UNIVERSITI MALAYSIA PAHANG

JUNE 2012

**UNIVERSITI MALAYSIA PAHANG**  
**FACULTY OF MECHANICAL ENGINEERING**

I certify that the project entitled “*Parametric Studies on Fatigue Failure Using Crack Initiation Method*” is written by *Mohd Fadzrul Hisyam bin Badarudin*. I have examined the final copy of this project and in our opinion; it is fully adequate in terms of scope and quality for the award of the degree of Bachelor of Engineering. I herewith recommend that it be accepted in partial fulfilment of the requirements for the degree of Bachelor of Mechanical Engineering.

*(JULIAWATI BINTI ALIAS)*

Examiner

Signature

### **SUPERVISOR'S DECLARATION**

I hereby declare that I have checked this project and in my opinion, this project is adequate in terms of scope and quality for the award of the degree of Bachelor of Mechanical Engineering.

Signature

Name of Supervisor : NASRUL AZUAN BIN ALANG

Position : LECTURER

Date : 25 JUNE 2012

### **STUDENT'S DECLARATION**

I hereby declare that the work in this project is my own except for quotations and summaries which have been duly acknowledged. The project has not been accepted for any degree and is not concurrently submitted for award of other degree.

Signature

Name : MOHD FADZRUL HISYAM BIN BADARUDIN

ID Number : MA08054

Date : 25 JUNE 2012

*Dedicated to my parents,  
Mr. Badarudin Abd. Manan and Mdm. Nursyamsiah Jisam Abdullah  
My family members,  
My mentors,  
And friends.  
May Allah bless all of you.*

## ACKNOWLEDGEMENTS

First and foremost, I am grateful and would like to express my sincere gratitude to my supervisor Mr. Nasrul Azuan bin Alang for his invaluable guidance, germinal ideas, continuous encouragement and constant support in making this research possible. He has always impressed me with his outstanding professional conduct, his strong conviction for science, and his belief that a Degree program is only a start of lifelong learning experiences. I am appreciating his consistent support from the first day I applied to graduate program until this moment. I am very grateful for his progressive vision about my training and his tolerance of my mistakes.

Sincerely, I also would like to express very special thanks to the all members of the staff of Faculty of Mechanical Engineering, who helped me in many ways including the preparation of this study especially to Assoc. Prof. Dr. Md. Mustafizur Rahman and Miss Nurazima binti Ismail, Mr. Hadi bin Abdul Salaam and Mr. Mohd Firdaus bin Hassan for their endless supports, guidance and knowledge in order to help me to complete this project. I would like to thank the authority of University Malaysia Pahang (UMP) for providing us with good environment and facilities to complete this study. Many special thanks go to members of the research group for their excellent co-operation, inspirations and supports during this study.

Finally, I acknowledge my sincere indebtedness and gratitude to my parents for their love, understanding and sacrifice throughout my life. An honourable mention goes my friends for their supports and concerns on me in completing this study. I cannot find the appropriate words that could properly describe my appreciation for their devotion, support and faith in my ability to attain my goals. I would like to acknowledge their comments and suggestions, which was crucial for the successful completion of this study.



## ABSTRACT

This thesis presents the parametric study on fatigue failure using crack initiation method analysis. In order to investigate the fatigue failure of AISI/SAE 1045 steel by varying the microstrain parameters under different loading cases and predict the crack initiation life, compact tension specimen model is used for this project. The finite element linear static analysis is done by using MSC Patran 2010 and MSC Nastran 2007 to determine the result of the stress distribution on the model. The fatigue analysis is conducted by using ANSYS 13.0 nCode DesignLife to determine the microstrain value that initiates the dynamic and static failure under three loading cases; compression-compression, compression-tension and tension-tension. The obtained microstrain values are then used to obtain the fatigue damage,  $D$  which is then used to predict the crack initiation life of the material. Using Palmgren-Milner rule, the value of  $D$  will obtain the crack initiation life cycle of the material,  $N_f$ . Based on the result, it has found that the most critical loading case for the fatigue and static failure are the tension-tension. The crack initiation life of the material is at high cycle fatigue, and able to stand about  $5 \times 10^6$  cycles without failure for every loading case. Meanwhile the static failure analysis has found that there is no crack initiation life, as it has failed at very low cycle in every loading case.

## ABSTRAK

Tesis ini membentangkan kajian kepelbagaian parameter terhadap kegagalan lesu dengan menggunakan prosedur analisis permulaan rekahan. Untuk mengkaji kegagalan lesu keluli AISI/SAE 1045 dengan mempelbagaikan parameter regangan mikro di bawah kes-kes pembebanan yang berbeza dan meramal jangka hayat permulaan keretakan, model spesimen tegangan padat digunakan untuk projek ini. Analisis statik mendatar unsur terhingga dilakukan dengan menggunakan perisian MSC Patran 2010 dan MSC Nastran 2007 untuk mendapatkan keputusan pengagihan tekanan terhadap model. Analisis kelesuan dijalankan menggunakan perisian ANSYS 13.0 nCode DesignLife untuk mendapatkan nilai regangan mikro yang memulakan kegagalan dinamik dan statik di bawah tiga kes bebanan; kes tekanan-tekanan, tekanan-tegangan, dan tegangan-tegangan. Dari nilai regangan mikro yang diperoleh, kemudian digunakan untuk mendapatkan nilai kerosakan lesu,  $D$  yang digunakan untuk meramal jangka hayat permulaan keretakan bahan tersebut. Dengan menggunakan hukum Palmgren-Milner, nilai  $D$  akan mendapatkan kitaran jangka hayat bahan tersebut,  $N_f$ . Dari hasil yang diperoleh, difahamkan bahawa kes bebanan yang paling kritikal untuk kegagalan lesu dan statik adalah kes bebanan tegangan-tegangan. Jangka hayat permulaan keretakan untuk bahan tersebut adalah pada kitaran lesu tinggi, dan mampu bertahan kira-kira  $5 \times 10^6$  kali kitaran untuk setiap kes bebanan. Sementara itu, analisis kegagalan statik mendapati bahawa tiada permulaan keretakan berlaku pada bahan tersebut, memandangkan bahan tersebut telah gagal pada kitaran yang sangat rendah, untuk setiap kes bebanan.

## TABLE OF CONTENTS

|   | <b>Pages</b> |
|---|--------------|
| <b>EXAMINER’S DECLARATION</b>                                 | ii           |
| <b>SUPERVISOR’S DECLARATION</b>                               | iii          |
| <b>STUDENT’S DECLARATION</b>                                  | iv           |
| <b>DEDICATION</b>   | v            |
| <b>ACKNOWLEDGEMENTS</b>                                       | vi           |
| <b>ABSTRACT</b>   | vii          |
| <b>ABSTRAK</b>  | viii         |
| <b>TABLE OF CONTENTS</b>                                      | ix           |
| <b>LIST OF TABLES</b>   | xi           |
| <b>LIST OF FIGURES</b>  | xii          |
| <b>LIST OF SYMBOLS</b>  | xvii         |
| <b>LIST OF ABBREVIATIONS</b>                                  | xviii        |
| <br><b>CHAPTER 1            INTRODUCTION</b>                  |              |
| <br>1.1            Project Background                         | 1            |
| 1.2            Problem Statement                              | 2            |
| 1.3            Project Objectives                             | 3            |
| 1.4            Project Scopes                                 | 3            |
| <br><b>CHAPTER 2            LITERATURE REVIEW</b>             |              |
| <br>2.1            Introduction                               | 4            |
| 2.2            AISI/SAE 1045 Steel                            | 5            |
| 2.2.1    Steel  | 5            |
| 2.2.2    Carbon Steel Classifications                         | 5            |
| 2.2.3    AISI/SAE 1045 Steel                                  | 6            |
| 2.3            Introduction of Metal Fatigue Failure Analysis | 7            |
| 2.3.1    Types of Fatigue Failure Analysis                    | 7            |
| 2.3.2    Finite Element Analysis (FEA)                        | 8            |
| 2.3.2.1    Pre-processing                                     | 9            |
| 2.3.2.2    Analysis   | 9            |

|     |                                |    |
|-----|--------------------------------|----|
|     | 2.3.2.3 Post-processing        | 9  |
| 2.4 | Crack Initiation               | 10 |
|     | 2.4.1 Fatigue                  | 10 |
|     | 2.4.2 Crack Initiation Life    | 10 |
| 2.5 | Specimen Geometry              | 11 |
|     | 2.5.1 Standard Test Specimen   | 11 |
|     | 2.5.2 Compact Tension Specimen | 11 |
| 2.6 | Summary                        | 13 |

### **CHAPTER 3            METHODOLOGY**

|     |                                |    |
|-----|--------------------------------|----|
| 3.1 | Introduction                   | 14 |
| 3.2 | Flow Chart                     | 14 |
| 3.3 | Methodology Steps              | 16 |
|     | 3.3.1 Linear Static Analysis   | 27 |
|     | 3.3.2 Fatigue Failure Analysis | 25 |

### **CHAPTER 4            RESULTS AND DISCUSSIONS**

|     |   |    |
|-----|---|----|
| 4.1 | Introduction                            | 33 |
| 4.2 | Finite Element Analysis Results         | 33 |
|     | 4.2.1 Input Parameters                  | 34 |
|     | 4.2.2 Crack Initiation Analysis Results | 34 |
| 4.3 | The Theoretical Failure Stress          | 72 |
| 4.4 | Crack Initiation Life                   | 74 |

### **CHAPTER 5            CONCLUSION AND RECOMMENDATIONS**

|     |                 |    |
|-----|-----------------|----|
| 5.1 | Conclusions     | 76 |
| 5.2 | Recommendations | 77 |

|                   |  |    |
|-------------------|--|----|
| <b>REFERENCES</b> |  | 78 |
|-------------------|--|----|

## LIST OF TABLES

| <b>Table No.</b> | <b>Title</b>  | <b>Page</b> |
|------------------|---|-------------|
| 2.1              | AISI/SAE 1045 steel element composition.                  | 6           |
| 2.2              | AISI/SAE 1045 steel mechanical properties                 | 7           |
| 3.1              | Material properties of the specimen                       | 21          |
| 3.2              | The variants of mesh seed sizes                           | 22          |
| 3.3              | Input parameter for crack initiation studies              | 27          |
| 4.1              | Input parameter for dynamic and static analysis studies   | 34          |
| 4.2              | Dynamic failure initiation microstrain and damage value   | 71          |
| 4.3              | Static failure initiation microstrain and damage value    | 72          |
| 4.4              | Theoretical failure stress at dynamic failure             | 73          |
| 4.5              | Theoretical failure stress at static failure              | 73          |
| 4.6              | Crack initiation life cycles for dynamic failure analysis | 74          |
| 4.7              | Crack initiation life cycles for static failure analysis  | 75          |

## LIST OF FIGURES

| <b>Figure No.</b> | <b>Title</b>  | <b>Page</b> |
|-------------------|---|-------------|
| 2.1               | CT specimen dimension                                       | 12          |
| 3.1               | The flowchart of the project methodology                    | 15          |
| 3.2               | Schematic diagram of compact tension specimen (CT specimen) | 16          |
| 3.3               | New model preference for the specimen analysis              | 17          |
| 3.4               | Geometry preferences for the specimen analysis              | 18          |
| 3.5               | Points of the specimen drawing                              | 19          |
| 3.6               | Curve of the specimen drawing                               | 19          |
| 3.7               | Created surface for the specimen drawing                    | 20          |
| 3.8               | Created curves before breaking the surface into parts       | 20          |
| 3.9               | Broken surfaces after curves deletion                       | 21          |
| 3.10              | Mesh seed for $L2 = 0.2$ .                                  | 22          |
| 3.11              | Mesh shape settings   | 23          |
| 3.12              | Created mesh on the specimen                                | 23          |
| 3.13              | Specimen with boundary layers                               | 24          |
| 3.14              | Time series generator network                               | 25          |
| 3.15              | Time Series Generator properties window                     | 26          |
| 3.16              | Generated time series interface                             | 27          |
| 3.17              | ASCII Translate setting interface                           | 28          |
| 3.18              | Strain-life analysis network                                | 29          |
| 3.19              | Strain-life properties setting                              | 30          |
| 3.20              | Material Map for the strain-life analysis                   | 31          |
| 3.21              | Strain-life result display                                  | 32          |

|      |  |    |
|------|--|----|
| 4.1  | Microstrain Value for Dynamic Failure Analysis for Compression-Compression Case at 1 Hz                | 35 |
| 4.2  | Damage Contour for Dynamic Failure Analysis for Compression-Compression Case at 1 Hz                   | 35 |
| 4.3  | Damage Contour at Notch Point for Dynamic Failure Analysis at for Compression-Compression Case at 1 Hz | 36 |
| 4.4  | Microstrain Value for Dynamic Failure Analysis for Compression-Compression Case at 2 Hz                | 37 |
| 4.5  | Damage Contour for Dynamic Failure Analysis for Compression-Compression Case at 2 Hz                   | 37 |
| 4.6  | Damage Contour at Notch Point for Dynamic Failure Analysis at for Compression-Compression Case at 2 Hz | 38 |
| 4.7  | Microstrain Value for Dynamic Failure Analysis for Compression-Compression Case at 3 Hz                | 39 |
| 4.8  | Damage Contour for Dynamic Failure Analysis for Compression-Compression Case at 3 Hz                   | 39 |
| 4.9  | Damage Contour at Notch Point for Dynamic Failure Analysis at for Compression-Compression Case at 3 Hz | 40 |
| 4.10 | Microstrain Value for Dynamic Failure Analysis for Compression-Tension Case at 1 Hz                    | 41 |
| 4.11 | Damage Contour for Dynamic Failure Analysis for Compression-Tension Case at 1 Hz                       | 41 |
| 4.12 | Damage Contour at Notch Point for Dynamic Failure Analysis at for Compression-Tension Case at 1 Hz     | 42 |
| 4.13 | Microstrain Value for Dynamic Failure Analysis for Compression-Tension Case at 2 Hz                    | 43 |
| 4.14 | Damage Contour for Dynamic Failure Analysis for Compression-Tension Case at 2 Hz                       | 43 |
| 4.15 | Damage Contour at Notch Point for Dynamic Failure Analysis at for Compression-Tension Case at 2 Hz     | 44 |
| 4.16 | Microstrain Value for Dynamic Failure Analysis for Compression-Tension Case at 3 Hz                    | 45 |

|      |   |    |
|------|---|----|
| 4.17 | Damage Contour for Dynamic Failure Analysis for Compression-Tension Case at 3 Hz                      | 45 |
| 4.18 | Damage Contour at Notch Point for Dynamic Failure Analysis at for Compression-Tension Case at 3 Hz    | 46 |
| 4.19 | Microstrain Value for Dynamic Failure Analysis for Tension-Tension Case at 1 Hz                       | 47 |
| 4.20 | Damage Contour for Dynamic Failure Analysis for Tension-Tension Case at 1 Hz                          | 47 |
| 4.21 | Damage Contour at Notch Point for Dynamic Failure Analysis at for Tension-Tension Case at 1 Hz        | 48 |
| 4.22 | Microstrain Value for Dynamic Failure Analysis for Tension-Tension Case at 2 Hz                       | 49 |
| 4.23 | Damage Contour for Dynamic Failure Analysis for Tension-Tension Case at 2 Hz                          | 49 |
| 4.24 | Damage Contour at Notch Point for Dynamic Failure Analysis at for Tension-Tension Case at 2 Hz        | 50 |
| 4.25 | Microstrain Value for Dynamic Failure Analysis for Tension-Tension Case at 3 Hz                       | 51 |
| 4.26 | Damage Contour for Dynamic Failure Analysis for Tension-Tension Case at 3 Hz                          | 51 |
| 4.27 | Damage Contour at Notch Point for Dynamic Failure Analysis at for Tension-Tension Case at 3 Hz        | 52 |
| 4.28 | Microstrain Value for Static Failure Analysis for Compression-Compression Case at 1 Hz                | 53 |
| 4.29 | Damage Contour for Static Failure Analysis for Compression-Compression Case at 1 Hz                   | 53 |
| 4.30 | Damage Contour at Notch Point for Static Failure Analysis at for Compression-Compression Case at 1 Hz | 54 |
| 4.31 | Microstrain Value for Static Failure Analysis for Compression-Compression Case at 2 Hz                | 55 |
| 4.32 | Damage Contour for Static Failure Analysis for Compression-Compression Case at 2 Hz                   | 55 |



|      |   |    |
|------|---|----|
| 4.33 | Damage Contour at Notch Point for Static Failure Analysis at for Compression-Compression Case at 2 Hz | 56 |
| 4.34 | Microstrain Value for Static Failure Analysis for Compression-Compression Case at 3 Hz                | 57 |
| 4.35 | Damage Contour for Static Failure Analysis for Compression-Compression Case at 3 Hz                   | 57 |
| 4.36 | Damage Contour at Notch Point for Static Failure Analysis at for Compression-Compression Case at 3 Hz | 58 |
| 4.37 | Microstrain Value for Static Failure Analysis for Compression-Tension Case at 1 Hz                    | 59 |
| 4.38 | Damage Contour for Static Failure Analysis for Compression-Tension Case at 1 Hz                       | 59 |
| 4.39 | Damage Contour at Notch Point for Static Failure Analysis at for Compression-Tension Case at 1 Hz     | 60 |
| 4.40 | Microstrain Value for Static Failure Analysis for Compression-Tension Case at 2 Hz                    | 61 |
| 4.41 | Damage Contour for Static Failure Analysis for Compression-Tension Case at 2 Hz                       | 61 |
| 4.42 | Damage Contour at Notch Point for Static Failure Analysis at for Compression-Tension Case at 2 Hz     | 62 |
| 4.43 | Microstrain Value for Static Failure Analysis for Compression-Tension Case at 3 Hz                    | 63 |
| 4.44 | Damage Contour for Static Failure Analysis for Compression-Tension Case at 3 Hz                       | 63 |
| 4.45 | Damage Contour at Notch Point for Static Failure Analysis at for Compression-Tension Case at 3 Hz     | 64 |
| 4.46 | Microstrain Value for Static Failure Analysis for Tension-Tension Case at 1 Hz                        | 65 |
| 4.47 | Damage Contour for Static Failure Analysis for Tension-Tension Case at 1 Hz                           | 65 |
| 4.48 | Damage Contour at Notch Point for Static Failure Analysis at for Tension-Tension Case at 1 Hz         | 66 |

|      |   |    |
|------|---|----|
| 4.49 | Microstrain Value for Static Failure Analysis for Tension-Tension Case at 2 Hz                | 67 |
| 4.50 | Damage Contour for Static Failure Analysis for Tension-Tension Case at 2 Hz                   | 67 |
| 4.51 | Damage Contour at Notch Point for Static Failure Analysis at for Tension-Tension Case at 2 Hz | 68 |
| 4.52 | Microstrain Value for Static Failure Analysis for Tension-Tension Case at 3 Hz                | 69 |
| 4.53 | Damage Contour for Static Failure Analysis for Tension-Tension Case at 3 Hz                   | 69 |
| 4.54 | Damage Contour at Notch Point for Static Failure Analysis at for Tension-Tension Case at 3 Hz | 70 |

## LIST OF SYMBOLS

|                   |  |
|-------------------|--|
| $D$               | Fatigue damage   |
| $E$               | Modulus of Elasticity  |
| $\varepsilon$     | Strain   |
| $f$               | Frequency  |
| $K_I$             | Stress intensity factor  |
| $N_f$             | Number of cycle to failure for a particular stress range and mean    |
| $N_i$             | Number of cycle to failure within a particular stress range and mean |
| $\nu$             | Poisson's ratio  |
| $P$               | Load   |
| $\sigma$          | Theoretical failure stress   |
| $\sigma'_F$       | Fatigue strength coefficient   |
| $S_{ut}$          | Ultimate Tensile Strength  |
| $W$               | Width  |
| $\frac{L_2}{L_1}$ | Mesh size ratio  |

**LIST OF ABBREVIATIONS**

|      |                                   |
|------|-----------------------------------|
| AISI | American Iron and Steel Institute |
| CT   | Compact tension                   |
| DCB  | Double cantilever beam            |
| FEA  | Finite Element Analysis           |
| SAE  | Society of Automotive Engineers   |
| SENB | Single edge notched bend          |
| US   | The United State                  |

## **CHAPTER 1**

### **INTRODUCTION**

#### **1.1 PROJECT BACKGROUND**

This project concerns about the parametric study on fatigue failure using crack initiation method. The effect of microstrain values and the frequency that applied to the specimen were investigated using finite element software. The analysis is applied on AISI/SAE 1045 steel (the following stated as AISI 1045 steel to refer AISI/SAE 1045 steel), which is widely used in the automotive applications. AISI 1045 steel was chosen for the project since that this material plays important roles in the engineering field. AISI 1045 steel is usually used as axles, bolts, connecting rods, studs, crankshafts, torsion bars, sockets, etc. So, this material has selected simply because of the importance of AISI 1045 steel in daily life applications, which are require high safety measures. Due to its wide use, there are also huge possibilities that it will be failed in their applications. Some of the failures are because of they become fatigue, due to the repeating force acted on the material and cause them unable to work perfectly and then fail.

Fatigue failure is a common type of failure which is hardly to determine their life span. Basically, this type of failure is started when a crack tip has appeared under certain circumstances which also known the crack initiation, allowing the crack to propagate, making the material become weaker by times. The crack propagation is commonly happened by the cyclic loads or forces that acted on the structure, which applied continuously along with time passes, though the forces and loads did not ever reach the ultimate strength of the material.

In order to estimate the life span of the metal structures, some experiments and analyses must be conducted. This is important to determine the limits of the materials before they are selected to be used in the design. The works on predicting the life cycle of AISI 1045 steel is started by determining the stress distribution on the material by conducting the linear static analysis. The analysis is done using standard compact tension (CT) specimen as the model testing, using MSC Patran 2010 and MSC Nastran 2007 softwares. The results of the analysis is then will be used as the reference to continue the study on parametric studies on fatigue failure of AISI 1045 steel using crack initiation method.

## **1.2 PROBLEM STATEMENT**

Since the industrial revolution there are lots of new machines were created to meet human needs in their daily activities and also the need of the development of the industrial activities. Since then, there are also lots of new materials used for the latest machines. The usages of the new machines bring the daily activities alive with the times.

However in the past days, the creations of the new machines were not considering one of the material weaknesses in their application which bring them into failure. The failure of the materials did a lot of damage and lost while some of the failures were also bring fatality to humans.

Basically, fatigue of materials occurs as they were used repeatedly subjected to reverse stresses over the time. When the materials reach its maximum cycles, it no longer can hold the load as it did before. Due to fatigue, the material fails and bring catastrophe to the mankind and also to the surroundings. Some of the catastrophes that involved fatality due to fatigue were two 1954 Comet jet planes were crashed due to metal fatigue. The first crash killed 29 passengers and a crew lost their lives. Three months later, the second crash killed fourteen passengers and seven crews (British Broadcasting Corporation). However, there was 34 years later, another airline catastrophe really did change the airline industry related to the material control. It was

1988 Aloha Flight 243 that a large section of the fuselage blown off, leaving dozens of passengers rode the plane in open-air breeze (Nolan, 2007).

Since then a lot of actions were taken to prevent any other catastrophe that happens due to fatigue. Huge number of engineers made the research on metal fatigue due to dynamic loading. Some of the tests were also involved the study of crack initiation which is then lead the further stage of fatigue failure.

### **1.3 PROJECT OBJECTIVES**

There are several objectives to be achieved in this study;

- (i) To investigate the fatigue failure of AISI 1045 steel by varying the microstrain parameters under different loading cases.
- (ii) To predict the crack initiation life of AISI 1045 steel by using crack initiation method.

### **1.4 PROJECT SCOPES**

This project is focusing on the parametric studies on fatigue failure using crack initiation method. This focus area is done based on the following aspects:

- (i) AISI 1045 steel is used as the material that to be studied.
- (ii) The crack initiation method by using damage equation is used to predict the initial life cycle of the material.
- (iii) Compact Tension Specimen (CT) is used as the model of the test.
- (iv) Linear Static Stress Analysis is conducted using MSC Patran 2010 and MSC Nastran 2007 software.
- (v) Fatigue Analysis is carried out using ANSYS 13.0 nCode DesignLife software.

## **CHAPTER 2**

### **LITERATURE REVIEW**

#### **2.1 INTRODUCTION**

The chronology of this chapter has been properly organized according to the sequence of this study. In this chapter, the readers will get chances to understand the idea on the importance of failure analysis in the engineering field. The brief of AISI/SAE 1045 steel in section (2.2) will give some information about steels, the properties and classifications. The main part of this section is briefing about AISI/SAE 1045 steel, which will be used for this project. Starting from section (2.3), readers will be given with a short overview about this project, by introducing the metal failure analysis including its analysis types. In the same section, the readers also will be introduced with an overview about finite element analysis (FEA) including the steps of FEA. Though the literature review about FEA is likely quite general, however this project uses MSC Patran and MSC Nastran as default FEA software for static linear analysis and ANSYS 13.0 nCode DesignLife for dynamic analysis; and in order to set up the model and run the analysis as well as obtaining the analysis result of the project. Section (2.4) is then will introduce about crack initiation with briefs about fatigue and crack initiation life. This section will bring the readers to the relations of fatigue damage value and crack initiation life cycles in order to precede this project into the analysis. The following sections will show the brief of the specimen geometry (2.7) will give an introduction about CT specimens while exposing some other specimens that exist for related kind of analysis which are likely almost or same to this project. However, CT specimen is the only specimen that will be discussed more than the others since that this project only use CT specimen in the analysis job to obtain the prediction of crack



initiation life cycle of AISI/SAE 1045 steel using CT specimen. The last section will give the summary of this chapter in proceeding to the next chapter of this project.

## **2.2 AISI/SAE 1045 STEEL**

### **2.2.1 Steel**

Metals and alloys are widely applied in engineering designs as they have many engineering properties. Some of the most used metal type in the engineering design is iron and its alloys which are also known as steel. It has accounted for huge production of metals and becoming the most favourite metal chosen by the engineers mainly because of the combination of good strength, toughness, and ductility at low cost. In smaller portions of steel types, there are variety of steel family such as plain-carbon steels, alloy steels, stainless steels, cast iron and copper alloys. They are widely used in manufacturing of various types of parts and tools, which are having the needs of high rotation and force acted on them. In other classification, steel is categorised as ferrous alloys, since it is based on iron alloys (Smith & Hashemi, 2006).

### **2.2.2 Carbon Steels Classifications**

The definition of The American Iron and Steel Institute (AISI) of carbon steel is; steel is considered to be carbon steel when no minimum content is specified or required for chromium, cobalt, columbium [niobium], molybdenum, nickel, titanium, tungsten, vanadium or zirconium, or any other element to be added to obtain a desired alloying effect; when the specified minimum for copper does not exceed 0.40 per cent; or when the maximum content specified for any of the following elements does not exceed the percentages noted: manganese 1.65, silicon 0.60, copper 0.60 (Key to Metals, 2011).

Carbon steel can be classified according to various deoxidation practices, which have effects on the steel properties. Variations of the carbon content in the steels also give a huge effect on the mechanical properties; with increasing the carbon content will lead to the increase the strength and hardness of the steel. Generally, carbon steels are

divided into groups, according to their carbon content, which the carbon steels that contain up to 2% total alloying elements and can be subdivided into low carbon steels, medium carbon steels, high carbon steels, and ultrahigh carbon steels.

The most widely used identification systems for carbon and alloy steels in the United State (US) is AISI and Society of Automotive Engineers (SAE), which are usually used four-digit identifications. The first digit of the identification is used to indicate the grouping by major alloying element, while the second digit in some instances suggests the relative percentage of the primary alloying element in the series. The remaining digits indicate the median carbon content in hundredths of a percent (Budinski & Budinski, 2010).

### 2.2.3 AISI/SAE 1045 Steel

AISI 1045 steel is designated as high carbon steel where the percentage of carbon in the elemental composition is higher than 0.3%. High carbon steel is one of the types of steel with more than 0.3% carbon. It is a tough and hard type of steel, due to its high amount of carbon content; however make it less formable steel compared to low carbon steel and medium carbon steel. High carbon steel's hardness makes it suitable for plow blades, shovels, bedsprings, cutting edges, or other high-wear applications (American Iron and Steel Institute). The elemental composition of AISI 1045 steel is shown in the Table 2.1.

**Table 2.1:** AISI/SAE 1045 steel element composition.

| <b>Element Composition (mass fraction, in %)</b> |              |
|--|--------------|
| <b>Parameter</b>                                 | <b>Value</b> |
| Aluminium (total)                                | 0.040        |
| Carbon   | 0.462        |
| Chromium   | 0.036        |

Source: National Institute of Standard and Technology (2012)

AISI 1045 steel is usually used in automotive industries in making car parts. Some of the parts are including axles, bolts, connecting rods, studs, crankshafts, torsion

bars, light gears, guide rods, etc. Thus, the applications of AISI 1045 steel acquire a lot of vibrations and cyclic loadings acted on the parts.

The usage of the AISI 1045 steel is considered by its mechanical properties which are usually hard and tough for high wear and tear. The mechanical properties of AISI 1045 steel are shown in Table 2.2.

**Table 2.2:** AISI/SAE 1045 steel mechanical properties.

| <b>Grade<br/>AISI/SAE</b> | <b>Hardness<br/>HB</b> | <b>Tensile<br/>Strength <math>S_{ut}</math><br/>MPa</b> | <b>Modulus of<br/>Elasticity <math>E</math><br/>GPa</b> | <b>Fatigue Strength<br/>Coefficient <math>\sigma'_F</math><br/>MPa</b> |
|---------------------------|------------------------|---|---|--|
| 1045                      | 225                    | 725   | 200   | 1225   |
| 1045                      | 410                    | 1450  | 200   | 1860   |
| 1045                      | 390                    | 1345  | 205   | 1585   |
| 1045                      | 450                    | 1585  | 205   | 1795   |
| 1045                      | 500                    | 1825  | 205   | 2275   |
| 1045                      | 595                    | 2240  | 205   | 2725   |

Source: Budynas & Nisbett (2010)

## 2.3 INTRODUCTION OF METAL FATIGUE FAILURE ANALYSIS

Since the growth of the technology of metallurgy engineering and the expanding of engineering knowledge based on the success of the high technology appliance in the human activities, there are so many latest inventions and innovations are using metal as the final products that meet the consumers. However, the important part of using metal is the prediction on the capability of the metal to work until it reaches the failure stage because of certain conditions that acted on the metal. Thus the study on predicting the working capability limit has known as the ‘failure analysis.’

### 2.3.1 Types of Fatigue Failure Analysis

Failure Analysis is a method which is gathering the data and doing the analysis to determine the cause of the failure. In general speaking, the metal failures could be

attributed by varying types of cases or the combination of two or more cases such as the improper material selection, design, maintenance, production defects, weather, workloads and the exposure of the metal to the working surroundings (Das, 1997).

The analysis might be done by doing the experiment on the materials by testing under certain conditions and sample types. Some of the failure analysis is done by testing the metals under static forces to get the ultimate strength of the material by applying the forces to the material until it fails. This type of failure analysis is usually done to determine the maximum load that can be applied on the material when it is used in the actual scenario. Besides, there is also another type of analysis which is newer in modern engineering which is dynamic testing. In a simple meaning, dynamic testing on the material is done to determine the maximum life of the material under certain circumstances which are might be or might not be related to the maximum load that can be applied on the material.

In another way, failure analysis also can be conducted by doing the simulated testing by using any engineering analysis software. In modern engineering, this method is likely more practical since that this method can optimize the source by reducing the cost, energy, time, and wasted sources. This kind of testing is also known as ‘Finite Element Analysis (FEA)’ under the method name of ‘Finite Element Method (FEM).’

### **2.3.2 Finite Element Analysis (FEA)**

FEA is a method that using the numerical methods to simulate and analyse the materials by finding the approximate solutions to the field problems (Widas, 1997). Though that FEA can be done by using manual calculation, however the development of modern engineering has made the analysis easier since that there is a lot of analysis software that produced to meet the engineering needs nowadays. The birth of the latest version of FEA software gives better results on the analysis and capable to analyse very complex problems. The latest FEA software is also capable to analyse for static, dynamic, heat and vibration analysis.

Basically, FEA is consisting of three major steps, pre-processing, analyser, and post-processing; which are the important parts in the analysis jobs by using the FEA.

### **2.3.2.1 Pre-processing.**

Pre-processing step is the stage where the user constructs a model of a part that to be analysed in which the geometry is divided into a number of discrete sub-regions, which is also called as ‘nodes’. The nodes are generated by building the mesh on the model. Some of the pre-processors are also can overlay mesh by importing pre-existing CAD files, besides of building the model itself in the pre-processors. When the nodes are ready, boundary conditions are then applied on the model along with the material types and properties (Roylance, 2011).

### **2.3.2.2 Analysis**

Analysis which is also known as solver is where the datasets prepared by the pre-processor is used as input to generate and reassemble acquired equations into the analysis to obtain the result (Roensch, 2008); by constructing and solving the linear and non-linear algebraic equation;

$$K_{ij}u_j = f_i \quad (2.1)$$

Where  $u$  and  $F$  are the displacements and externally applied forces at the nodal points and  $K$  is the system stiffness matrix. Matrix  $K$  is varies depending on the type of problem that is to be analysed. The analysis job is done by the software and the final results of the analysis are depending on the setups during the pre-processing.

### **2.3.2.3 Post-processing**

Post-processing is the last step of the FEA analysis which is the process of the investigation of the results after pre-processing and solving processes. The results obtained from the analysis will be assisted with graphical and managed result data. During the end of this period, the final conclusions or predictions of the study might be addressed depending on the pre-processing setup and analysis jobs result.

## 2.4 CRACK INITIATION

### 2.4.1 Fatigue

Fatigue mechanism knowledge is an essential in order to consider various technical conditions which will affect the specimen fatigue life and fatigue crack growth, such as material surface quality, residual stress and environmental influence. It is also important for the analysis of fatigue properties of an engineering structure and designs.

The fatigue life is usually split to a crack initiation period and a crack growth period. The initiation period usually including the microcrack growth, but it is too small to be detected by naked eyes. The next period of the fatigue life, the crack is growing until complete failure, which is also known as crack propagation. The crack propagation started because of the uneven stress distribution on a micro level, with the stress concentration at the crack tip. It then makes the neighbouring grains becoming weaker by times and another slip system has been activated (Schijve, 2001).

### 2.4.2 Crack Initiation Life

Crack initiation life is usually predicted by using local stress-strain approach, which is the most widely accepted approach to predict the crack initiation life. By postulating the number of the cycles required to initiate a crack in the initial zone,  $N_i$  to be equal to the number of cycles to produce failure of the specimen in a laboratory test under the same cyclic strains and stresses, this concept has been illustrated as the notch at the critical zone, which indicate as the initiation of the crack (Collins, 2003).

In the calculation of crack initiation life, the value of fatigue damage,  $D$  is used in order to obtain the number of cycles to initiate the crack. The equation of the fatigue damage value is obtained from Palmgren-Milner rule, for the accumulated damage,  $\sum D$  is expressed as the equation below, where  $N_i$  is the number of cycles within a particular stress range and mean while  $N_f$  is the number of cycles to failure for a particular stress range and mean (Abdullah, *et. al*, 2011).

$$\sum D = \sum \frac{N_i}{N_f} \quad (2.2)$$

The equation is then extracted with the fatigue damage value for each cycle, and it can be obtained by the equation below.

$$D = \frac{1}{N_f} \quad (2.2)$$

From the damage values that obtained from every cycle, they are then can be determine the value of the crack initiation cycle by obtaining the value of  $N_f$ .

## **2.5 SPECIMEN GEOMETRY**

### **2.5.1 Standard Test Specimens**

Standard test specimens are used for experimental application to determine fatigue life of materials. The specimens that are selected depend on the type of fatigue test, since those not all standard specimens are suitable for any type of tests. The types are included compact tension specimen (CT), single edge notched bend specimen (SENB), double cantilever beam specimen (DCB) and others. CT specimen usually used for fatigue crack analysis, which is a notched sample. Notched sample is used to create fatigue crack by cycling the sample to the maximum and the minimum loads. When it comes the time where the fatigue crack started to appear at the notch, it will expand trough the sample. It is a good representation of the real situation of fatigue crack scenario.

### **2.5.2 Compact Tension Specimen**

As proposed by William H. Hartt (Hartt, 1991) in his on assesses and characterizes the fatigue properties of several new high strength structural steels under





## **2.6 SUMMARY**

Overall of this chapter has clarified the overview of relation of study of fatigue failure by using crack initiation method with narrowed scope, of AISI/SAE 1045 steel as the main material for this project. However, there is also some analysis about determining the crack initiation life cycle of the material in using CT specimen as analysis model. All specifications discussed in this chapter will be used to proceed to the analysis job, in order to achieve the objective of this project.

## **CHAPTER 3**

### **METHODOLOGY**

#### **3.1 INTRODUCTION**

This chapter will be elaborating the methodology applied for this project, starting from the specimen modelling stage until the documentation of the analysis result. The methodology for this project is taken by following the proper method of using finite element method to determine the final results of the analysis. The first analysis part is the linear static analysis, while the second part of the analysis is the fatigue failure analysis. The result of the linear static analysis will be used for the fatigue failure analysis in order to obtain the final results of this project.

#### **3.2 FLOW CHART**

This project methodology is visualized into a constructed flow chart to show the general overview of this project. The flow chart is shown in Figure 3.1.

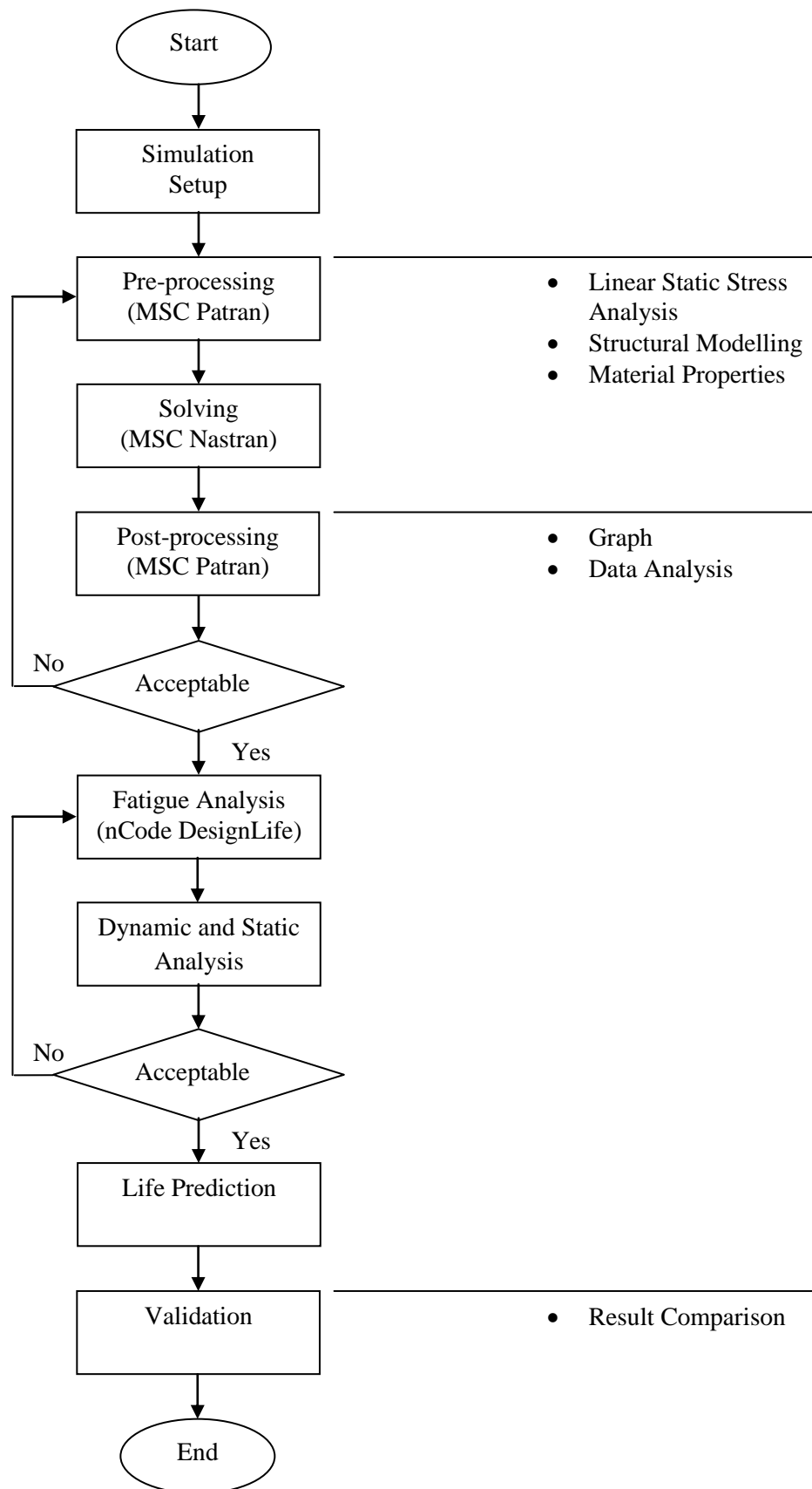


**Figure 3.1:** The flowchart of the project methodology.

### 3.3 METHODOLOGY STEPS

The methodology of the project mainly consists of two parts which are linear static analysis and fatigue analysis. Both parts are also divided into several activities that follow the analysis flows. Before the analysis started, CT specimen is selected for the analysis. A standard dimension of CT specimen is used for the analysis, and the dimension of the CT specimen used for this project is shown in Figure 3.2:

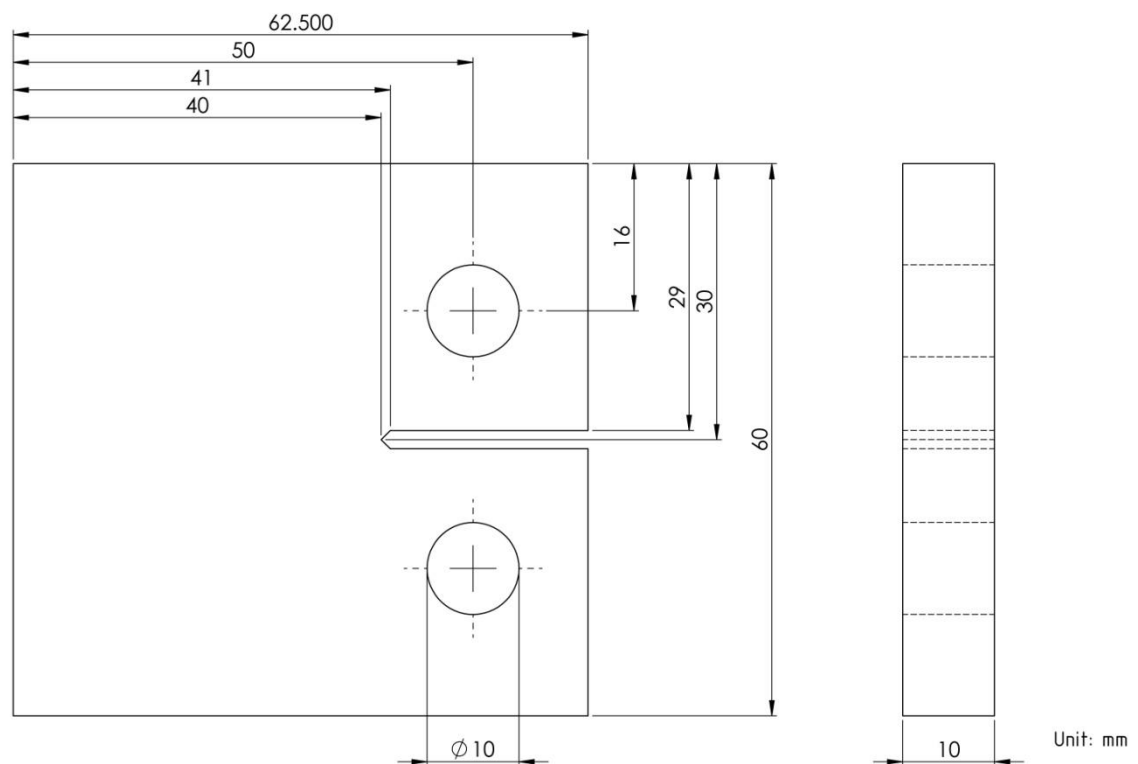


**Figure 3.2:** Schematic diagram of compact tension specimen (CT specimen).

Since the CT specimen is symmetrical, the analysis will be conducted on the top part of the specimen. This is because of it is assumed that the results of the analysis will be obtained as same as the bottom, regarding to the symmetrical shape.

The first part of the analysis is linear static which is the prerequisite of the fatigue analysis. The linear static analysis is firstly started by considering the variables and parameters which are related to the analysis. Some of the variables and parameters that

are related to the analysis are the type of specimen, the material properties, the measurement units, and the software that will be used for the project. In this project, MSC Patran 2010 and MSC Nastran 2007 are the software that has been selected to be used for analysis. Thus, the following methodology shown is taken from their latest interface of the softwares.

### 3.2.1 Linear Static Analysis

The structure modelling is created using MSC Patran by referring to the specimen dimensions. Modelling process is started by drawing the specimen model in MSC Patran by creating points, curve and surface. Before the drawing is started, new model preference was set as default setting as shown in Figure 3.3.

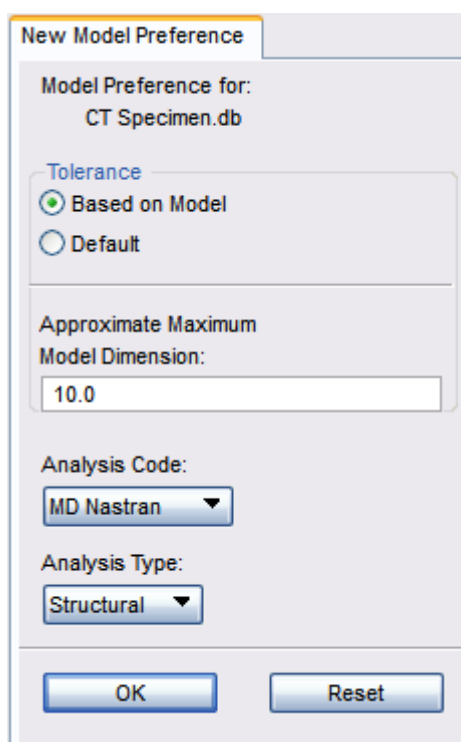


**Figure 3.3:** New model preference for the specimen analysis.

When it is completed, the geometry preferences have to be set to millimetres in the 'Geometry Scale Factor' section as shown in Figure 3.4. The other sections are left as default setting.

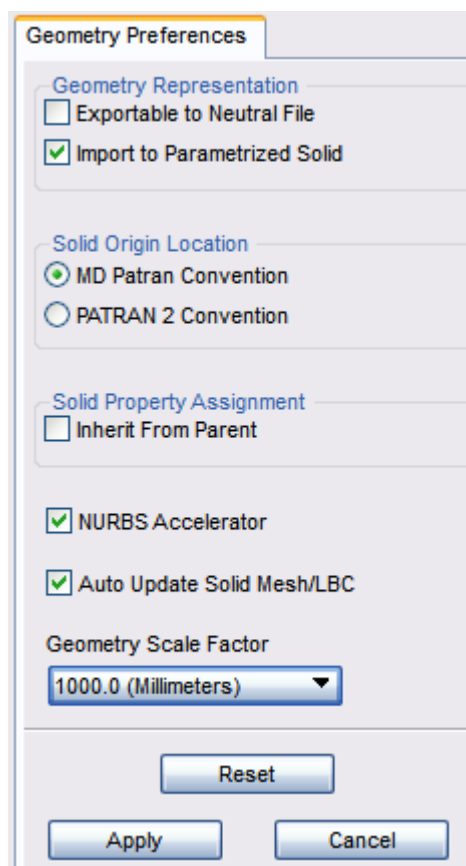


**Figure 3.4:** Geometry preferences for the specimen analysis.

When the preferences setting is done, the specimen drawing is started by create the specimen edge points. The origin point with coordinate  $[0, 0, 0]$  is used in the drawing. The other points are created by referring the dimensions of the specimen. The edge points of the drawing are shown in the Figure 3.5.



**Figure 3.5:** Points of the specimen drawing.

When the points are created, the curves are created by connecting between the points. Hence, a circle is created for the specimen hole in the analysis by using 2D Circle option. The completed curves are shown in Figure 3.6.

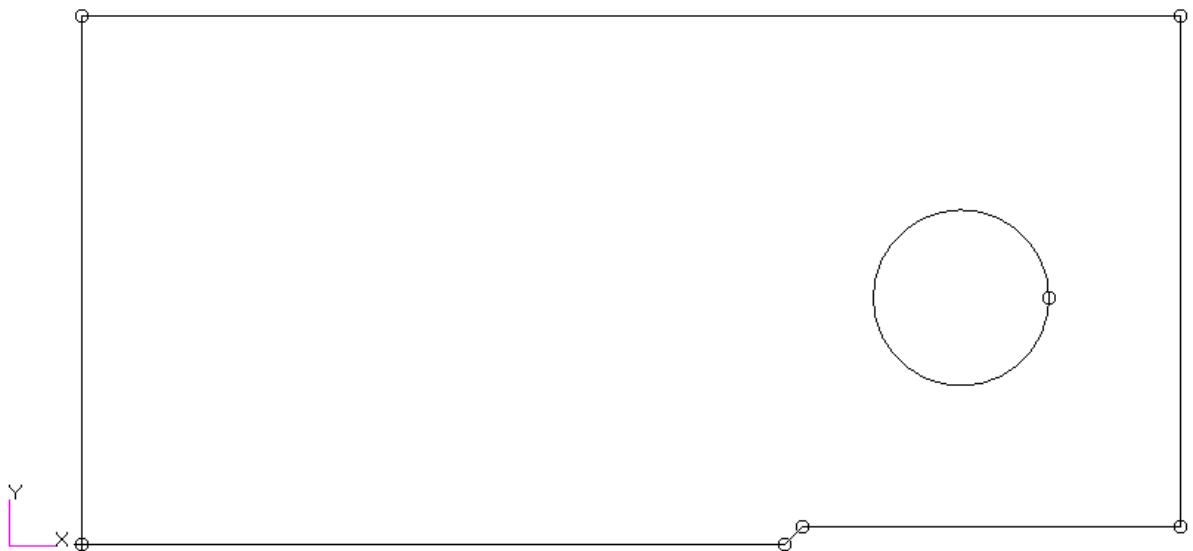


**Figure 3.6:** Curve of the specimen drawing.

Then, the specimen drawing is converted into a surface which is then looked as in Figure 3.7; while the curves are deleted from the drawing. The surface is selected

because the specimen is too thin as the thickness of the specimen is 10 mm. Thus, it is assumed as two dimensional analysis.



**Figure 3.7:** Created surface for the specimen drawing.

The surface is then broken into several parts for the preparation of creating mesh on the specimen as shown in Figure 3.8. The methods used for breaking the surface are broken by curves and points. The hole is also broken into eight parts for creating a structured mesh for the analysis. The broken surfaces are shown in Figure 3.9.

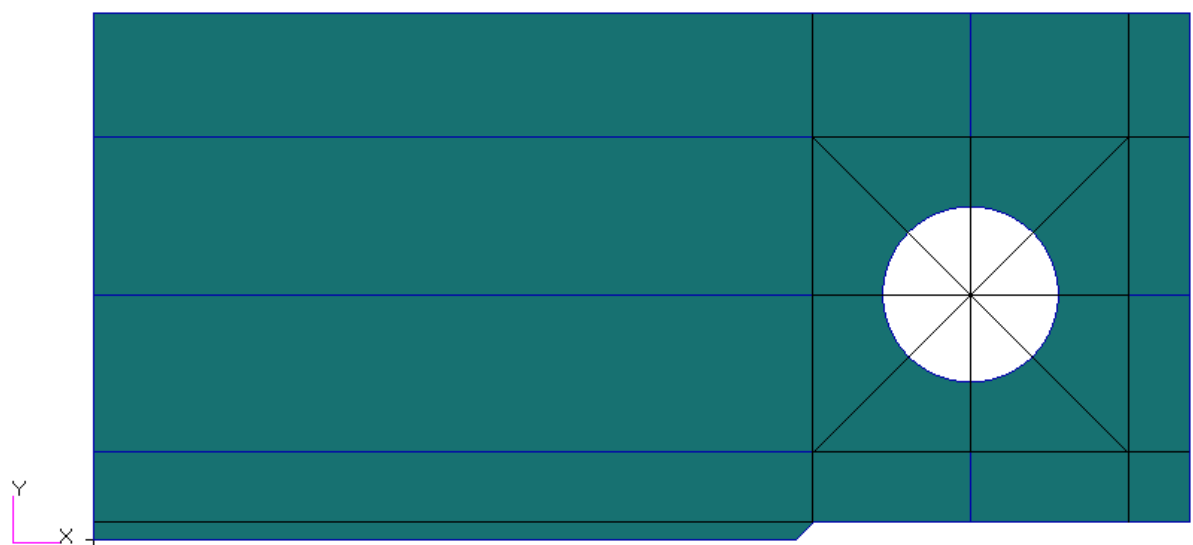


**Figure 3.8:** Created curves before breaking the surface into parts.





**Figure 3.9:** Broken surfaces after curves deletion.

Then, the material properties of the specimen are applied by using the following properties of high carbon steel are shown in Table 3.1.

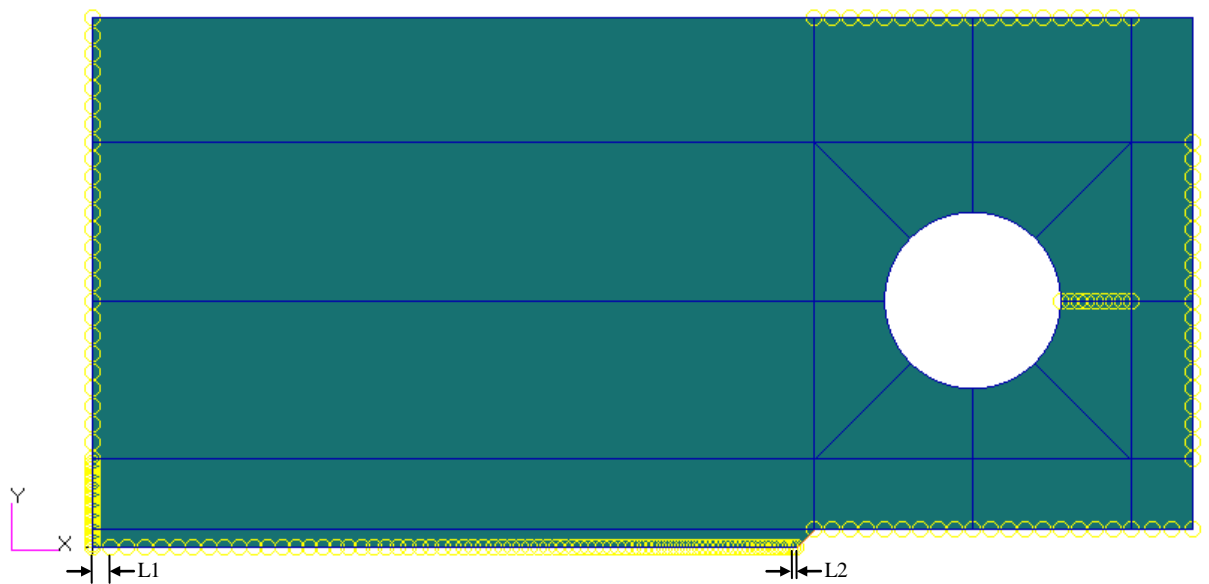
**Table 3.1:** Material properties of the specimen

| <b>Material Properties</b> |         |
|----------------------------|---------|
| Modulus of elasticity, $E$ | 205 GPa |
| Poisson's ratio, $\nu$     | 0.29    |

Hence, the mesh is created when the material properties of high carbon steel has been applied to the specimen. In the most of the part, uniform meshing is used while one way bias meshing is applied on the critical part of the specimen. The mesh seed is firstly created on the specimen before the actual mesh is applied. Uniform mesh seed with 1.0 mm is applied to the most part of the specimen, 0.5 mm is applied to the close part of the hole. Meanwhile, the one way biased mesh seeds are applied to the lowest part of the specimen so that they will create an arranged mesh with smaller mesh size is located at the closest node to the crack tip which is represented as L2. The bigger mesh size (presented as L1) is located at the furthest node from the crack tip. The sizes of the smaller mesh are differing regarding on the following L2/L1 ratios as shown in Table 3.2. The applied biased mesh seeds are shown in Figure 3.10:

**Table 3.2:** The variants of mesh seed sizes.

| Mesh seed size |     |
|----------------|-----|
| L1             | L2  |
| 1.0            | 0.1 |
| 1.0            | 0.2 |
| 1.0            | 0.3 |
| 1.0            | 0.4 |
| 1.0            | 0.5 |
| 1.0            | 0.6 |
| 1.0            | 0.7 |
| 1.0            | 0.8 |
| 1.0            | 0.9 |

**Figure 3.10:** Mesh seed for  $L2 = 0.2$ .

After setting up the mesh seeds, the mesh is created on the specimen by selecting on all the specimen surfaces. In the settings option as shown in Figure 3.11, the mesh element shape is set to 'Quad' that represent as rectangular mesh, IsoMesh is selected for the mesher selection, and Quad4 is selected for the topology setting.

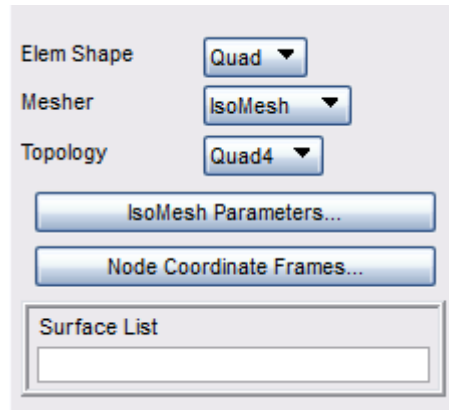


**Figure 3.11:** Mesh shape settings.

The global edge length automatically calculated after selecting the surfaces that will be created with mesh. The automated length is left as the computer done automatically as shown in Figure 3.12. After the mesh has been created, the meshes are then made equivalence so to make the mesh from all parts are connected together.

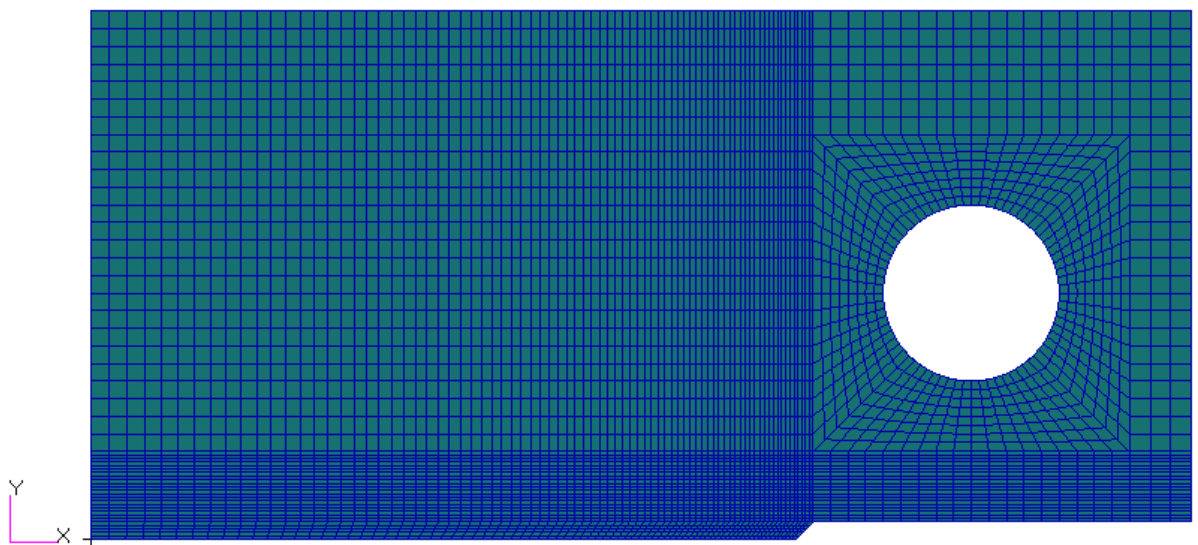


**Figure 3.12:** Created mesh on the specimen.

When the meshing is completed, the boundary conditions are set on the model as shown in Figure 3.13. It is set by fixing the bottom edge of the critical area and giving positive force on the hole in the model by using total load selection.

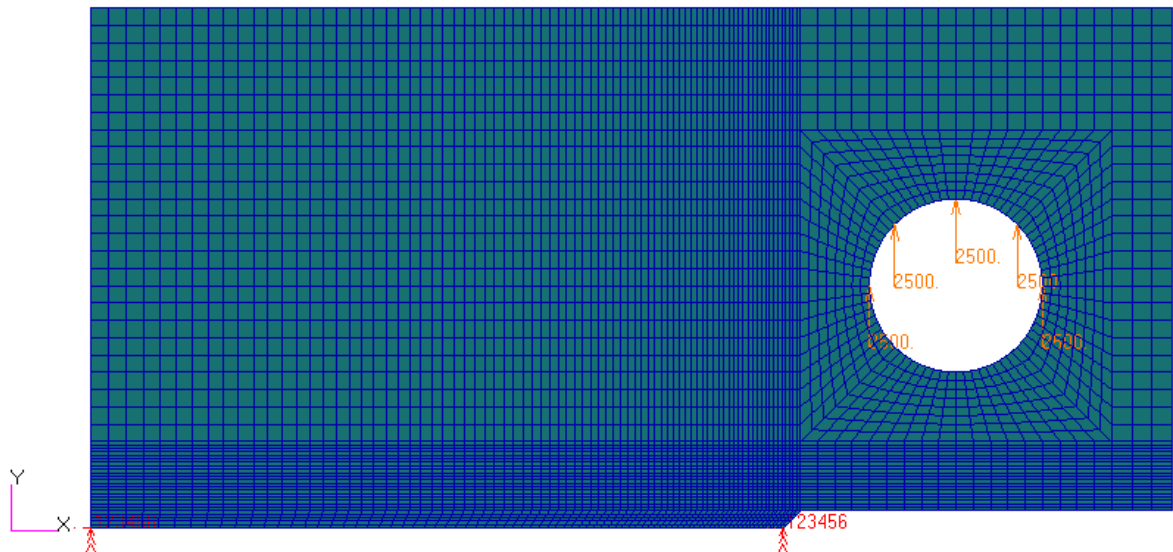


**Figure 3.13:** Specimen with boundary layers.

During the analysis setup, the analysis method is set to ‘Analysis Deck’ and the linear static is chosen for ‘Solution Type’. In order to create a file that will be used for ANSYS 13.0 nCode DesignLife, the format for output file was set to ‘op2’ file by clicking on ‘Solution Parameter’ button which will open a new pop up window. The output file format can be set by clicking on the ‘Results Output Format’ and once again will open a new pop up window. Tick on the ‘OP2’ selection and select ‘OK’ for all appeared windows to return to the main interface. Then, ‘bdf’ file is produced when ‘Apply’ button is hit.

The analysis is then started by using MSC Nastran 2007. To set up the analysis, the produced ‘bdf’ file from previous step is selected when MSC Nastran 2007 is running. Hence, the analysis is started when the ‘Run’ button is hit.

After the analysis was done, the results were read by selecting the ‘Access’ Result’ options in analysis toolbar. The results are then used as a input data for the following fatigue analysis.

### 3.2.2 Fatigue Failure Analysis

Fatigue analysis started when all static analysis has completed and the results have been obtained from the post-processor. For fatigue analysis, the major steps are mostly same which are consisting of pre-processing, analysis and post-processing.

In ANSYS 13.0 nCode DesignLife software, there are several procedures needed to be followed which are generating time series, converting time series into input data, importing the produced 'op2' file from the previous analysis, material setting, run the analysis and obtaining the result.

A time series generation network is created in order to generate the time series. Time Series Generator box is dragged into the workspace from the right sidebar under the Input Glyphs. Then, the Data Value Display and XY Display boxes are dragged into the workspace from the Display Glyphs. The Time Series Generator box is then linked with the display boxes to create linked network as shown as in Figure 3.14.

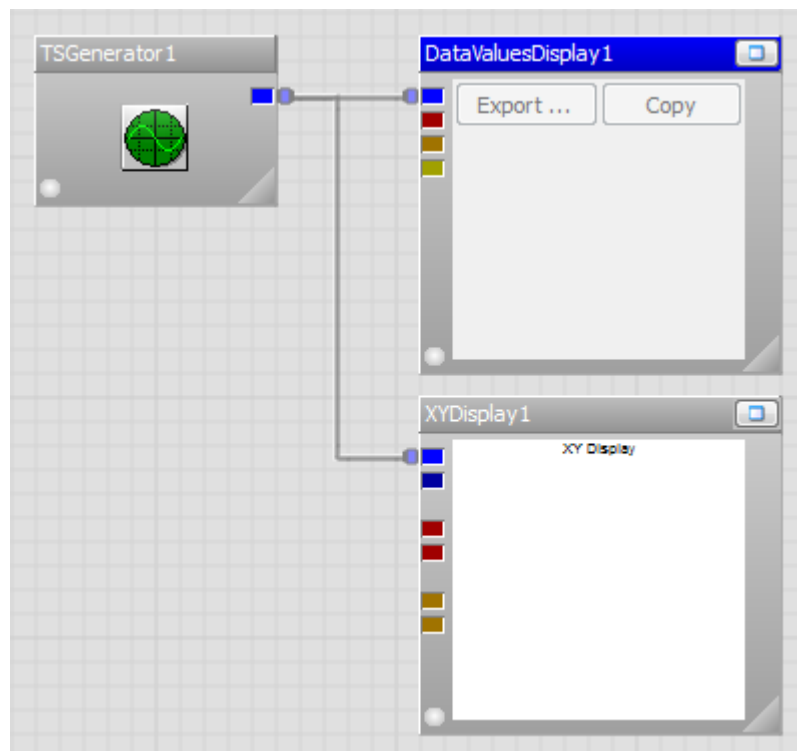


**Figure 3.14:** Time series generator network.

The properties setting for the Time Series Generator is then opened by double clicking on the Time Series Generator box. A pop up window is then appeared as shown in Figure 3.15.

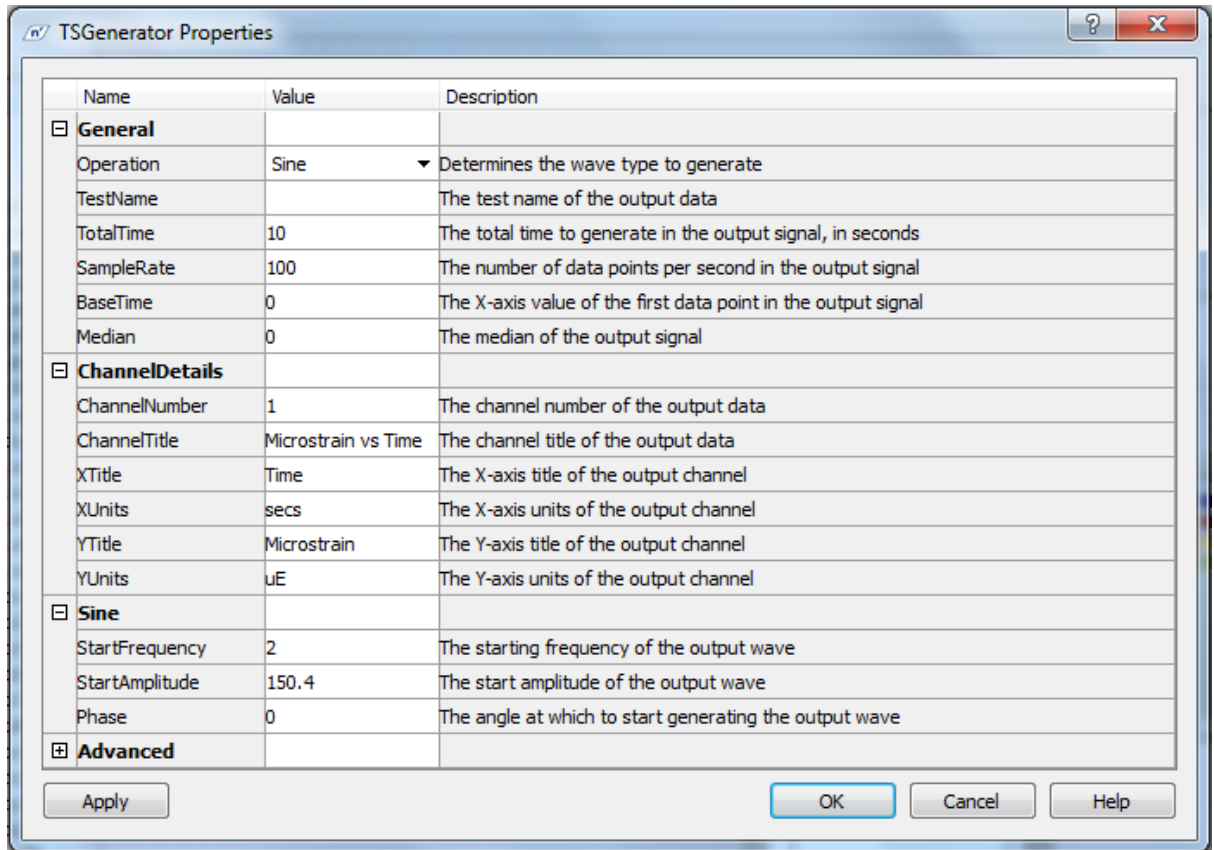


**Figure 3.15:** Time Series Generator properties window.

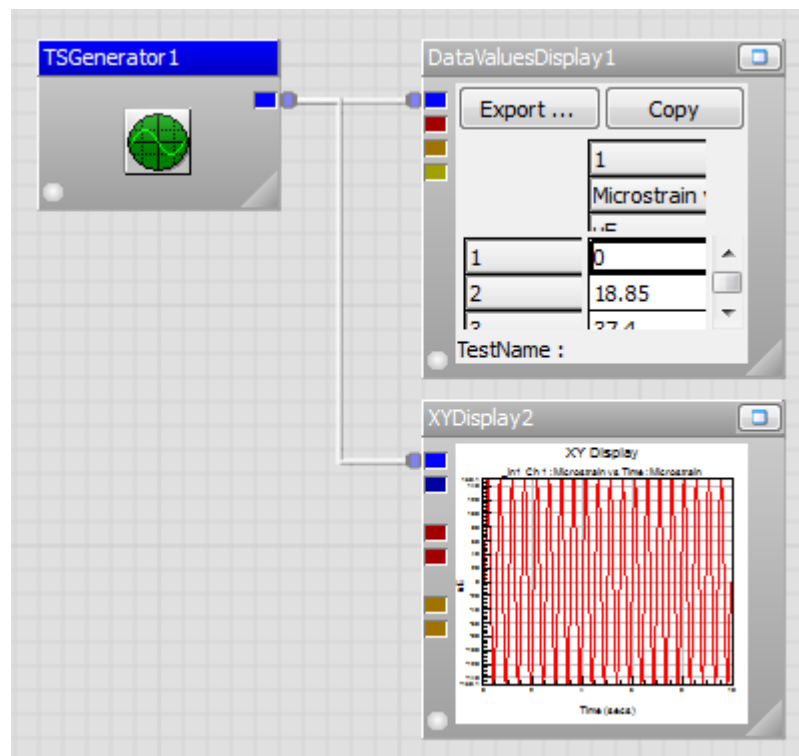
The Time Series Generator Properties is a setting window that controls the type of operation of the time series, the time settings, input value and units, input frequency and the amplitude, and the initial phase angle. For this study, the analysis is run as sine operation with constant frequency and amplitude, as the study is not concern about the amplitude or frequency variation in a time series.

The time series input properties set up is shown in the Figure 3.15. The input parameters that set into the Time Series Generator are depending on the study case types are listed in Table 3.3.

**Table 3.3:** Input parameter for crack initiation studies.

| Case                    | Frequency | Time Sample | Phase angle |
|-------------------------|-----------|-------------|-------------|
| Compression–Compression | 1 Hz      | 100         | 90°         |
|                         | 2 Hz      | 100         | 90°         |
|                         | 3 Hz      | 100         | 90°         |
| Compression–Tension     | 1 Hz      | 100         | 0°          |
|                         | 2 Hz      | 100         | 0°          |
|                         | 3 Hz      | 100         | 0°          |
| Tension–Tension         | 1 Hz      | 100         | 270°        |
|                         | 2 Hz      | 100         | 270°        |
|                         | 3 Hz      | 100         | 270°        |

When all settings are completed, OK button is hit to return to the main software interface. Then, the time series generation is ran when the Run button is hit. The end of the time series generation is shown in the Figure 3.16.

**Figure 3.16:** Generated time series interface.

Both display boxes are resulted to view the time series in numerical values in the Data Value Display box while the time series graph is shown in the XY Display box.

The following steps are the method to export the data value before convert the data value as the input parameter.

After the time series has generated, the Export button in the Data Value Display box is clicked and a popup window appeared. A name for the time series is given and the exported time series data are saved into 'csv' file. Then, export the data values into ASCII data.

To convert the file, the ASCII Translate button at the most left sidebar in the software interface is clicked and a small popup window appeared. The saved time series is chosen for the next step. 'Time Series' in the 'Convert To' selection is chosen and the next button is clicked to move to the next settings, as shown in Figure 3.17.

Layout

Number of header lines: 8 Line number for channel titles: 3

Number of channels: Line number for units: 5

(If blank, number of channels will be auto-detected)

Fields

☐ Tab separated ☒ Comma separated ☐ Space separated

☐ Semi-colon separated ☐ Fixed width: 10

Decimal Character

☒ . (period) ☐ , (comma)

Columns to

Exclude

Preview: Truncated to first 300 rows

|   | 1          | 2       | 3                   |
|---|------------|---------|---------------------|
| 1 | #HEADER    |         |                     |
| 2 | #TITLES    |         |                     |
| 3 |            |         | Microstrain vs Time |
| 4 | #UNITS     |         |                     |
| 5 |            |         | uE                  |
| 6 | #DATATYPES |         |                     |
| 7 | Huge       | Double  | Float               |
| 8 | #DATA      |         |                     |
| 9 | 1          | 0.00000 | -7.105E-15          |

Help < Back Next > Cancel

**Figure 3.17:** ASCII Translate setting interface.





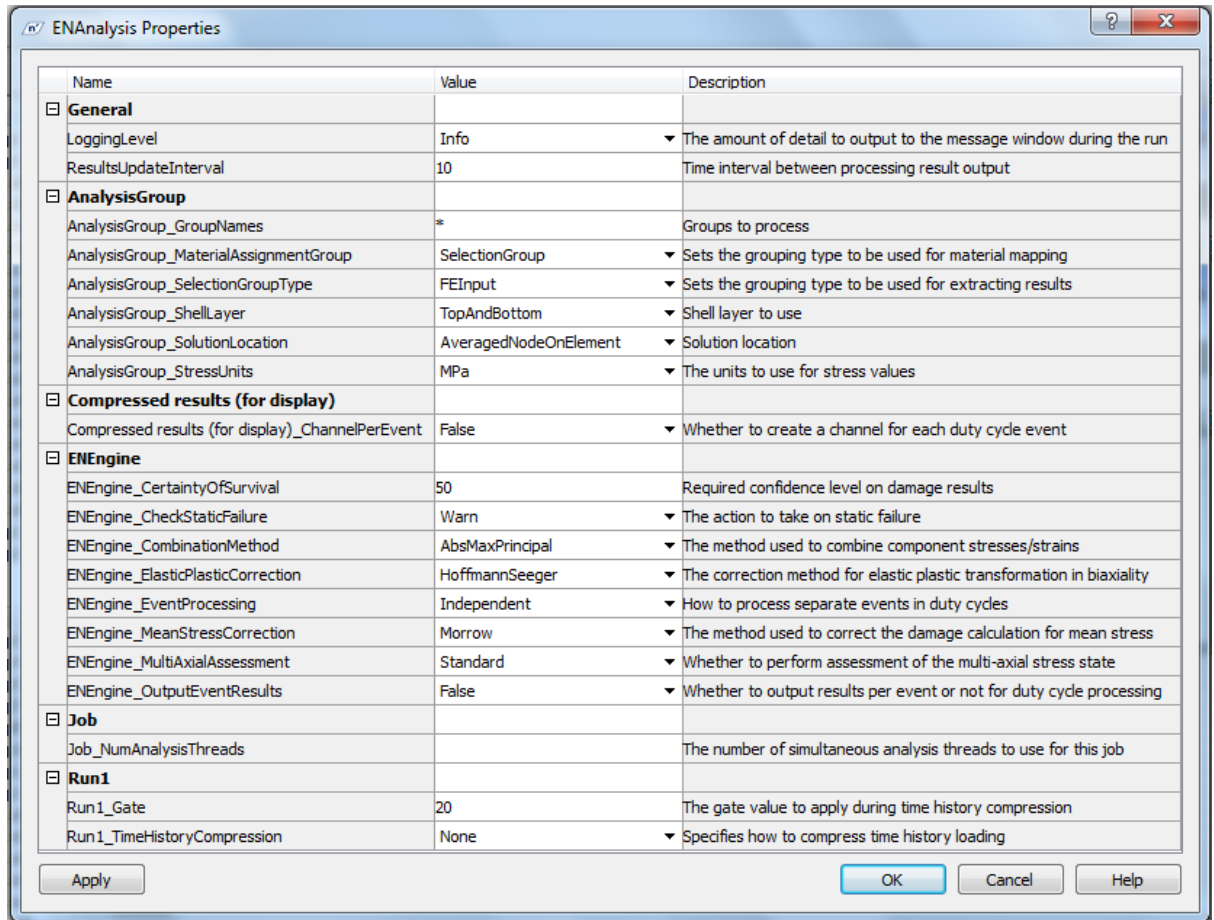


**Figure 3.19:** Strain-life properties setting.

The settings are leaved as default and the mean stress correction is set as Morrow. OK button is clicked to return to the main interface. Then, Material Mapping is opened by right clicking on the FEAnalysis box, and Edit Material Mapping is selected. ‘Yes’ button is clicked if a small popup window appears. Then, a window is appeared as shown in Figure 3.20 in order to set the material for the model.

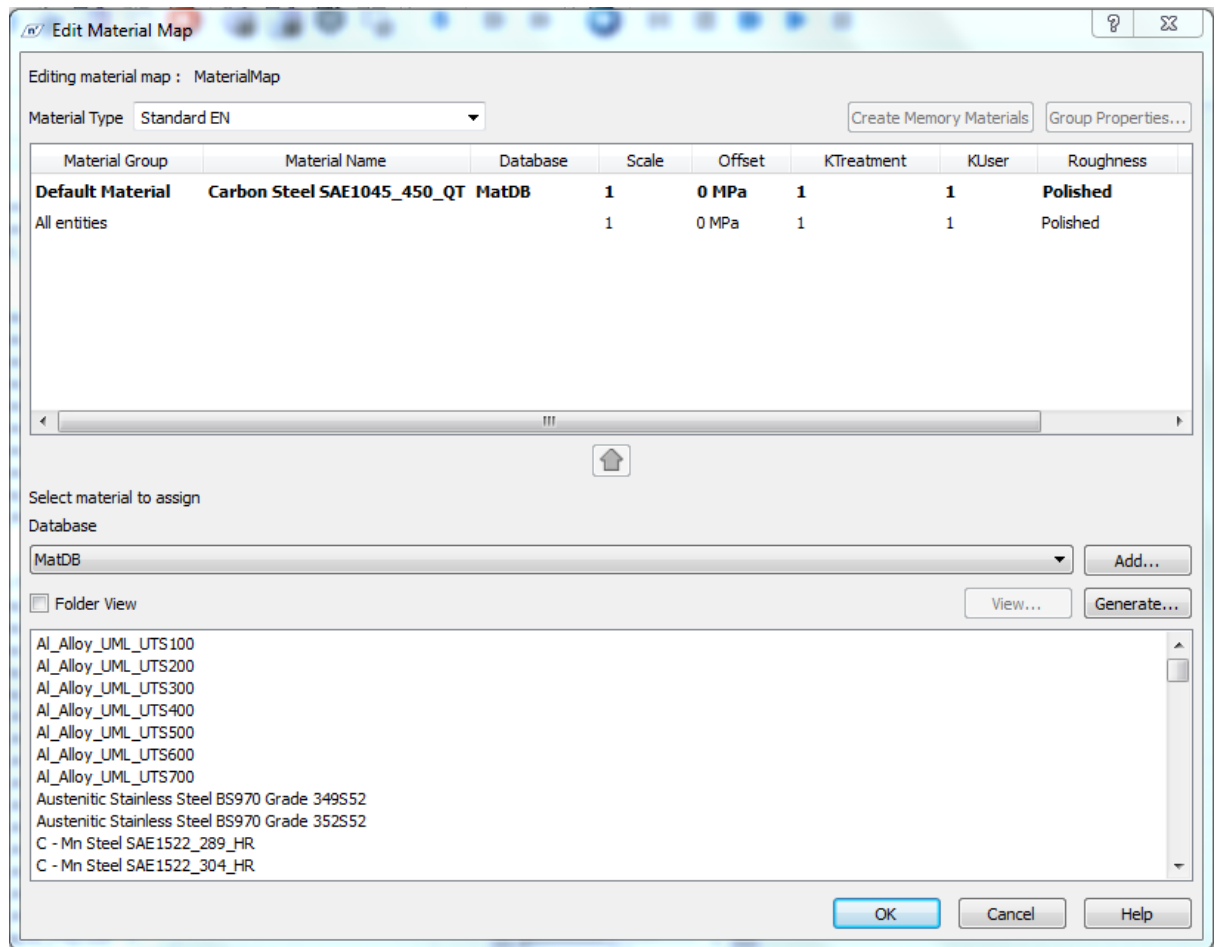


**Figure 3.20:** Material Map for the strain-life analysis.

Carbon Steel SAE1045\_450\_QT is chosen from the selection at the bottom of the window and the 'up' arrow at the centre of the window is clicked to insert the material into the Default Material group. When it has done, OK button is clicked to return to the workspace.

When all settings has completed, Run button is clicked to start the analysis. The results of the analysis are then shown as in Figure 3.21.

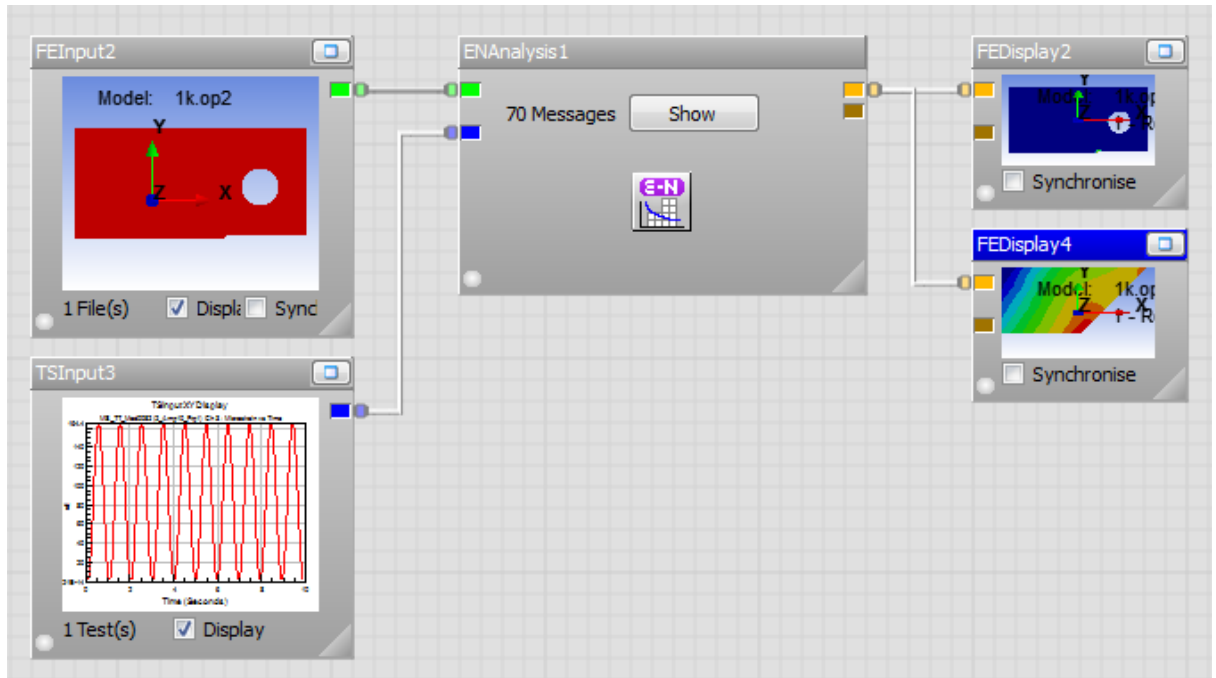


**Figure 3.21:** Strain-life result display.

The time series input is then changed to the other time series until the strain value at the initiation of dynamic and static failure has determined. The dynamic failure initiation is indicated by the beginning of the failure damage on the analysis model while the static failure initiation is indicated by the beginning of the static failure damage which is represented with purple colour.

The obtained results are then analyzed and discussed in order to draw a conclusion for this study.

## **CHAPTER 4**

### **RESULTS AND DISCUSSIONS**

#### **4.1 INTRODUCTION**

This chapter will analyze and discuss about the results of the analysis, beginning with the finite element an analysis result which is included the input parameter used for the analysis and the crack initiation analysis result. The following subchapters are discussing about the theoretical failure stress and the crack initiation life of the analysis design.

#### **4.2 FINITE ELEMENT ANALYSIS RESULTS**

The finite element analysis is consisting of three different cases which are the types of microstrain effect acted on the specimen. The cases that done on the specimen are tension-tension, compression-tension and compression-compression which are representing the different cases of loading acting on the material in the real applications.

In the real application, the loading types may happen in one of the cases or the combination of two or more cases in simultaneously. However, this study is using those three different cases separately to indicate the initiation point of static and dynamic failure damage to the material under the microstrain effects.

#### 4.2.1 Input Parameters.

The parametric studies on the specimen using the microstrain effect are consisting of several parameters that are needed to consider in obtaining the result. The studies are separated by the initial point of static and dynamic failure and the effect of microstrain frequency acted on the specimen. The parameters of the studies are listed in the Table 4.1.

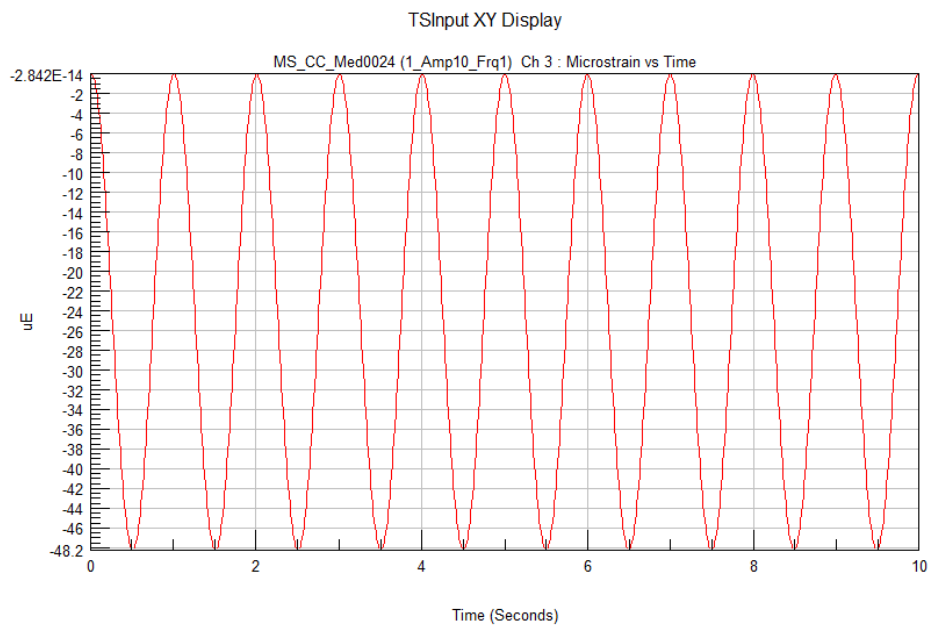
**Table 4.1:** Input parameter for dynamic and static analysis studies.

| Case                    | Frequency | Time Sample | Phase angle | Period |
|-------------------------|-----------|-------------|-------------|--------|
| Compression–Compression | 1 Hz      | 100         | 90°         | 10 s   |
|                         | 2 Hz      | 100         | 90°         | 10 s   |
|                         | 3 Hz      | 100         | 90°         | 10 s   |
| Compression–Tension     | 1 Hz      | 100         | 0°          | 10 s   |
|                         | 2 Hz      | 100         | 0°          | 10 s   |
|                         | 3 Hz      | 100         | 0°          | 10 s   |
| Tension–Tension         | 1 Hz      | 100         | 270°        | 10 s   |
|                         | 2 Hz      | 100         | 270°        | 10 s   |
|                         | 3 Hz      | 100         | 270°        | 10 s   |

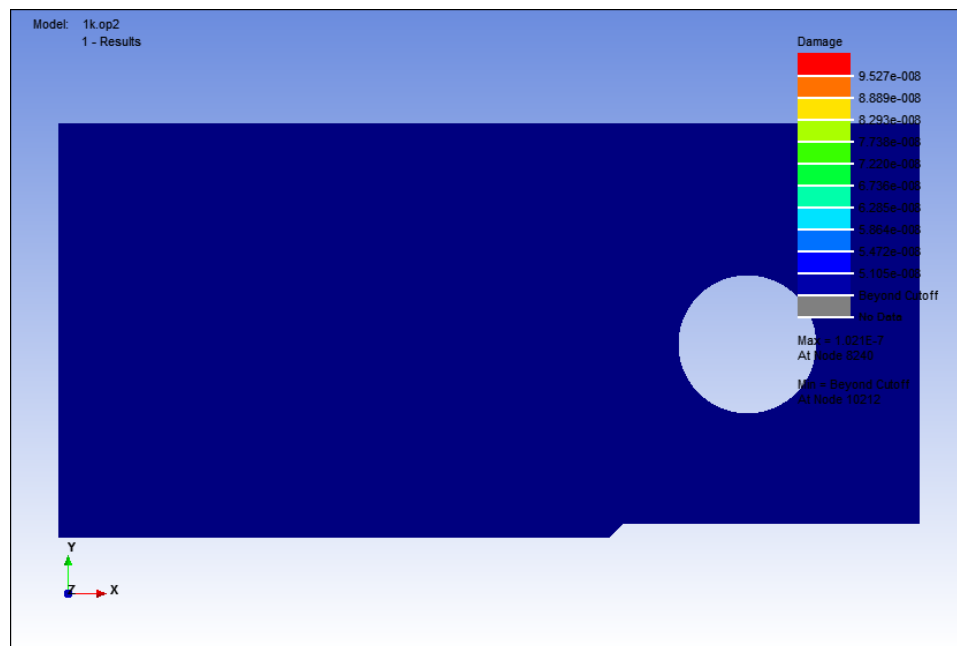
#### 4.2.2 Crack Initiation Analysis Results

In the static and dynamic failure in the crack initiation studies, the static and dynamic initiation failure is obtained by varying the microstrain value that applied on the specimen. The failure is obtained by the damage occurs on the specimen when the microstrain values are high enough to start the static and dynamic failure.

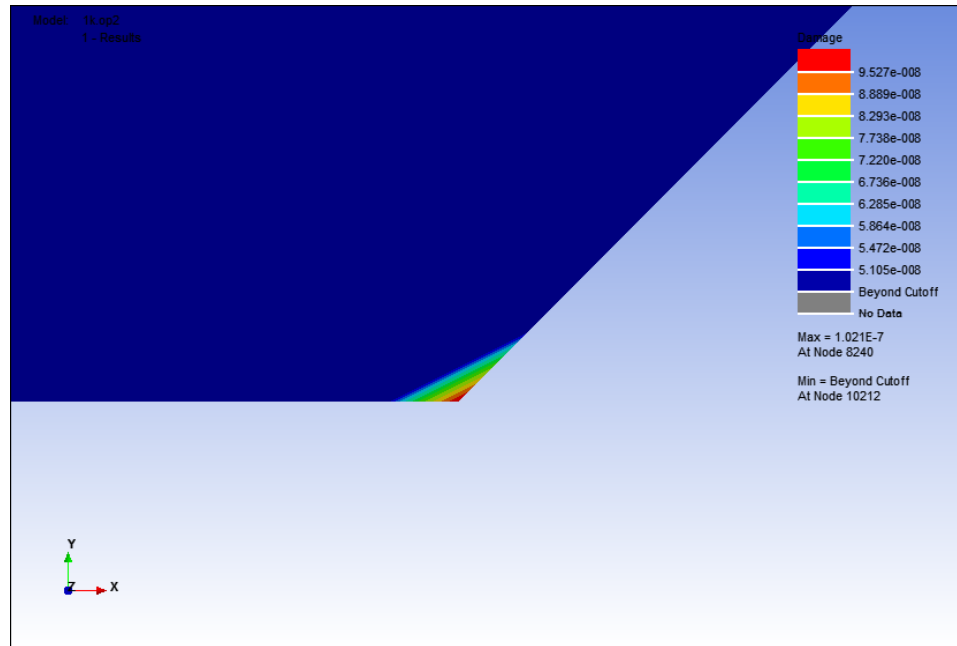
The microstrain value that applied on the specimen is actually the input value of the analysis, which then obtaining the damage of the failure on the specimen. Figure 4.1 until Figure 4.27 show the analysis results for all cases for dynamic failure while Figure 4.28 until Figure 4.34 show the results for all cases for static failure.



**Figure 4.1:** Microstrain value for dynamic failure analysis for compression-compression case at 1 Hz.



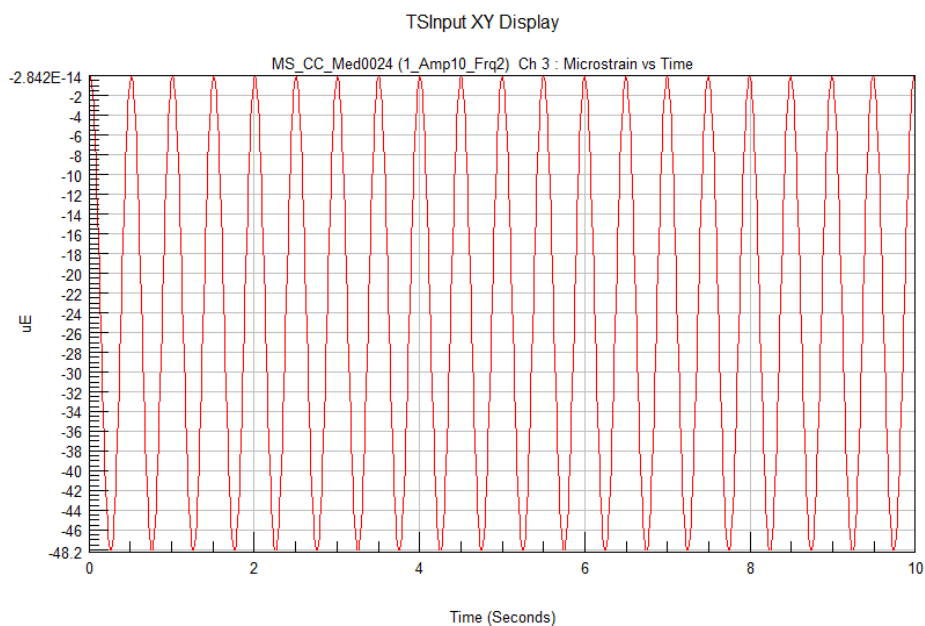
**Figure 4.2:** Damage contour for dynamic failure analysis for compression-compression case at 1 Hz.



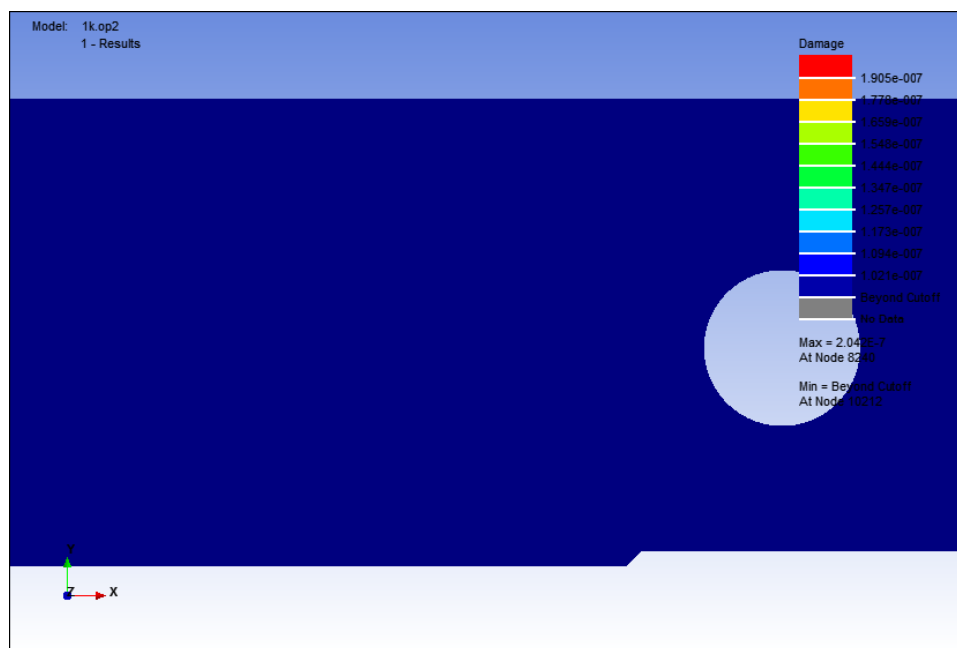
**Figure 4.3:** Damage contour at notch point for dynamic failure analysis at for compression-compression case at 1 Hz.

Figure 4.1 shows that the value of the microstrain that initiate the fatigue failure for compression-compression loading case for dynamic failure analysis at 1 Hz. At  $48.2 \mu\epsilon$ , the fatigue failure started and the damage value obtained was  $9.257 \times 10^{-8}$ . The fatigue failure that occurs on the model is very small, as shown in Figure 4.2. Figure 4.3 shows the affected area where the fatigue failure started at the notch point of the model.

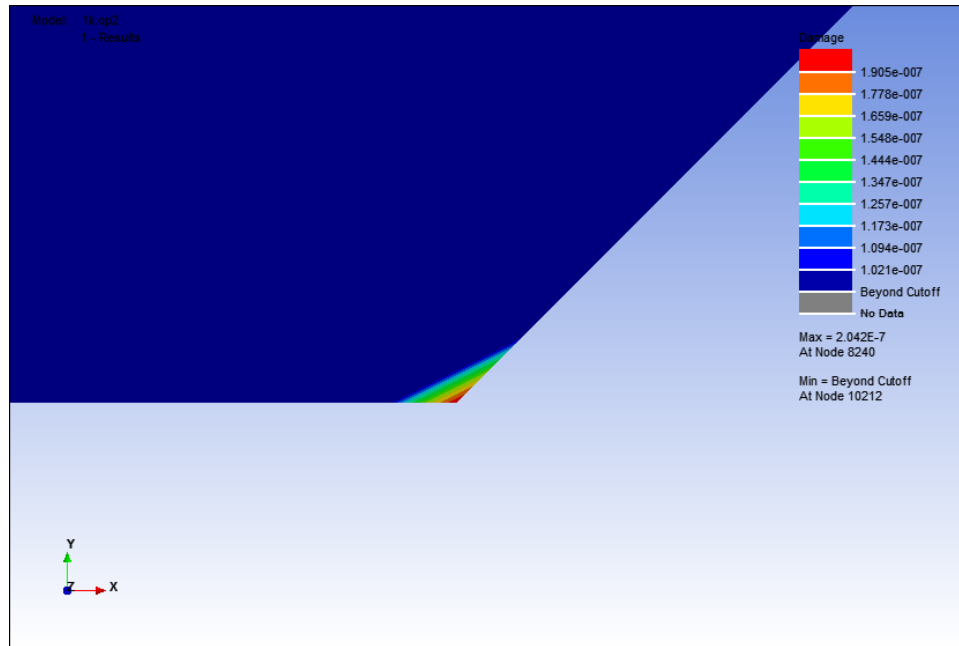




**Figure 4.4:** Microstrain value for dynamic failure analysis for compression-compression case at 2 Hz.

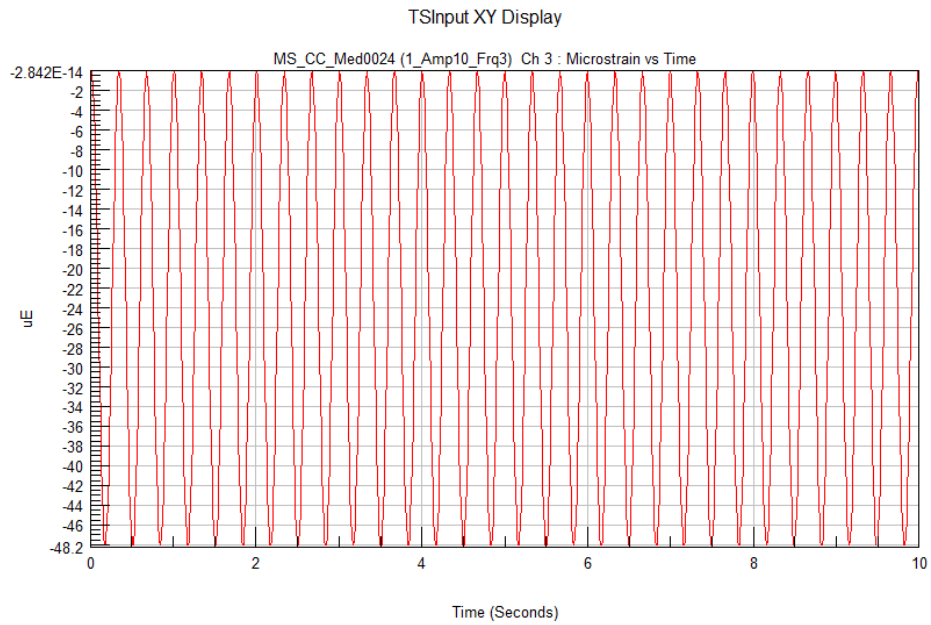


**Figure 4.5:** Damage contour for dynamic failure analysis for compression-compression case at 2 Hz.

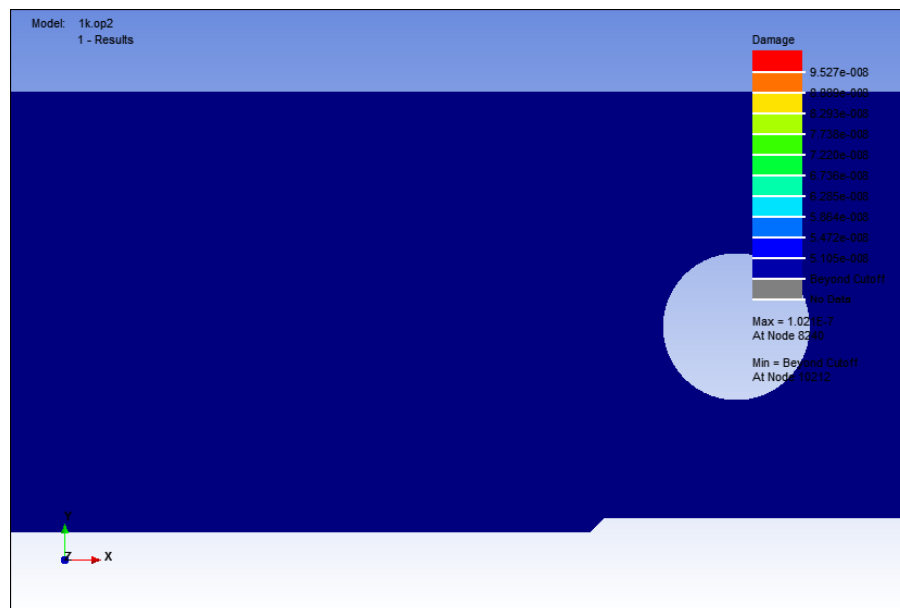


**Figure 4.6:** Damage contour at notch point for dynamic failure analysis at for compression-compression case at 2 Hz.

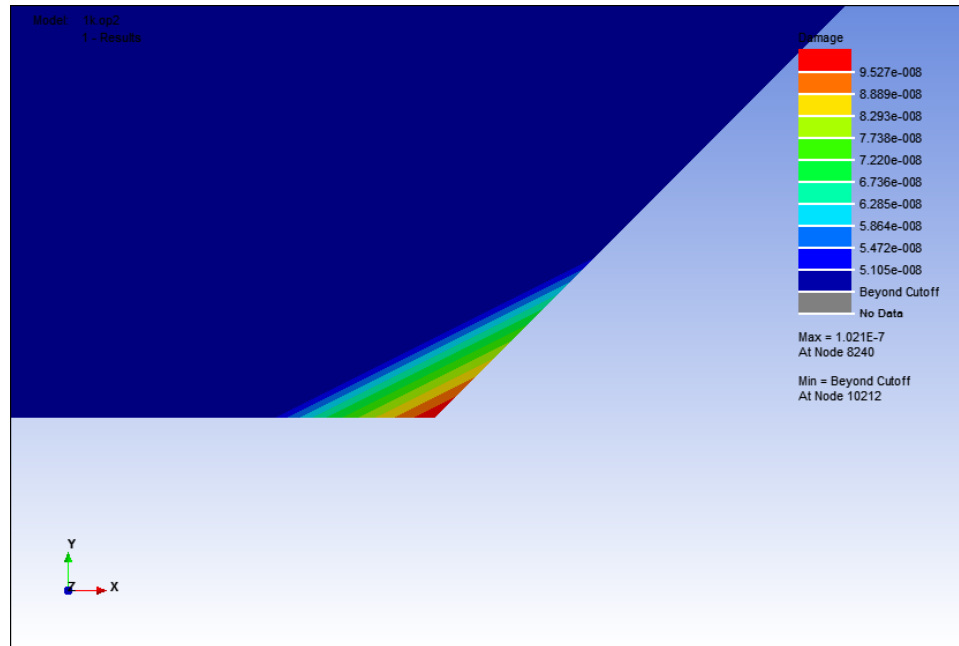
Using the same microstrain value with the cyclic frequency of 2 Hz as shown in Figure 4.4, the damage value that obtained was  $1.905 \times 10^{-7}$ . As same as the previous result, the fatigue failure that occurs on the model was very small, as shown in Figure 4.5. However, the damage value that obtained was different as it gets higher. Figure 4.6 shows the notch point of the model, which is the critical point of the fatigue failure initiation has occur.



**Figure 4.7:** Microstrain value for dynamic failure analysis for compression-compression case at 3 Hz.

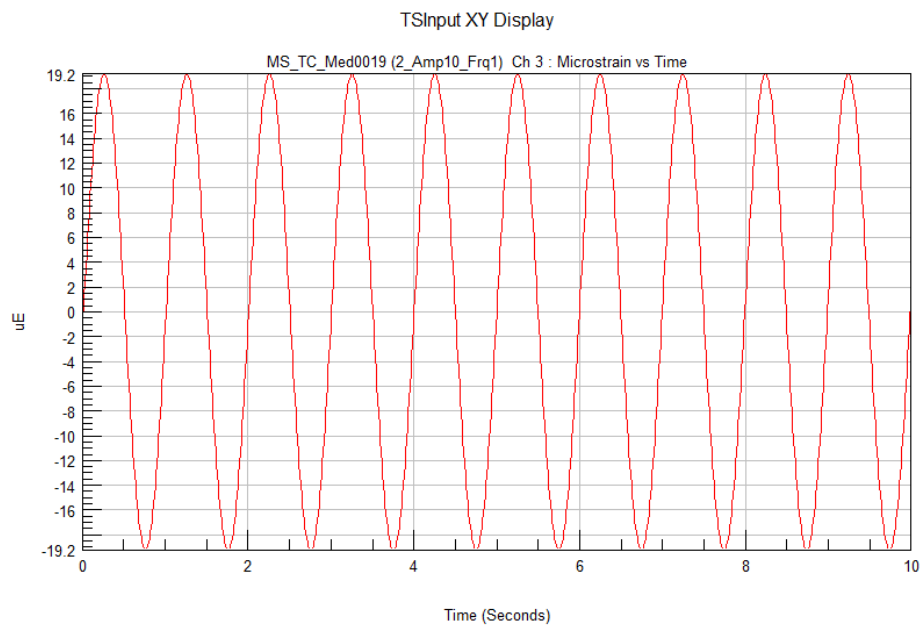


**Figure 4.8:** Damage contour for dynamic failure analysis for compression-compression case at 3 Hz.

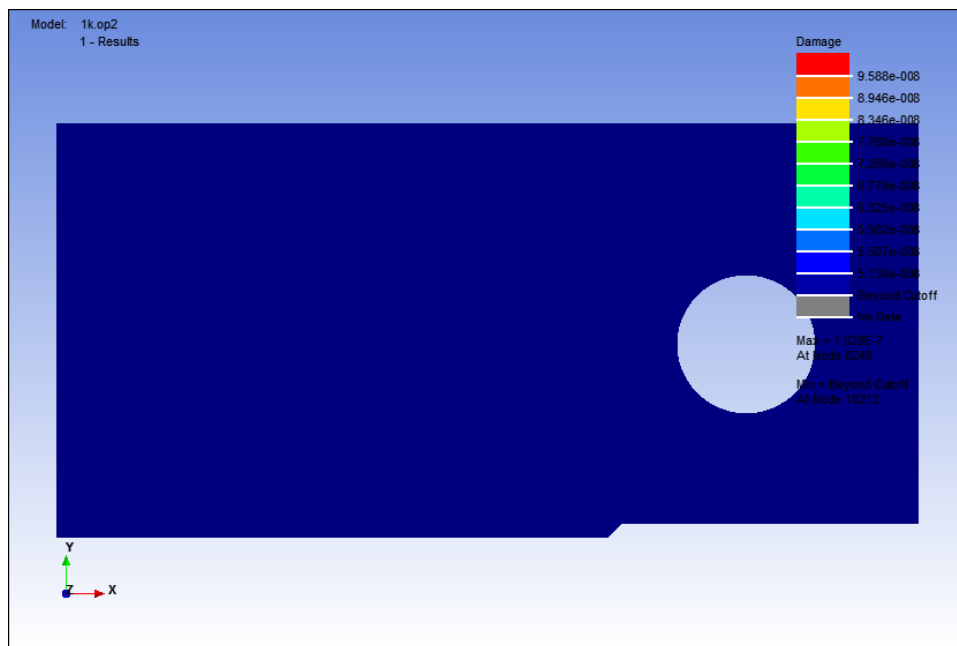


**Figure 4.9:** Damage contour at notch point for dynamic failure analysis at for compression-compression case at 3 Hz.

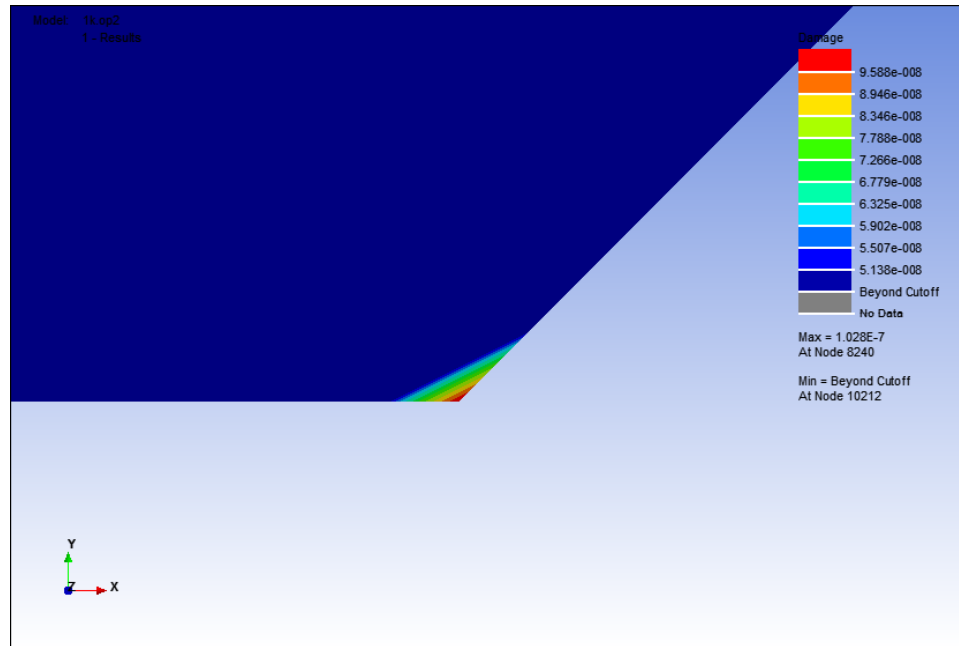
At 3 Hz, with the same value of microstrain at  $48.2 \mu\epsilon$  as shown in Figure 4.7; the damage that obtained was  $9.527 \times 10^{-8}$ . The damage that occur was still very small as shown in Figure 4.8 and Figure 4.9 but the damage value that obtained shows that it has returned to the value as same as the analysis result at 1 Hz.



**Figure 4.10:** Microstrain value for dynamic failure analysis for compression-tension case at 1 Hz.

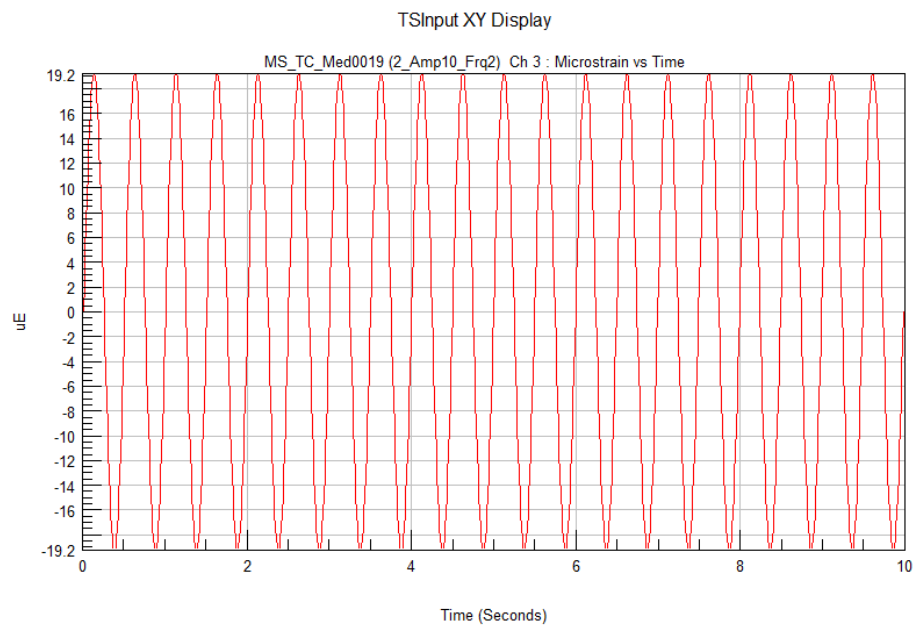


**Figure 4.11:** Damage contour for dynamic failure analysis for compression-tension case at 1 Hz.

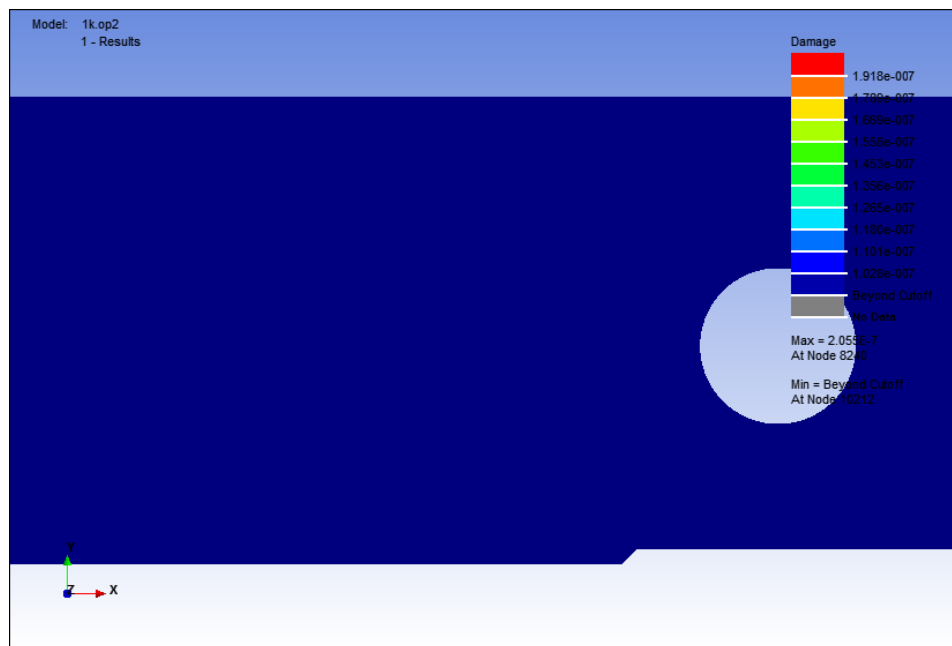


**Figure 4.12:** Damage contour at notch point for dynamic failure analysis at for compression-tension case at 1 Hz.

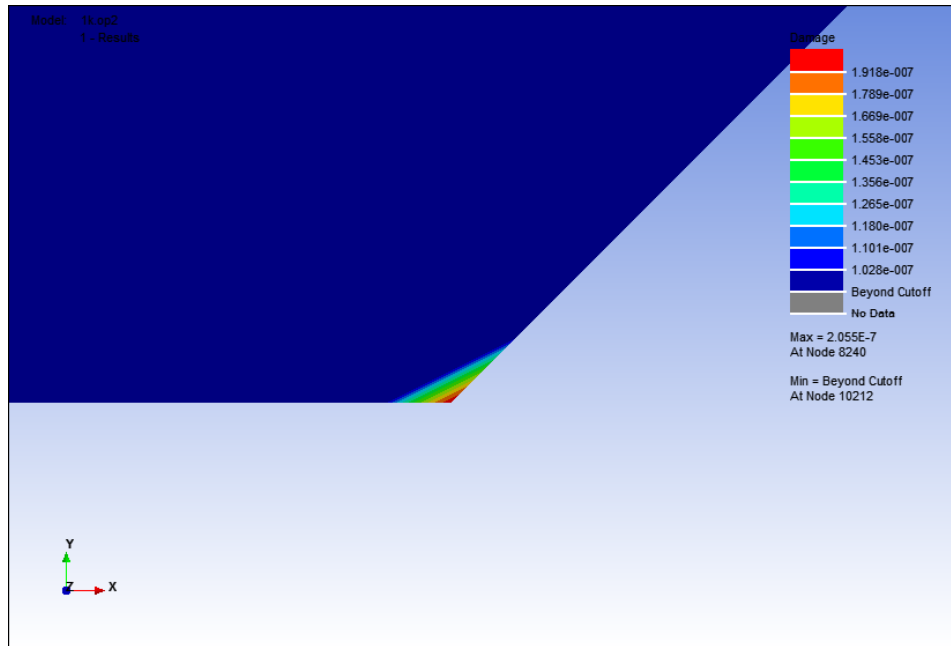
Figure 4.10 shows that the value of the microstrain that initiate the fatigue failure for compression-tension loading case for dynamic failure analysis at 1 Hz. At microstrain range of  $38.4 \mu\epsilon$ , the fatigue failure initiated and the damage value obtained was  $9.588 \times 10^{-8}$ . The fatigue failure that occurs on the model is very small, as shown in figure 4.11. Figure 4.12 shows the affected area where the fatigue failure started at the notch point of the model.



**Figure 4.13:** Microstrain value for dynamic failure analysis for compression-tension case at 2 Hz.



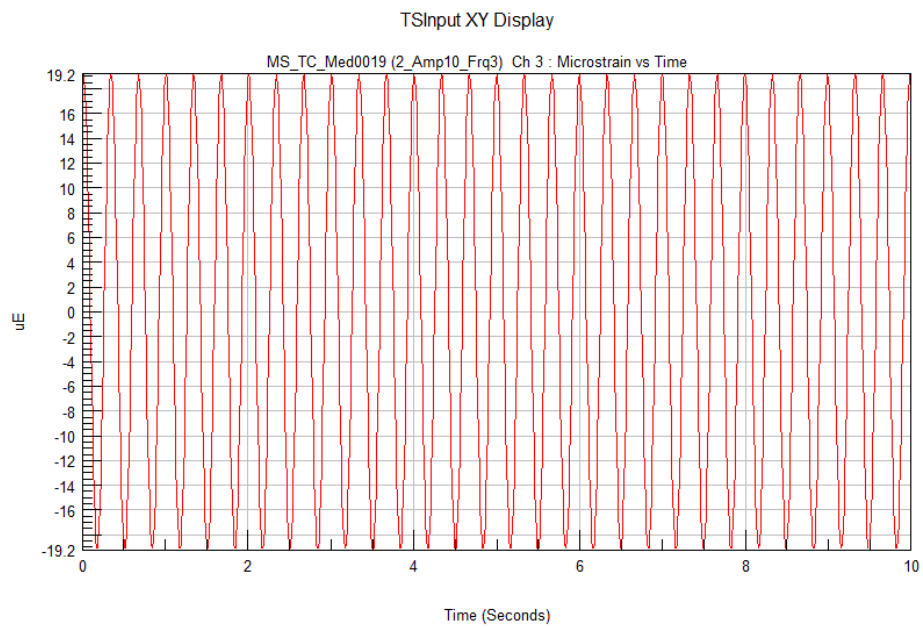
**Figure 4.14:** Damage contour for dynamic failure analysis for compression-tension case at 2 Hz.



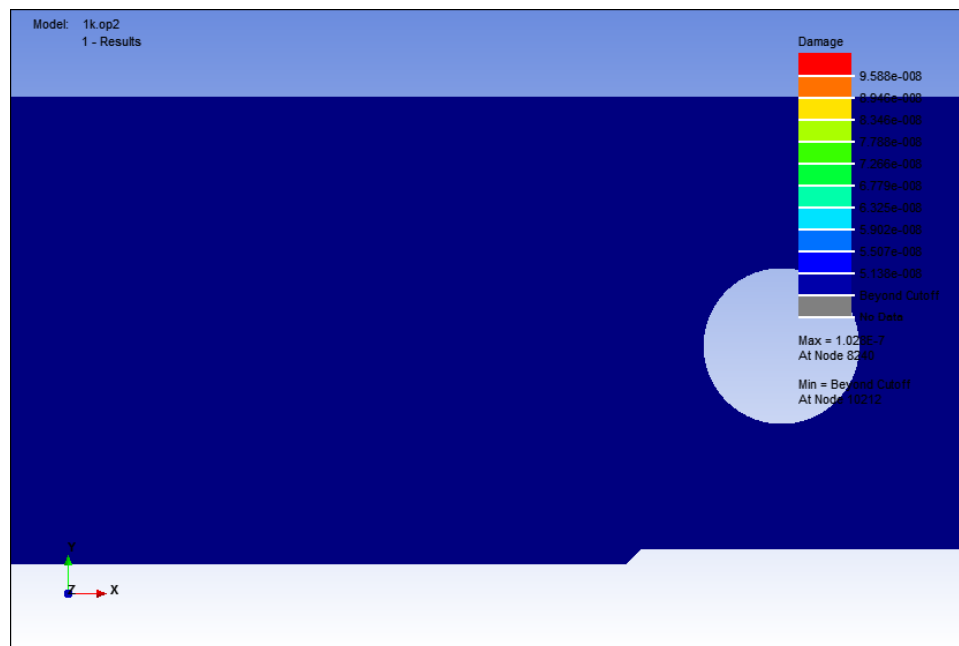
**Figure 4.15:** Damage contour at notch point for dynamic failure analysis at for compression-tension case at 2 Hz.

At 2 Hz, the damage value that obtained was  $1.918 \times 10^{-7}$  and the fatigue failure that occurs was still small, as shown in Figure 4.14 and Figure 4.15. Using the same microstrain value as the analysis at 1 Hz with the different frequency of 2 Hz as shown in Figure 4.13, the damage value get bigger than the previous analysis.

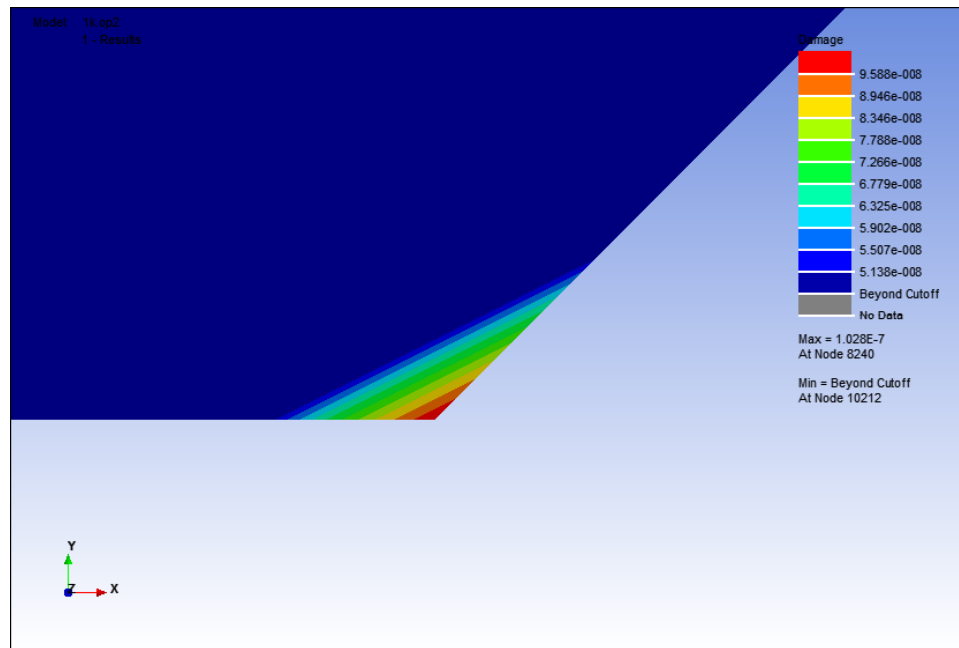




**Figure 4.16:** Microstrain value for dynamic failure analysis for compression-tension case at 3 Hz.

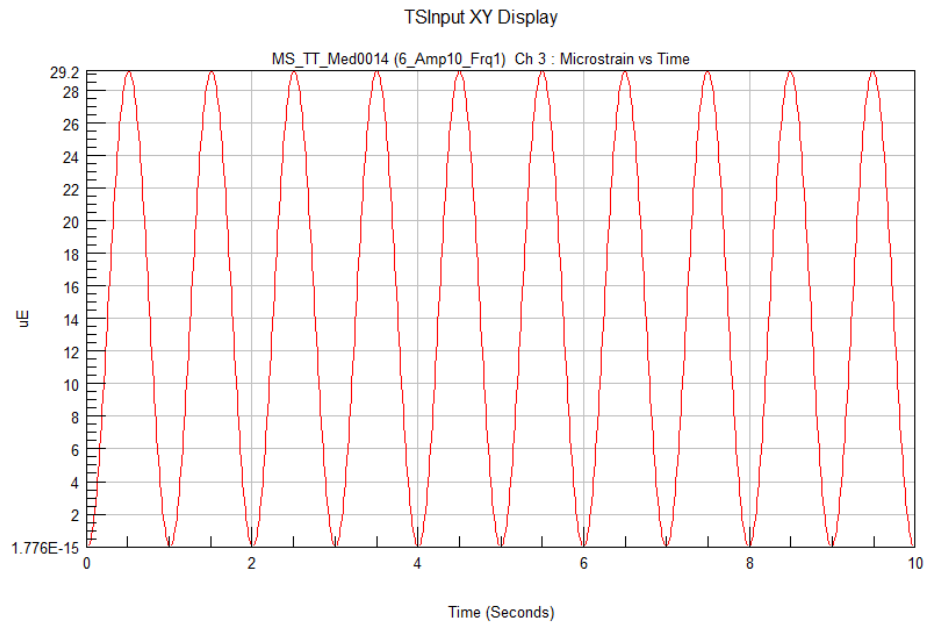


**Figure 4.17:** Damage Contour for Dynamic Failure Analysis for Compression-Tension Case at 3 Hz.

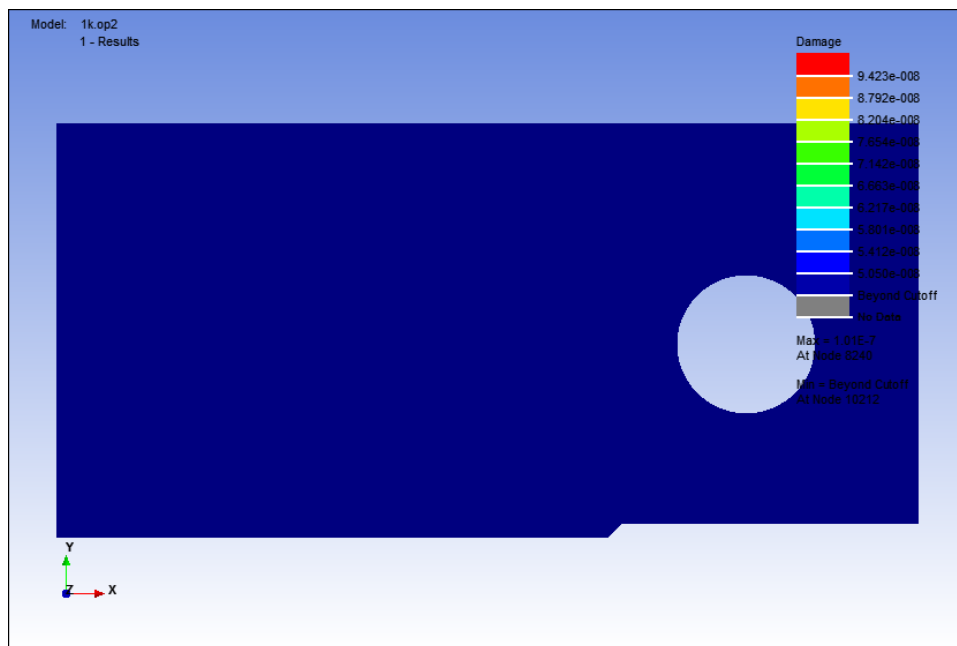


**Figure 4.18:** Damage contour at notch point for dynamic failure analysis at for compression-tension case at 3 Hz.

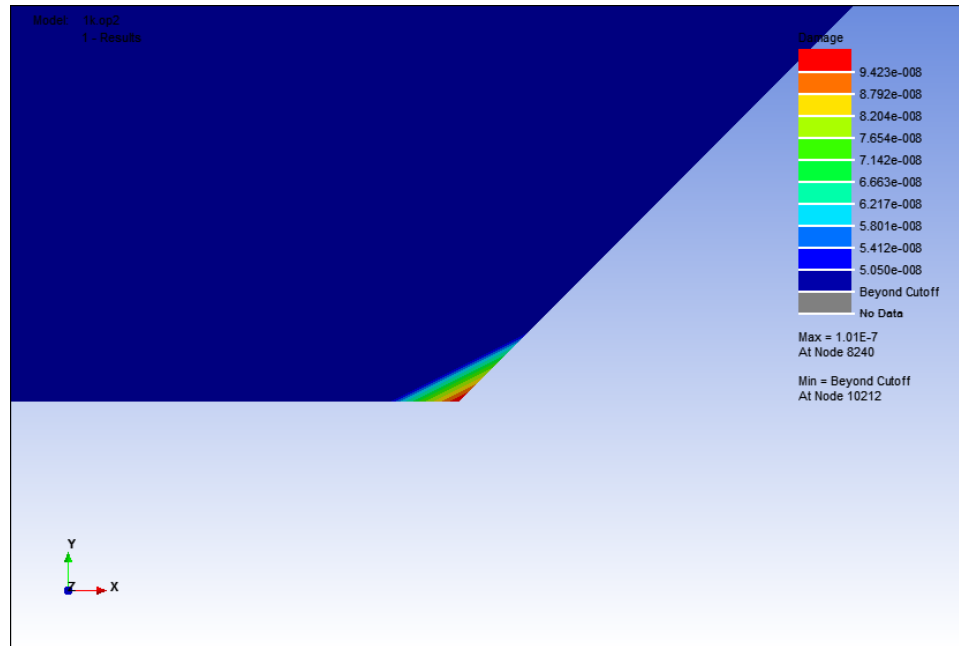
The damage value that obtained from the analysis at 3 Hz shows that the value has returned to the value of  $9.588 \times 10^{-8}$  as shown in Figure 4.17 and Figure 4.18. In this analysis, the microstrain range value was still same as in 1 Hz and 2 Hz analysis. The change of frequency of 3 Hz as shown in Figure 4.16 did not make the damage value become higher but it has returned to the same value as the analysis at 1 Hz instead.



**Figure 4.19:** Microstrain value for dynamic failure analysis for tension-tension case at 1 Hz.

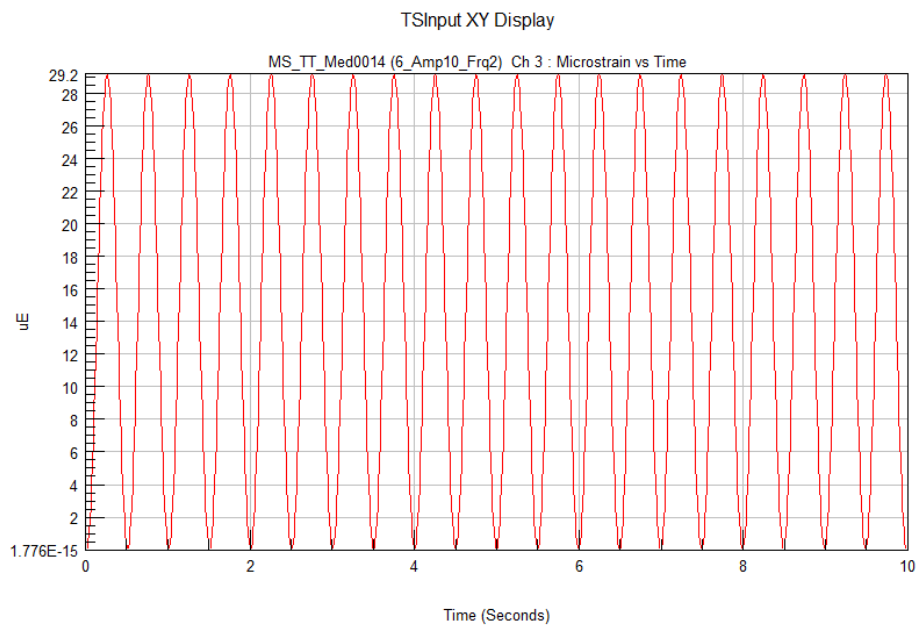


**Figure 4.20:** Damage contour for dynamic failure analysis for tension-tension case at 1 Hz.

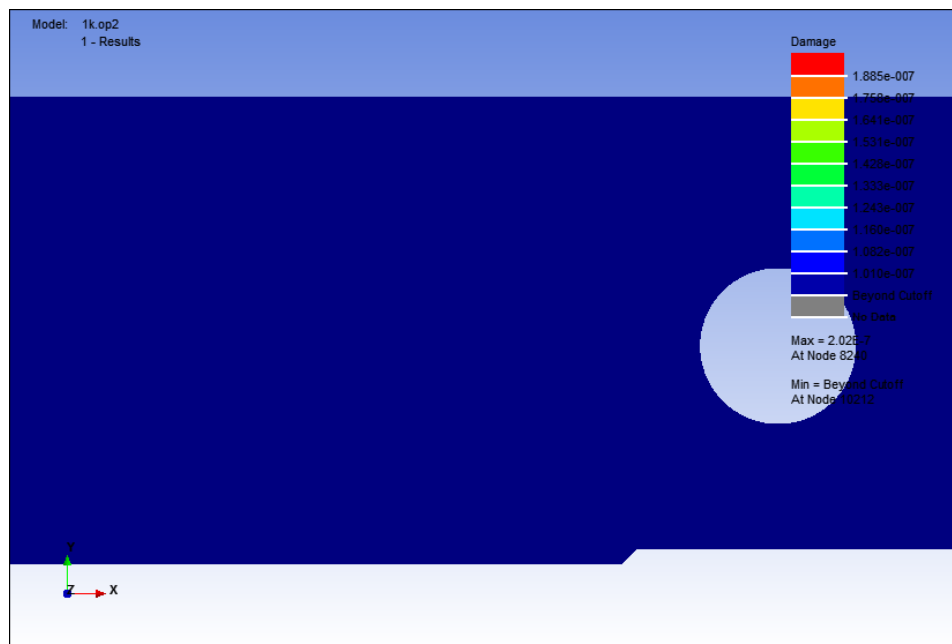


**Figure 4.21:** Damage contour at notch point for dynamic failure analysis at for tension-tension case at 1 Hz.

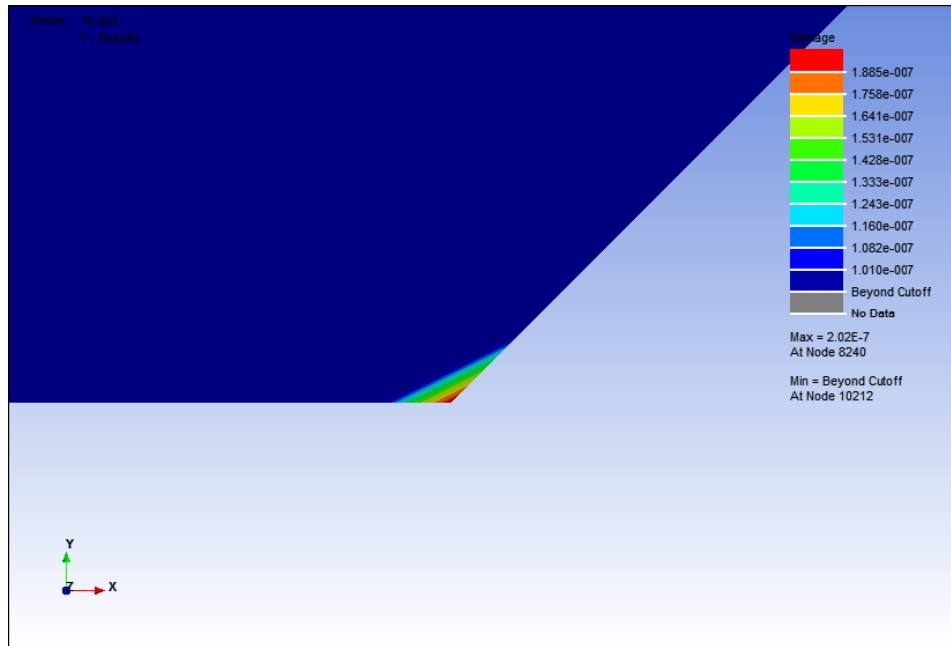
In the tension-tension loading case, the microstrain value that initiated the fatigue failure was  $29.2 \mu\epsilon$ . The effect of the microstrain value at 1 Hz as shown in Figure 4.19 obtained the damage value of  $9.423 \times 10^{-8}$  and the fatigue failure that occurs was still very small as same as the other loading cases for dynamic failure analysis, as shown in Figure 4.20. Figure 4.21 shows the critical notch area which the fatigue failure has started.



**Figure 4.22:** Microstrain value for dynamic failure analysis for tension-tension case at 2 Hz.

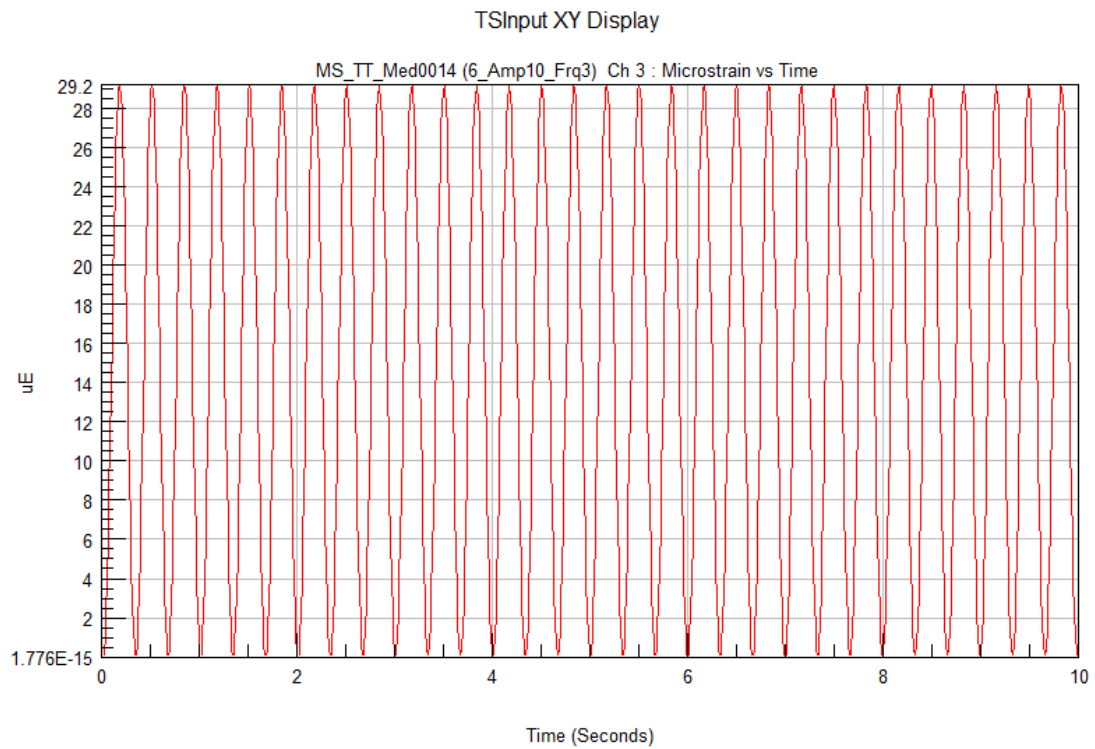


**Figure 4.23:** Damage contour for dynamic failure analysis for tension-tension case at 2 Hz.

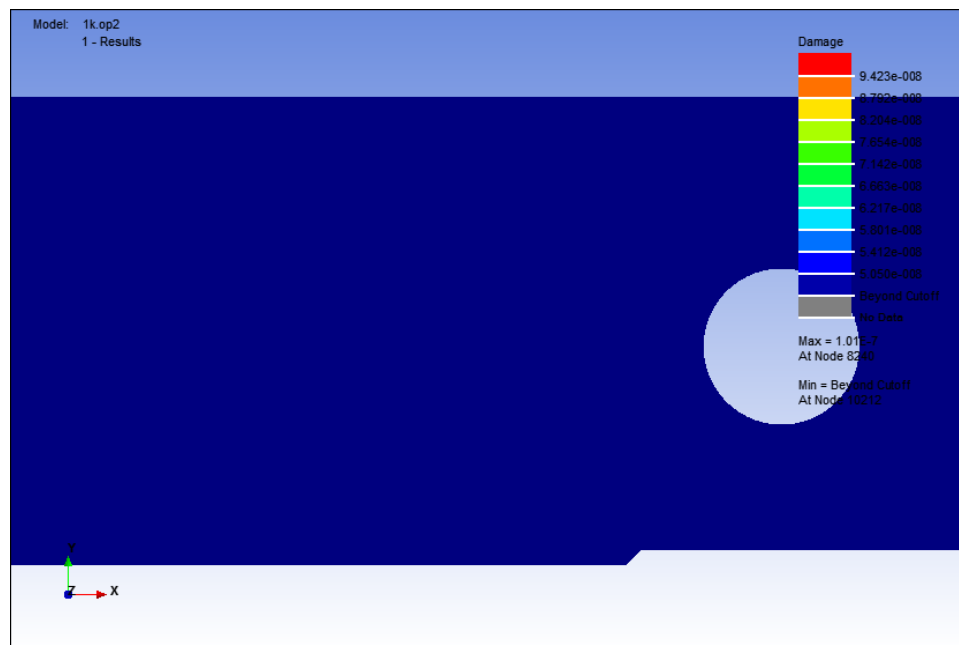


**Figure 4.24:** Damage contour at notch point for dynamic failure analysis at for tension-tension case at 2 Hz.

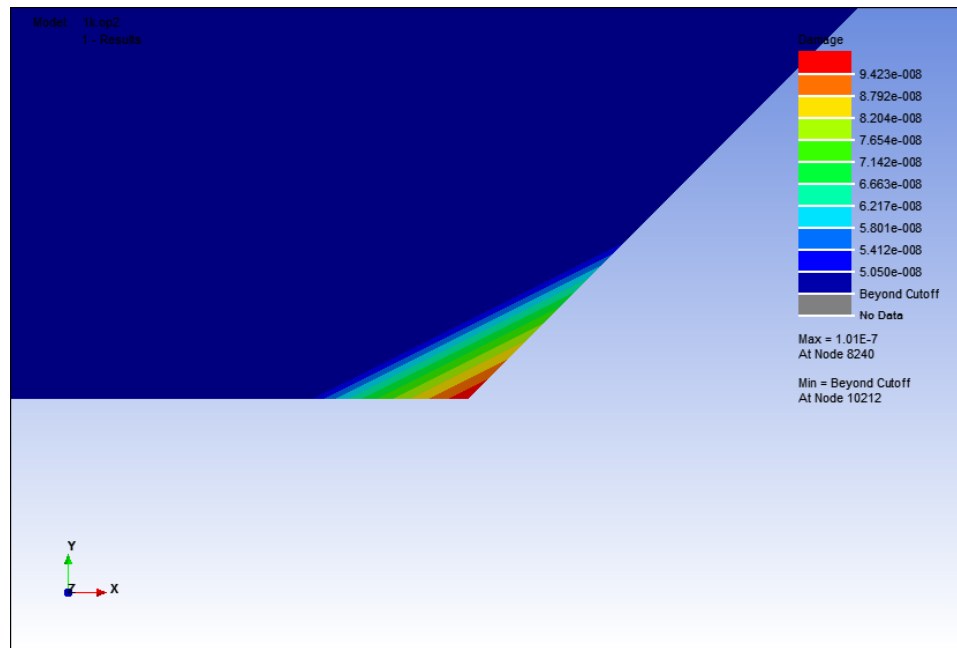
At 2 Hz with the same microstrain value as shown in figure 4.22, the damage value that obtained was  $1.885 \times 10^{-7}$  which is higher than the damage value at 1 Hz. Figure 4.23 shows that the fatigue failure that occur on the model was still small and Figure 4.24 shows the fatigue failure that initiate at the critical notch point of the model.



**Figure 4.25:** Microstrain value for dynamic failure analysis for tension-tension case at 3 Hz.



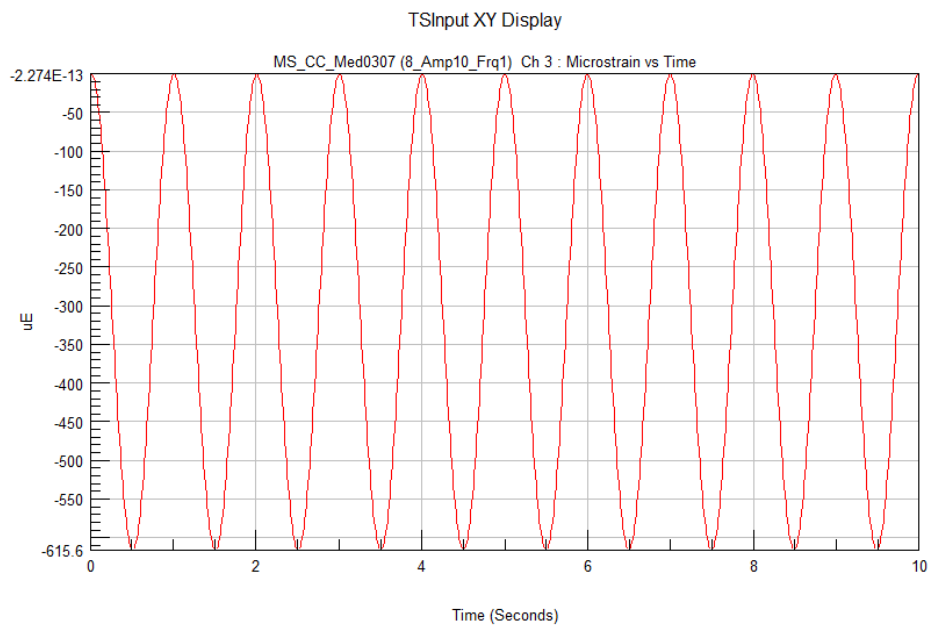
**Figure 4.26:** Damage contour for dynamic failure analysis for tension-tension case at 3 Hz.



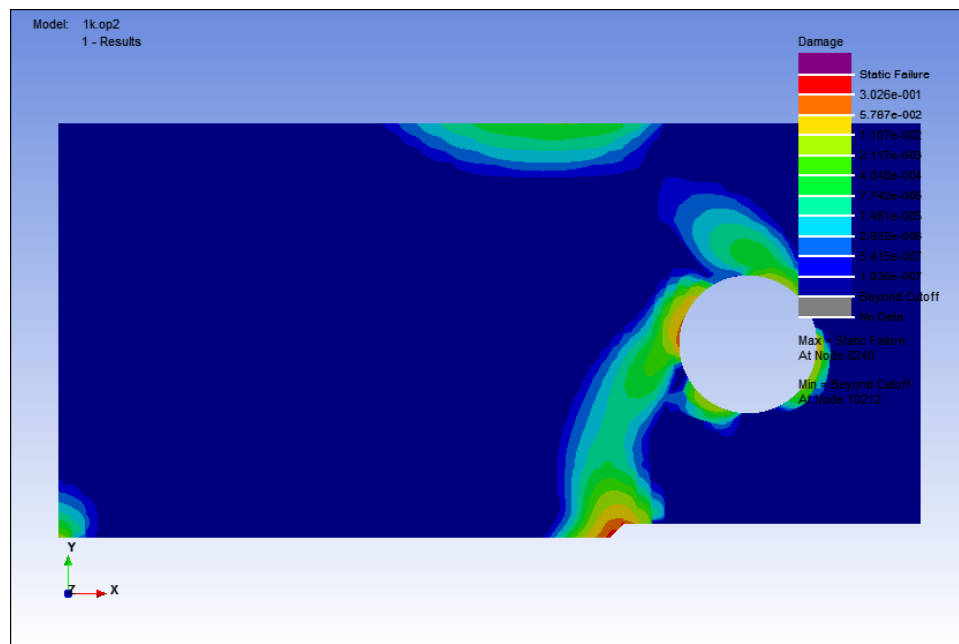
**Figure 4.27:** Damage contour at notch point for dynamic failure analysis at for tension-tension case at 3 Hz.

The damage value that obtained for the microstrain of  $29.2 \mu\epsilon$  at frequency of 3 Hz as shown in Figure 4.25 was  $9.423 \times 10^{-8}$ . The result shows that the damage value was returned to the same value as at 1 Hz. Still, the fatigue failure that occurs was still very small at the critical notch point of the model as shown in Figure 4.26 and Figure 4.27.

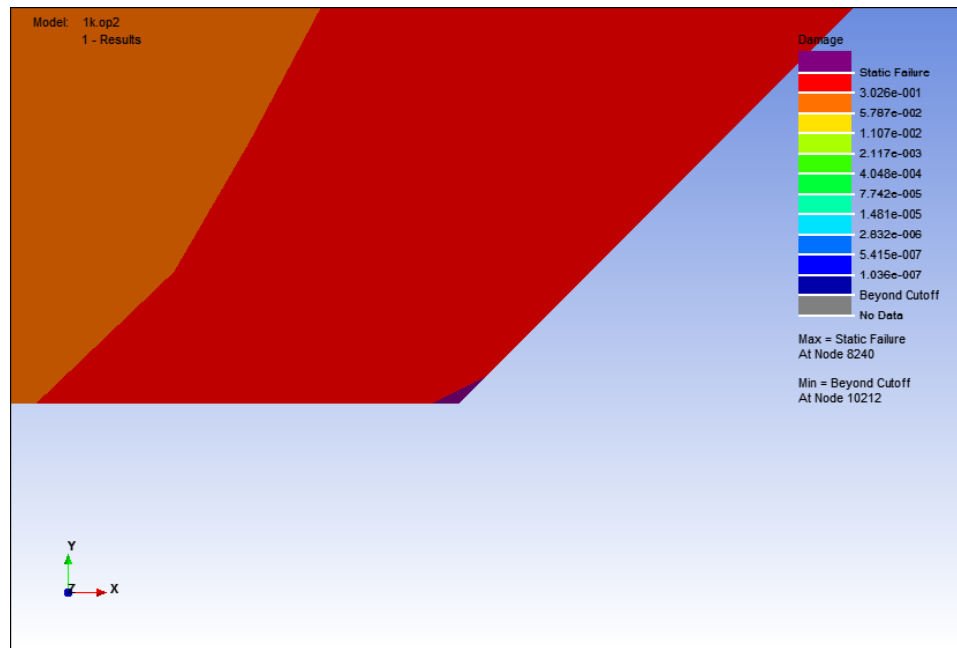




**Figure 4.28:** Microstrain value for static failure analysis for compression-compression case at 1 Hz.

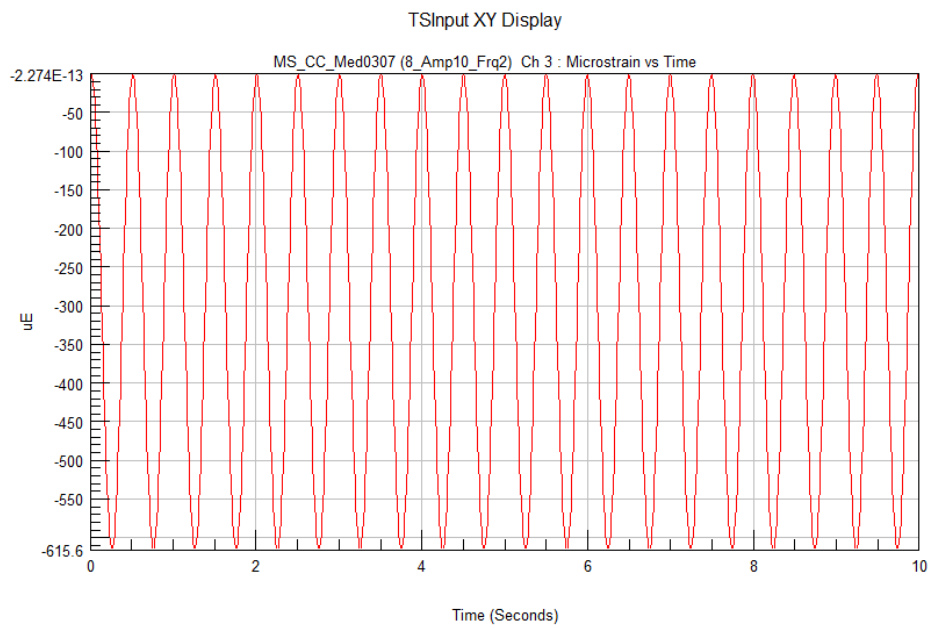


**Figure 4.29:** Damage contour for static failure analysis for compression-compression case at 1 Hz.

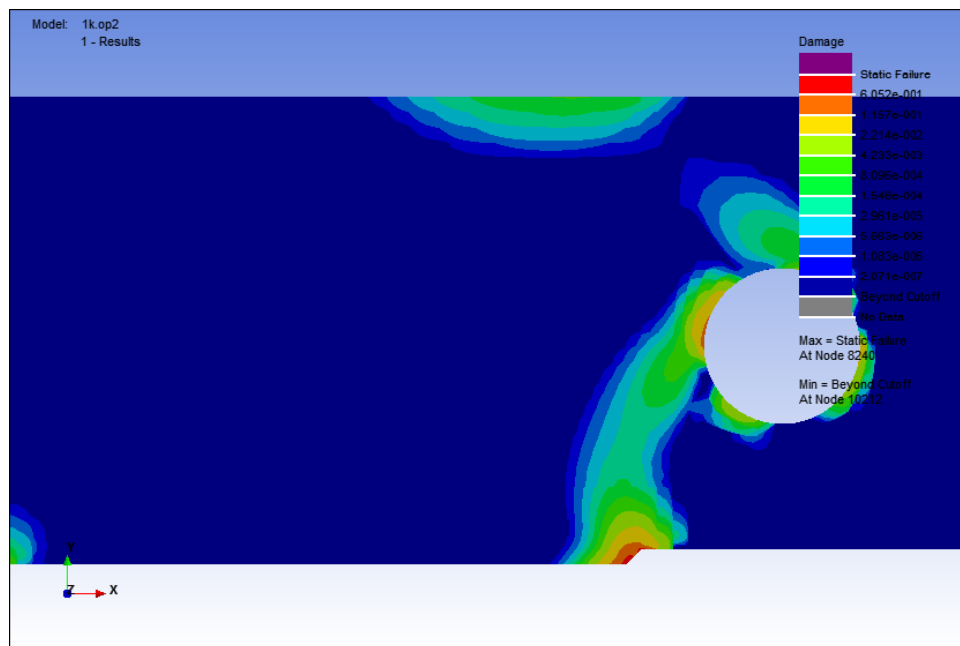


**Figure 4.30:** Damage contour at notch point for static failure analysis at for compression-compression case at 1 Hz.

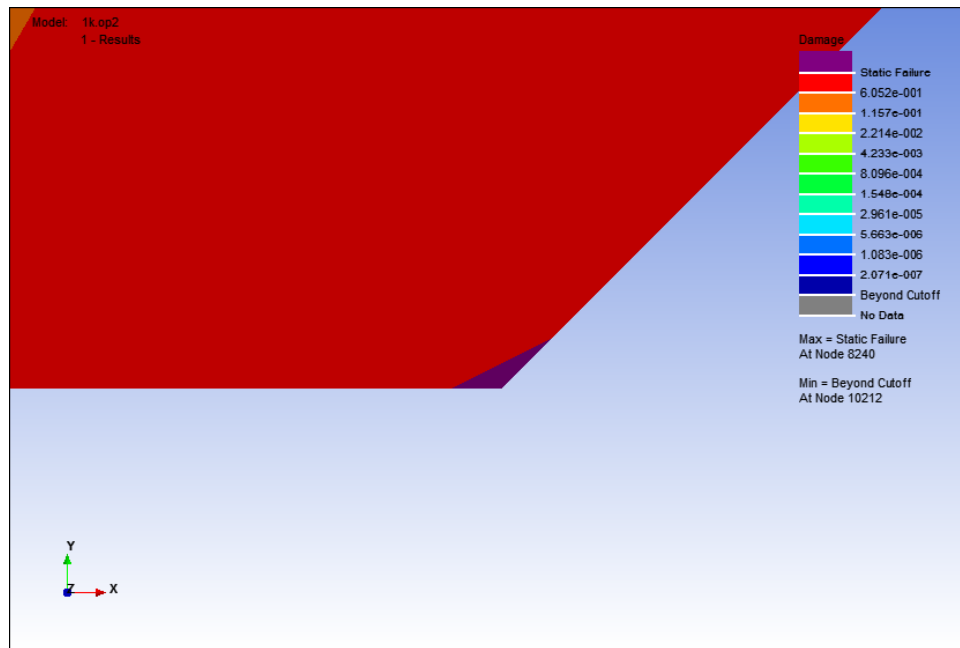
Figure 4.28 shows that the value of the microstrain that fail the model for compression-compression loading case for static failure analysis at 1 Hz. At  $615.6 \mu\epsilon$ , the static failure started and the damage value obtained was  $3.026 \times 10^{-1}$ . The damage area that occurs on the model is huge, as shown in figure 4.29. However Figure 4.30 shows the affected area where the static failure started at the notch point of the model.



**Figure 4.31:** Microstrain value for static failure analysis for compression-compression case at 2 Hz.

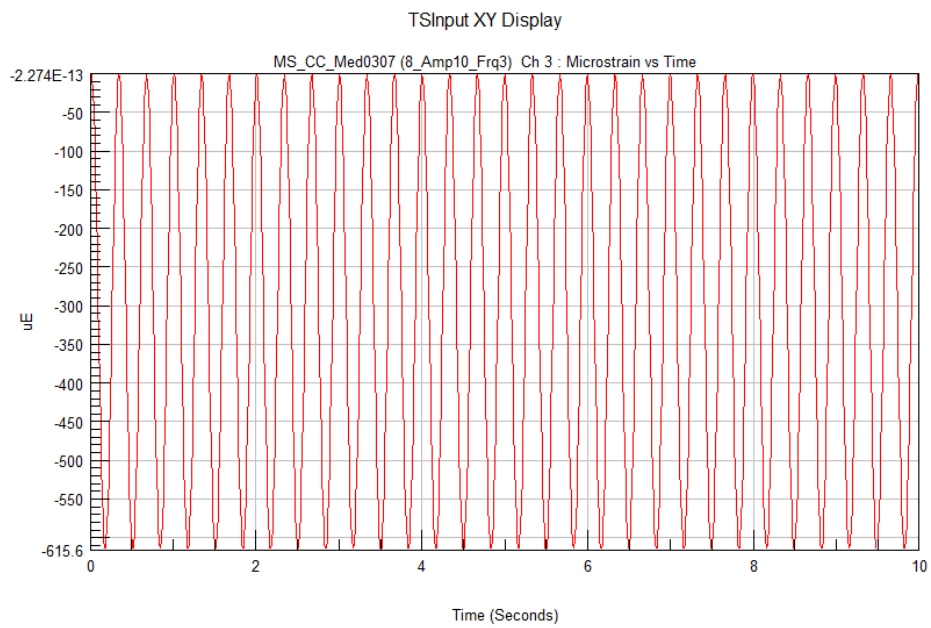


**Figure 4.32:** Damage contour for static failure analysis for compression-compression case at 2 Hz.

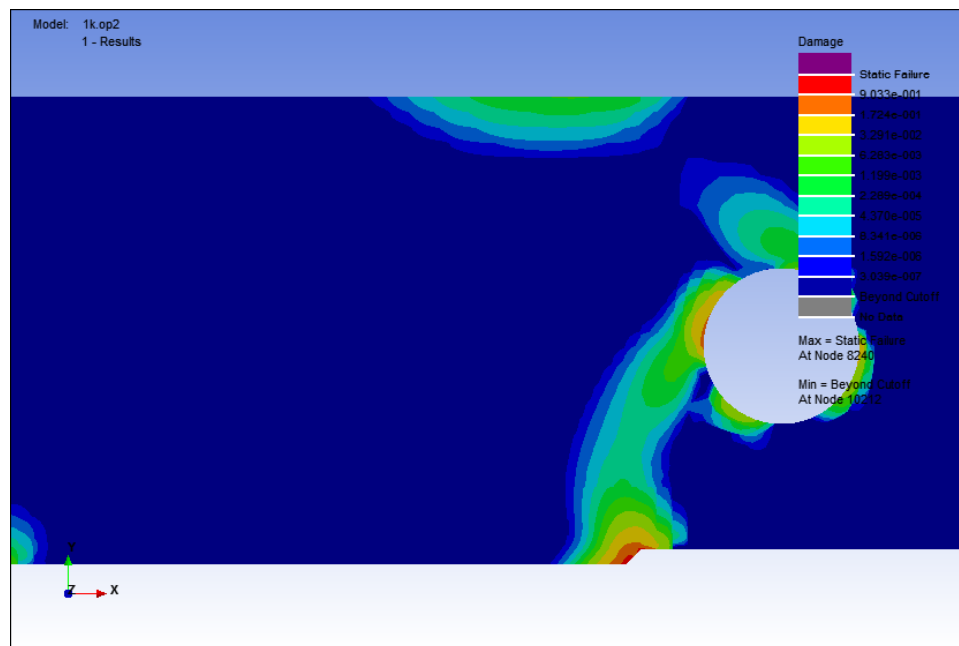


**Figure 4.33:** Damage contour at notch point for static failure analysis at for compression-compression case at 2 Hz.

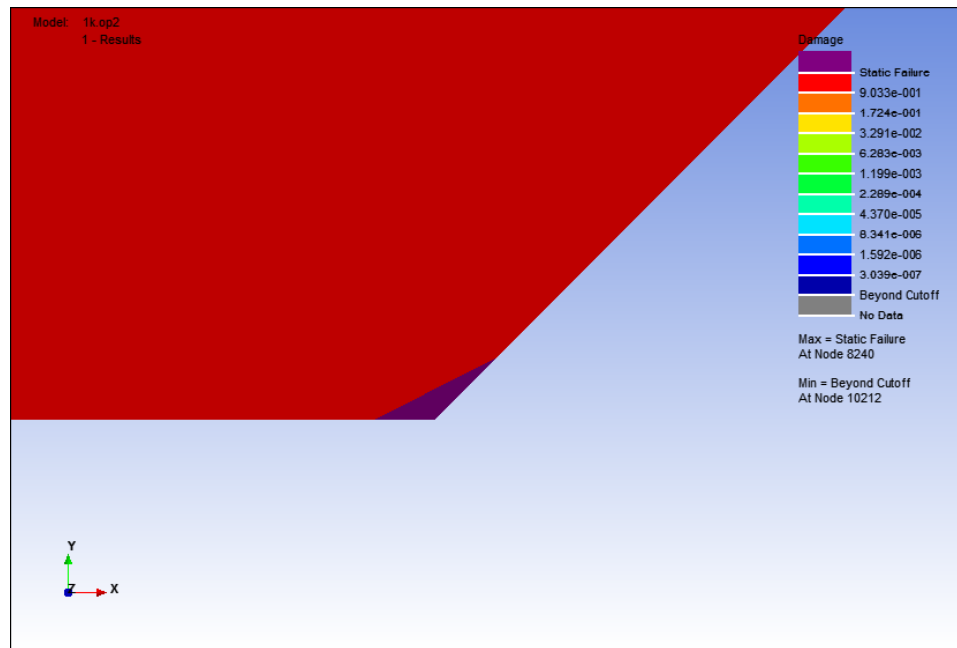
Using the same microstrain value with the cyclic frequency of 2 Hz as shown in Figure 4.31, the damage value that obtained was  $6.052 \times 10^{-1}$ . As same as the previous result, the damage area that occurs on the model was huge, as shown in Figure 4.32. However, the damage value that obtained was different as it gets higher. Figure 4.33 shows the notch point of the model, which is the critical point of the static failure has occur.



**Figure 4.34:** Microstrain value for static failure analysis for compression-compression case at 3 Hz.

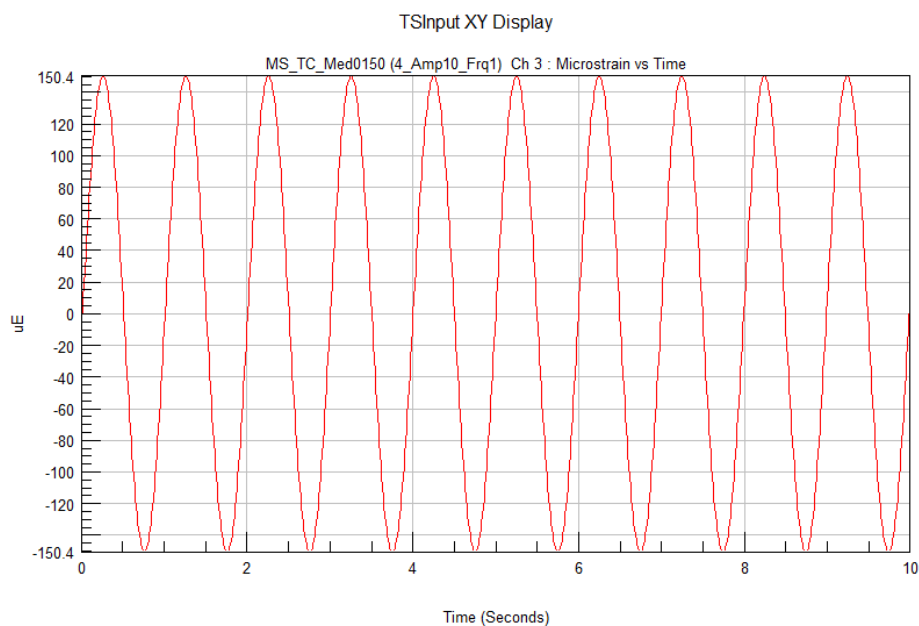


**Figure 4.35:** Damage contour for static failure analysis for compression-compression case at 3 Hz.

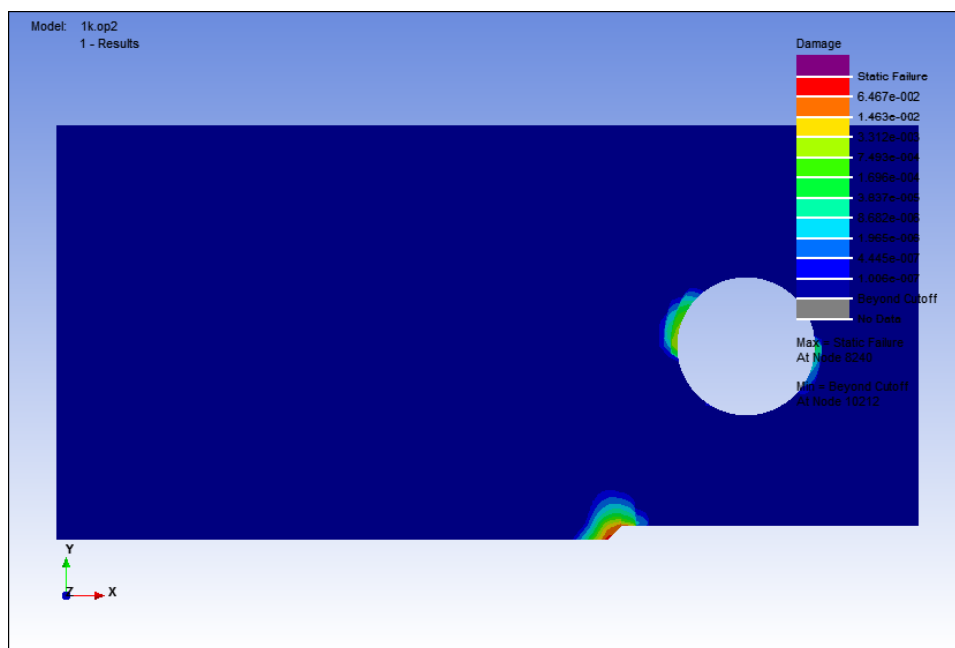


**Figure 4.36:** Damage contour at notch point for static failure analysis at for compression-compression case at 3 Hz.

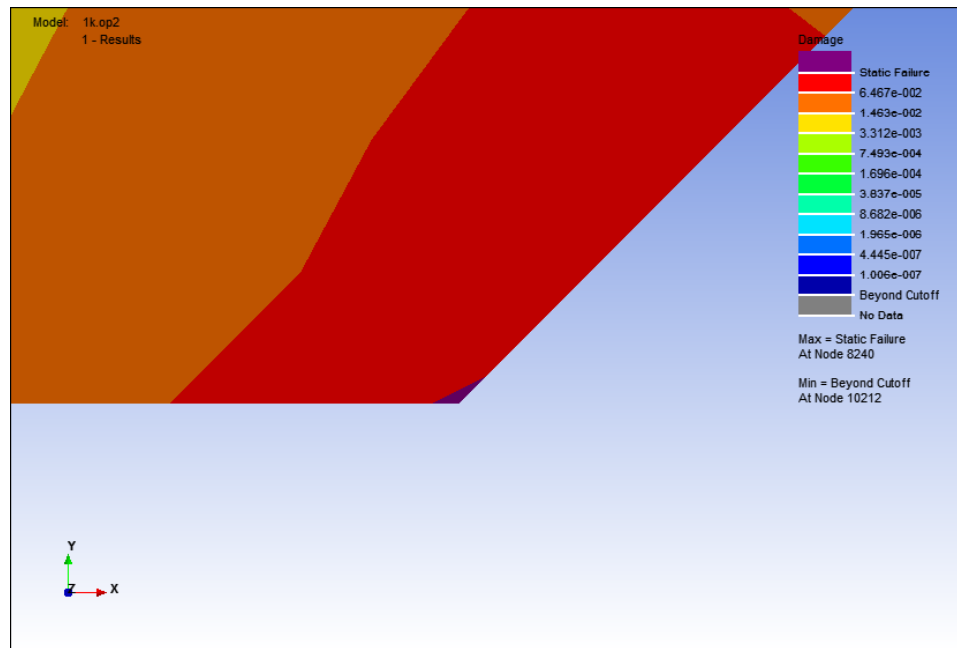
At 3 Hz, with the same value of microstrain at  $615.6 \mu\epsilon$  as shown in Figure 4.34; the damage that obtained was  $9.033 \times 10^{-1}$ . The damage area that occurs was still huge as shown in Figure 4.35 and Figure 4.36 shows the notch area of the model which the static failure has occurs. The damage value that obtained shows that it has increased higher than the damage value of the microstrain frequency at 1 Hz and 2 Hz.



**Figure 4.37:** Microstrain value for static failure analysis for compression-tension case at 1 Hz.



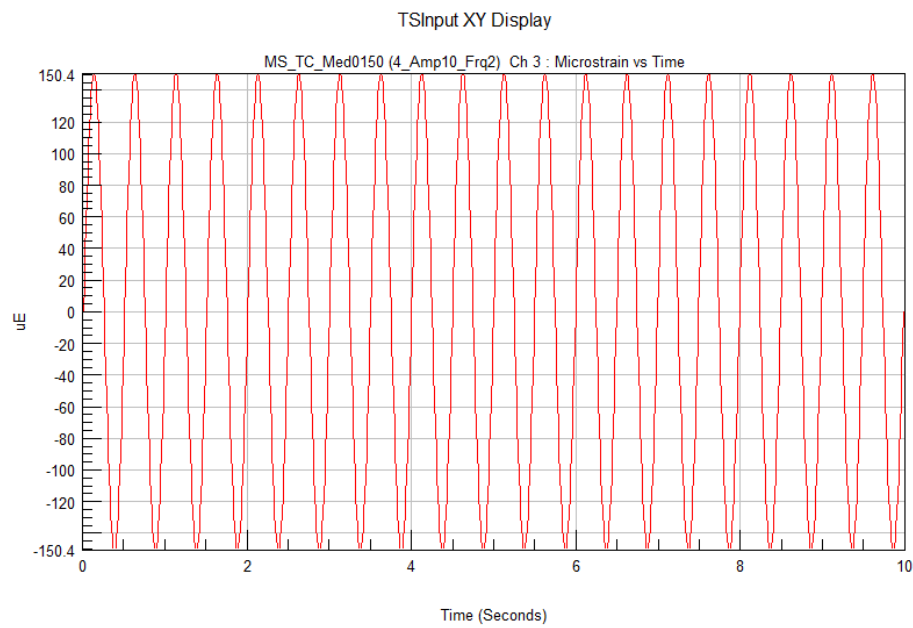
**Figure 4.38:** Damage Contour for static failure analysis for compression-tension case at 1 Hz.



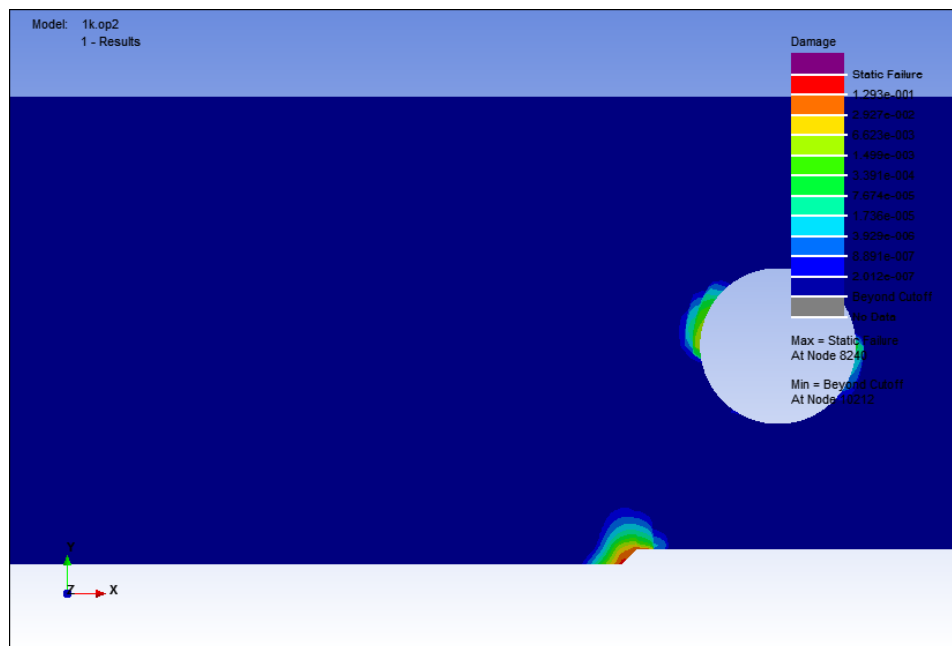
**Figure 4.39:** Damage contour at notch point for static failure analysis at for compression-tension case at 1 Hz.

Figure 4.37 shows that the value of the microstrain that initiate the failure for compression-tension loading case for static failure analysis at 1 Hz. At microstrain range of  $300.8 \mu\epsilon$ , the fatigue failure initiated and the damage value obtained was  $6.467 \times 10^{-2}$ . The damage area that on the model is small but can visible in the FEA result, as shown in figure 4.11. Figure 4.12 shows the affected area where the static failure occurs at the notch point of the model.





**Figure 4.40:** Microstrain value for static failure analysis for compression-tension case at 2 Hz.



**Figure 4.41:** Damage contour for static failure analysis for compression-tension case at 2 Hz.

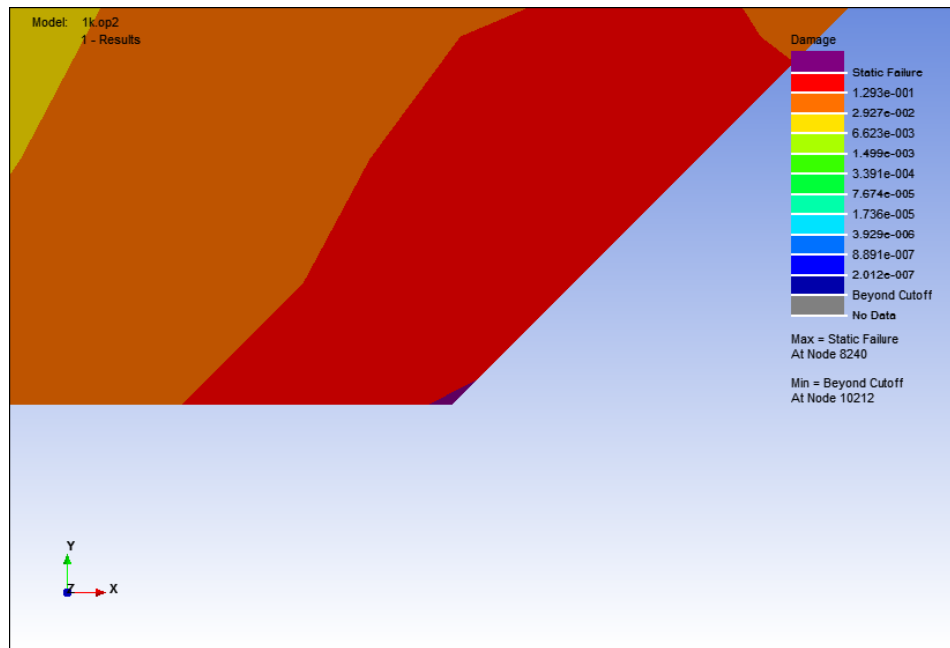


**Figure 4.42:** Damage contour at notch point for static failure analysis at for compression-tension case at 2 Hz.

At 2 Hz, the damage value that obtained was  $1.293 \times 10^{-1}$  and the damage area that was small, as shown in Figure 4.41 and Figure 4.42. Using the same microstrain value as the analysis at 1 Hz with the different frequency of 2 Hz as shown in Figure 4.40, the damage value get bigger than the previous analysis.

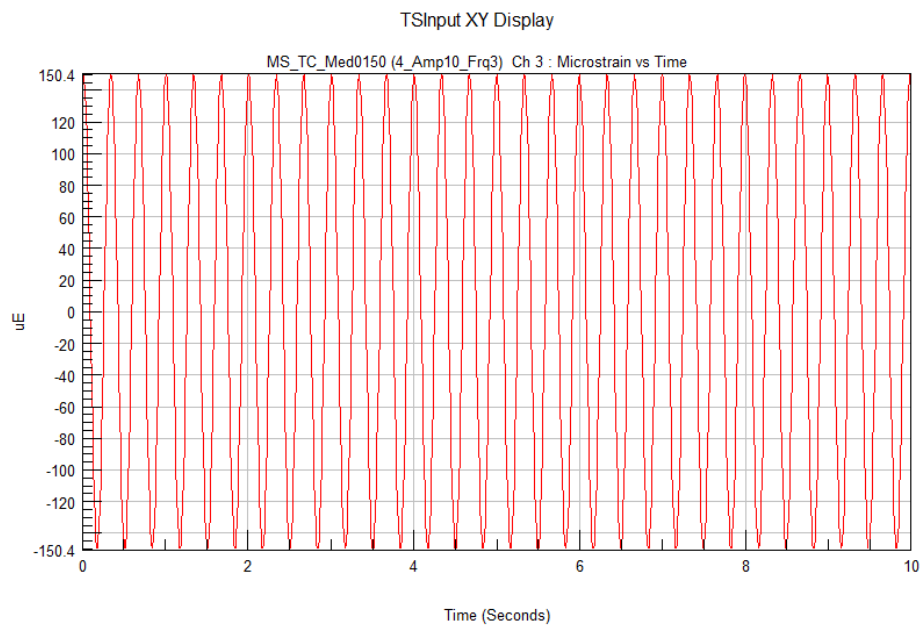


**Figure 4.43:** Microstrain value for static failure analysis for compression-tension case at 3 Hz.

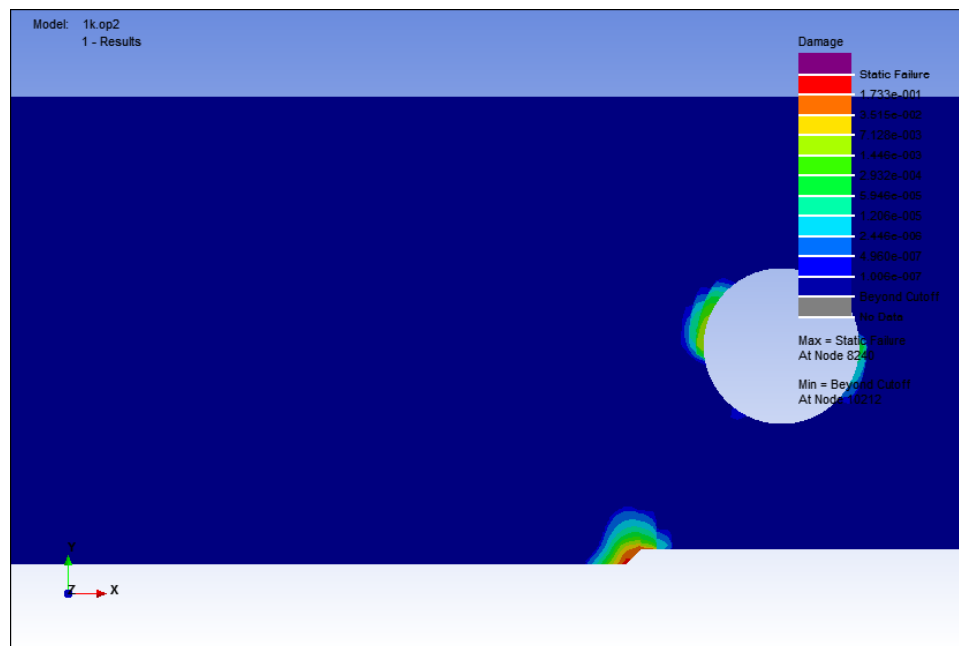


**Figure 4.44:** Damage contour for static failure analysis for compression-tension case at 3 Hz.

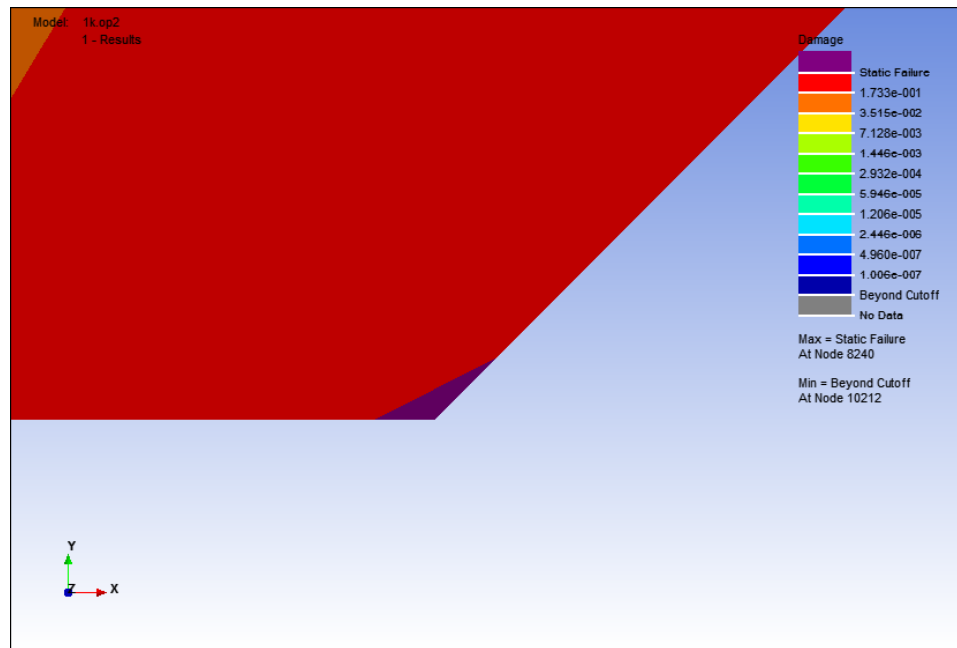


**Figure 4.45:** Damage contour at notch point for static failure analysis at for compression-tension case at 3 Hz.

The damage value that obtained from the analysis at 3 Hz shows that the damage value was  $1.733 \times 10^{-1}$  as shown in Figure 4.44 and Figure 4.15. In this analysis, the microstrain range value was still same as in 1 Hz and 2 Hz analysis. The change of frequency of 3 Hz as shown in Figure 4.43 has increased higher than the results at 1 Hz and 2 Hz.

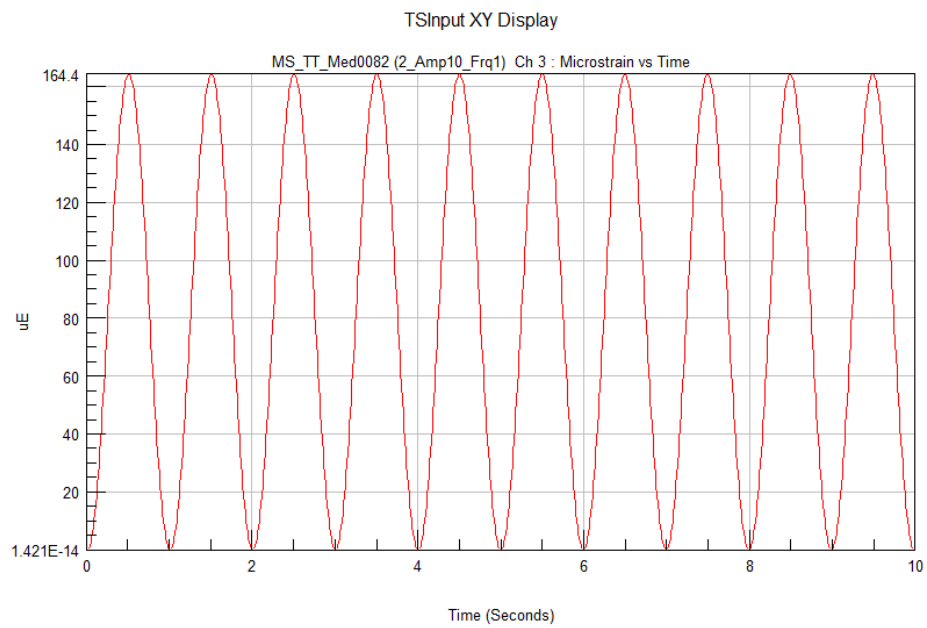


**Figure 4.46:** Microstrain value for static failure analysis for tension-tension case at 1 Hz.

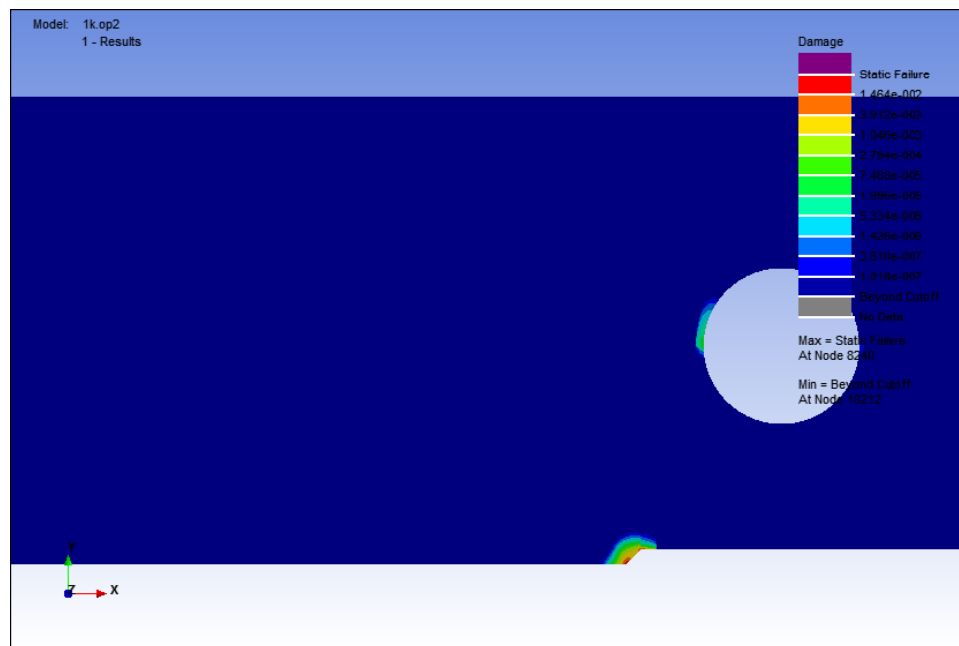


**Figure 4.47:** Damage Contour for static failure analysis for tension-tension case at 1 Hz.

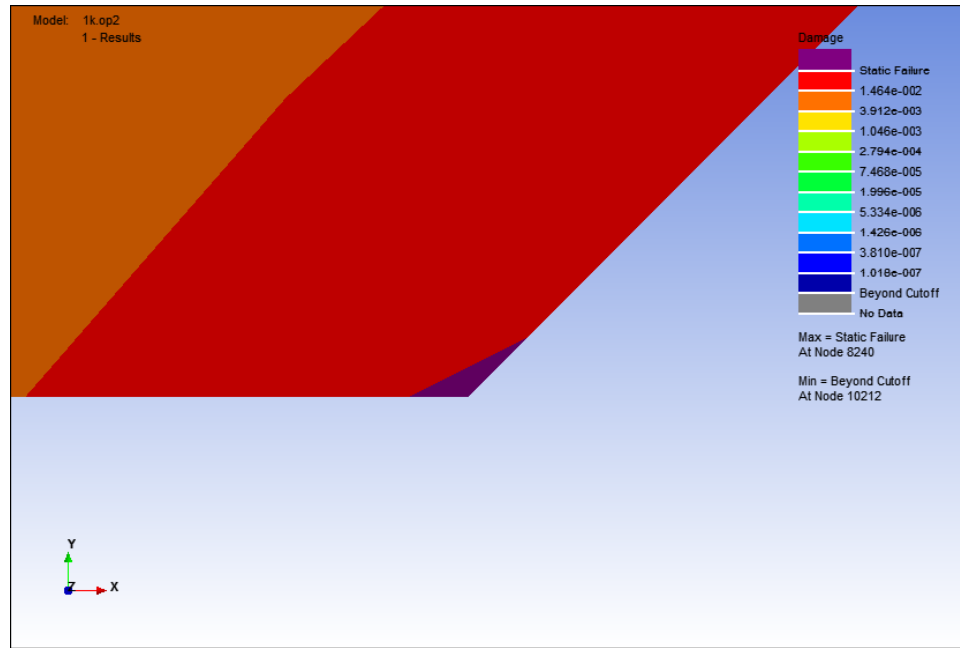


**Figure 4.48:** Damage contour at notch point for static failure analysis at for tension-tension case at 1 Hz.

In the tension-tension loading case, the microstrain value that initiated the fatigue failure was  $164.4 \mu\epsilon$ . The effect of the microstrain value at 1 Hz as shown in Figure 4.46 obtained the damage value of  $1.464 \times 10^{-2}$  and the damage area was smaller than the tension-tension loading case, as shown in Figure 4.20. Figure 4.21 shows the critical notch area which the static failure has started.

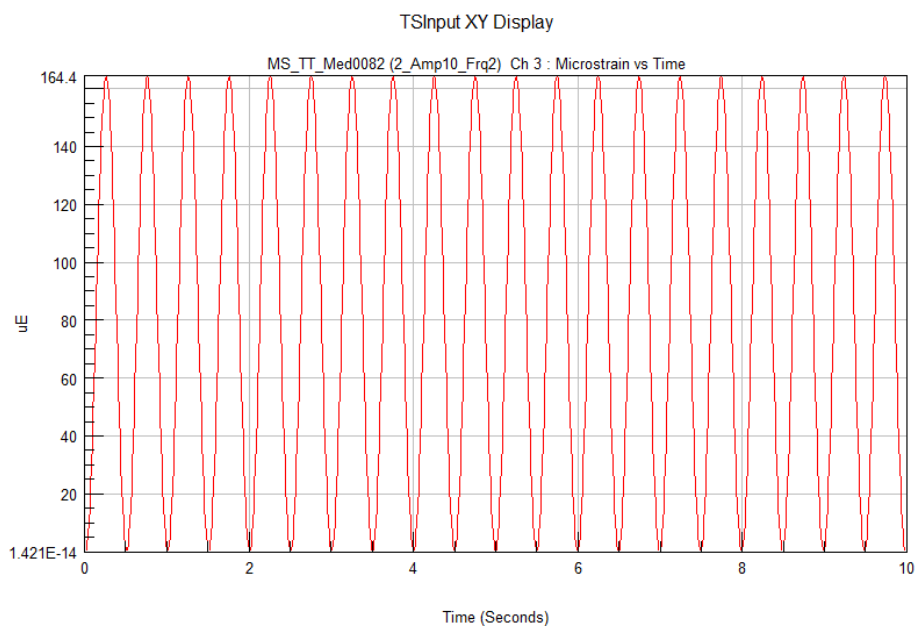


**Figure 4.49:** Microstrain value for static failure analysis for tension-tension case at 2 Hz.

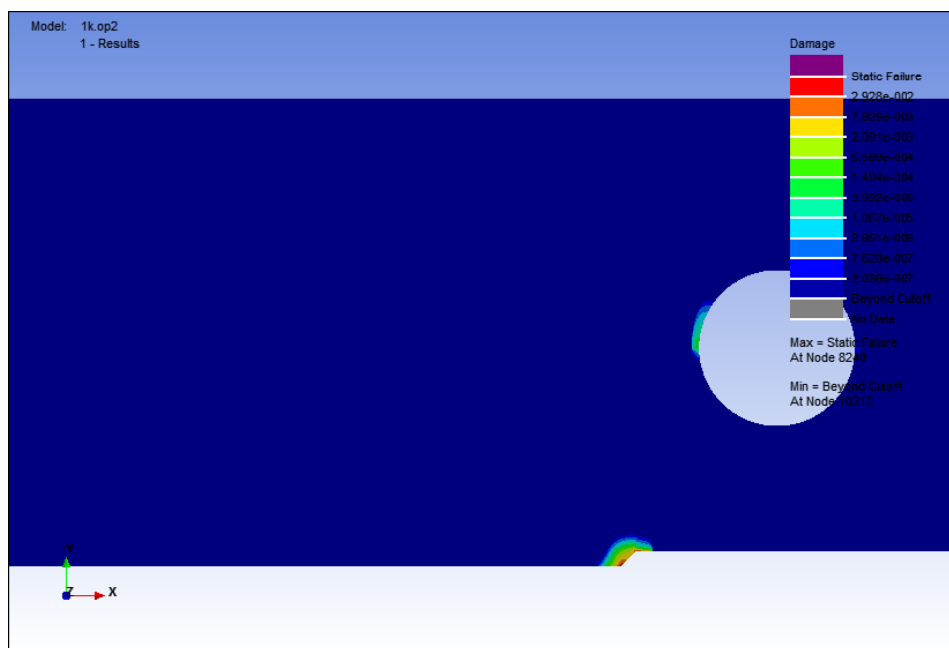


**Figure 4.50:** Damage contour for static failure analysis for tension-tension case at 2 Hz.

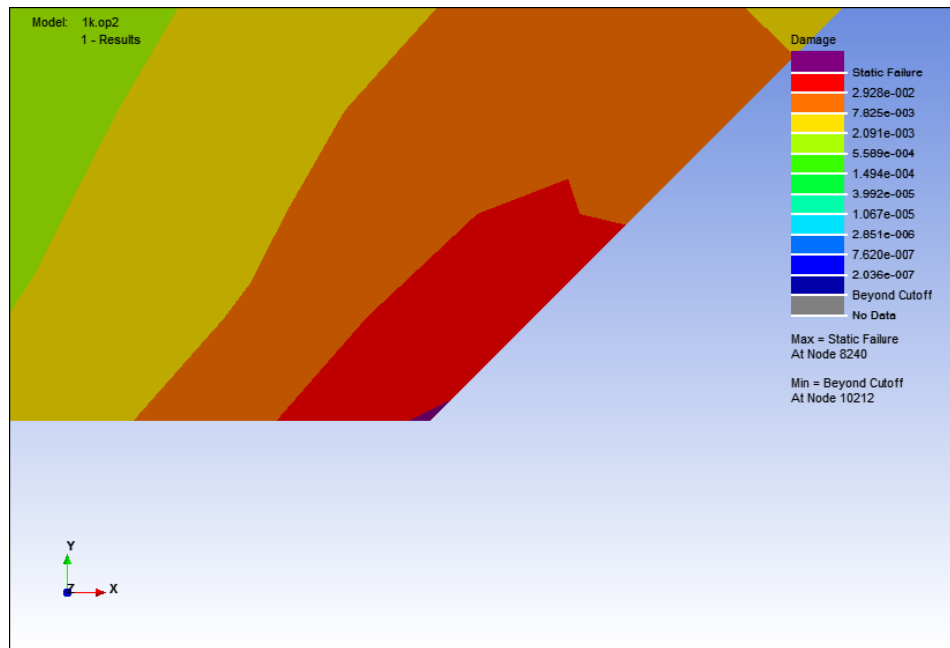


**Figure 4.51:** Damage contour at notch point for static failure analysis at for tension-tension case at 2 Hz.

At 2 Hz with the same microstrain value, as shown in figure 4.49, the damage value that obtained was  $2.926 \times 10^{-2}$  which is higher than the damage value at 1 Hz. Figure 4.50 shows that the damage area that occur on the model was still small and Figure 4.51 shows the static failure that initiate at the critical notch point of the model.



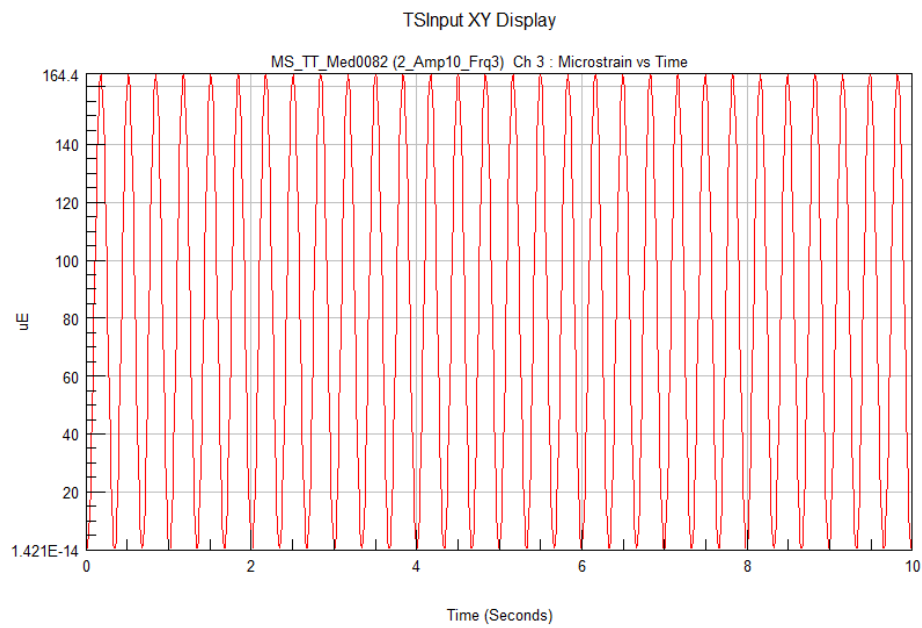


**Figure 4.52:** Microstrain value for static failure analysis for tension-tension case at 3 Hz.

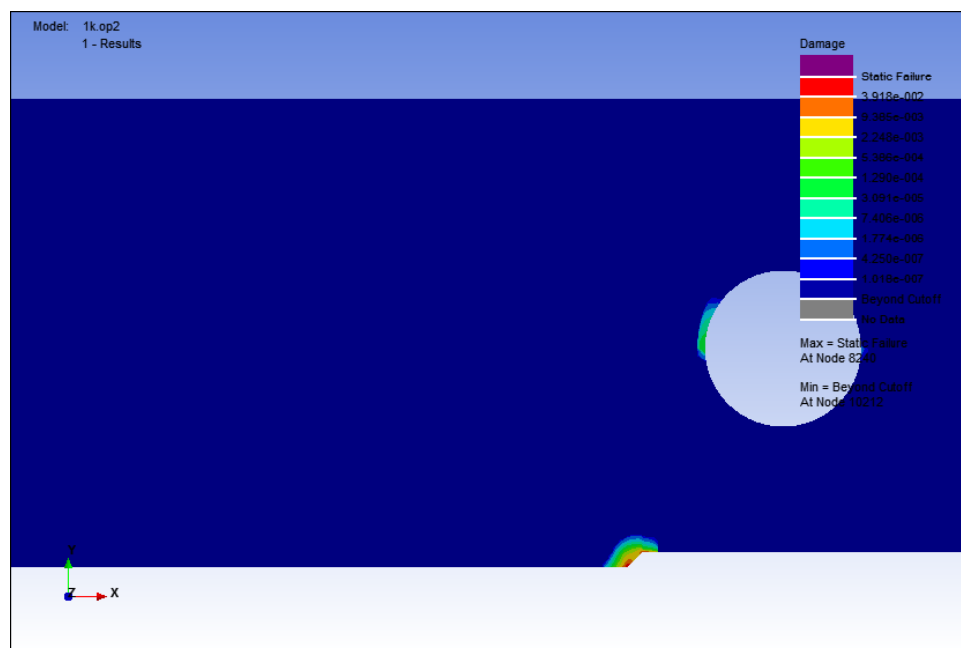


**Figure 4.53:** Damage contour for static failure analysis for tension-tension case at 3 Hz.

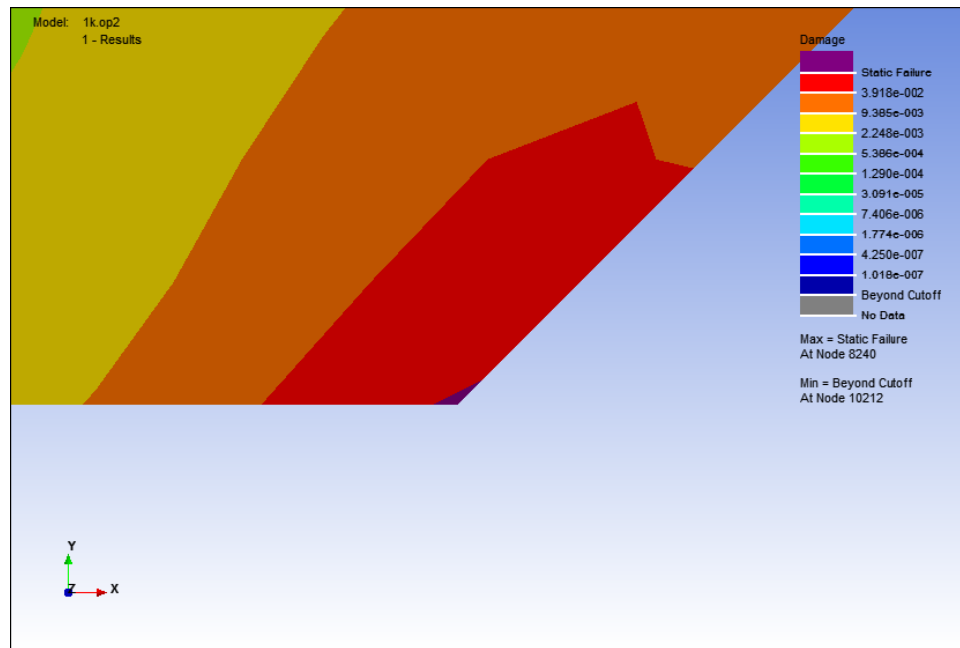


**Figure 4.54:** Damage contour at notch point for static failure analysis at for tension-tension case at 3 Hz.

The damage value that obtained for the microstrain of  $164.4 \mu\epsilon$  at frequency of 3 Hz as shown in Figure 4.52 was  $3.918 \times 10^{-2}$ . The result shows that the damage value was increased. Still, the damage area that occurs was small but visible in the FEA result is shown in Figure 4.53. The critical notch point of the model is shown in Figure 4.54.

From the results shown in the Figure 4.1 – 4.54, the results of the analysis for every case on dynamic and static failure are different where the compression-compression case has resulted the greatest damage contour area compared to the other cases, while the tension-tension resulted the smallest damage contour area. The value of the microstrain and the damage for the initial static and dynamic failures that obtained from the analysis results are shown in the Table 4.2.

**Table 4.2:** Dynamic failure initiation microstrain and damage value.

| Case                    | Frequency, $f$ | Microstrain, $\varepsilon$ |             |            | Damage                 |
|-------------------------|----------------|----------------------------|-------------|------------|------------------------|
|                         |                | Minimum                    | Median      | Maximum    |                        |
| Compression-Compression | 1 Hz           | - 48.2 $\mu$               | -24.1 $\mu$ | 0          | $9.257 \times 10^{-8}$ |
|                         | 2 Hz           | - 48.2 $\mu$               | -24.1 $\mu$ | 0          | $1.905 \times 10^{-7}$ |
|                         | 3 Hz           | - 48.2 $\mu$               | -24.1 $\mu$ | 0          | $9.257 \times 10^{-8}$ |
| Compression-Tension     | 1 Hz           | - 19.2 $\mu$               | 0           | 19.2 $\mu$ | $9.588 \times 10^{-8}$ |
|                         | 2 Hz           | - 19.2 $\mu$               | 0           | 19.2 $\mu$ | $1.918 \times 10^{-7}$ |
|                         | 3 Hz           | - 19.2 $\mu$               | 0           | 19.2 $\mu$ | $9.588 \times 10^{-8}$ |
| Tension-Tension         | 1 Hz           | 0                          | 14.6 $\mu$  | 29.2 $\mu$ | $9.423 \times 10^{-8}$ |
|                         | 2 Hz           | 0                          | 14.6 $\mu$  | 29.2 $\mu$ | $1.885 \times 10^{-7}$ |
|                         | 3 Hz           | 0                          | 14.6 $\mu$  | 29.2 $\mu$ | $9.423 \times 10^{-8}$ |

The results shows that the dynamic failure is only occur when the maximum value of microstrain which applied on the specimen is at 48.2  $\mu\varepsilon$  for compression-compression case, 38.4  $\mu\varepsilon$  for compression-tension case and 29.2  $\mu\varepsilon$  for tension-tension case. There are no dynamic failure occur for microstrain values applied on the specimen less than the obtained values. Regarding to the value, the dynamic failure had resulted the starting amount of microstrain where the crack start to initiate at the notch of the specimen.

In the other hand, despite of varying the frequency of the microstrain effect on the specimen, the value only differ when  $f = 2$  Hz while the values of the damage while  $f = 1$  Hz and  $f = 3$  Hz are same. Therefore, these results show that the frequency difference did not affect the result of the damage value and the initiation of the crack on the analysis sample.

Along with the analysis, there are the static failures of the specimen, where in this point, the specimen at the notch point start to fail. With the same parameter used in the dynamic failure analysis, the values of microstrain are increased to determine the initial value where the static failure is starting to occur. The values of the microstrain and the damage of the specimen are shown in Table 4.3.

**Table 4.3:** Static failure initiation microstrain and damage value.

| Case                    | Frequency, $f$ | Microstrain, $\varepsilon$ |               |             | Damage                 |
|-------------------------|----------------|----------------------------|---------------|-------------|------------------------|
|                         |                | Minimum                    | Median        | Maximum     |                        |
| Compression-Compression | 1 Hz           | - 615.6 $\mu$              | - 307.8 $\mu$ | 0           | $3.026 \times 10^{-1}$ |
|                         | 2 Hz           | - 615.6 $\mu$              | - 307.8 $\mu$ | 0           | $6.052 \times 10^{-1}$ |
|                         | 3 Hz           | - 615.6 $\mu$              | - 307.8 $\mu$ | 0           | $9.033 \times 10^{-1}$ |
| Compression-Tension     | 1 Hz           | - 150.4 $\mu$              | 0             | 150.4 $\mu$ | $6.467 \times 10^{-2}$ |
|                         | 2 Hz           | - 150.4 $\mu$              | 0             | 150.4 $\mu$ | $1.293 \times 10^{-1}$ |
|                         | 3 Hz           | - 150.4 $\mu$              | 0             | 150.4 $\mu$ | $1.733 \times 10^{-1}$ |
| Tension-Tension         | 1 Hz           | 0                          | 82.2 $\mu$    | 164.4 $\mu$ | $1.464 \times 10^{-2}$ |
|                         | 2 Hz           | 0                          | 82.2 $\mu$    | 164.4 $\mu$ | $2.928 \times 10^{-2}$ |
|                         | 3 Hz           | 0                          | 82.2 $\mu$    | 164.4 $\mu$ | $3.918 \times 10^{-2}$ |

At the shown values for every case, they show that the static value started to occur when the microstrain value has reached 615.6  $\mu\varepsilon$  for compression-compression case, 300.8  $\mu\varepsilon$  for compression-tension case and 164.4  $\mu\varepsilon$  for tension-tension case. In this case, the higher value of the microstrain will affect the damage value of the static failure of the analysis sample at notch point.

For the different frequency analysis, there are effects of the microstrain frequency applied on the specimen and the damage results. Every case show that the damage value increased for higher microstrain frequency applied on the specimen. This shows that the microstrain frequency affected the static failure damage, while they did not give a large influence in dynamic failure. This phenomenon may occur because of the high value of the microstrain applied on the specimen, which also obviously high enough to influence the result of the static failure.

### 4.3 THE THEORETICAL FAILURE STRESS

From the value of the Young's Modulus of Elasticity,  $E$  of AISI 1045 steel; the theoretical failure stress value,  $\sigma$  on the initiation of the crack can be determined by multiplying the value of the microstrain,  $\varepsilon$  with Young's Modulus,  $E$  of AISI 1045 steel which is obtained from the Young's Modulus equation, as shown in Eqn. (4.1).

$$\sigma = E\varepsilon \quad (4.1)$$

The value of the microstrain is obtained from the value of the initial point of the dynamic and static failure from the analysis. Note that these theoretical failure stress values are the values of the stress that applied at the pinhole of the analysis specimen which lead to the failure of the analysis specimen.

The theoretical failure stresses for every case at dynamic failure are shown in Table 4.4 while the theoretical failure stresses for every case at static failure are shown in table 4.5.

**Table 4.4:** Theoretical failure stress at dynamic failure.

| Case                    | Theoretical failure stress, $\sigma$ |
|-------------------------|--------------------------------------|
| Compression-Compression | 4.941 MPa                            |
| Compression-Tension     | 3.936 MPa                            |
| Tension-Tension         | 2.993 MPa                            |

**Table 4.5:** Theoretical failure stress at static failure.

| Case                    | Theoretical failure stress, $\sigma$ |
|-------------------------|--------------------------------------|
| Compression-Compression | 63.099 MPa                           |
| Compression-Tension     | 30.832 MPa                           |
| Tension-Tension         | 16.851 MPa                           |

The obtained theoretical failure stress result at dynamic failure shows that the crack started to initiate when the load applied on the specimen are 4.941 MPa for compression-compression case, 3.936 MPa for compression-tension case and 2.993 MPa for tension-tension case.

Meanwhile the theoretical failure stress at static failure shows that the specimen begin to fail at the point of the specimen notch when the load applied on the specimen

are 63.099 MPa for compression-compression case, 30.832 MPa for compression-tension case and 16.851 MPa for tension-tension case.

The results are different by the cases because the effect of the analysis specimen dimension used for the analysis. As the failure started at the notch of the sample, the highest stress intensity occurs at the specimen notch. Due to the different cases of loading, the notch reached the weakest point at the lowest stress when experiencing the tension-tension loading while it reached the weakest point at the highest stress when experiencing the compression-compression loading.

#### 4.4 CRACK INITIATION LIFE

As suggested by Abdullah (Abdullah, *et. al*, 2011), crack initiation life can be obtained from the damage value that acquired from the analysis. From the results shown in Table 4.2 and Table 4.3, the crack initiation life for the dynamic analysis and the static analysis are determined by using Eqn. (2.2) as shown in the Table 4.6 and Table 4.7.

**Table 4.6:** Crack initiation life cycles for dynamic failure analysis.

| Case                    | Frequency, $f$ | Damage                 | Cycles, $N_f$      |
|-------------------------|----------------|------------------------|--------------------|
| Compression-Compression | 1 Hz           | $9.257 \times 10^{-8}$ | $1.08 \times 10^7$ |
|                         | 2 Hz           | $1.905 \times 10^{-7}$ | $5.25 \times 10^6$ |
|                         | 3 Hz           | $9.257 \times 10^{-8}$ | $1.08 \times 10^7$ |
| Compression-Tension     | 1 Hz           | $9.588 \times 10^{-8}$ | $1.04 \times 10^7$ |
|                         | 2 Hz           | $1.918 \times 10^{-7}$ | $5.21 \times 10^6$ |
|                         | 3 Hz           | $9.588 \times 10^{-8}$ | $1.04 \times 10^7$ |
| Tension-Tension         | 1 Hz           | $9.423 \times 10^{-8}$ | $1.06 \times 10^7$ |
|                         | 2 Hz           | $1.885 \times 10^{-7}$ | $5.31 \times 10^6$ |
|                         | 3 Hz           | $9.423 \times 10^{-8}$ | $1.06 \times 10^7$ |

**Table 4.7:** Crack initiation life cycles for static failure analysis.

| Case                        | Frequency, $f$ | Damage                 | Cycles, $N_f$ |
|-----------------------------|----------------|------------------------|---------------|
| Compression-<br>Compression | 1 Hz           | $3.026 \times 10^{-1}$ | 3.31          |
|                             | 2 Hz           | $6.052 \times 10^{-1}$ | 1.65          |
|                             | 3 Hz           | $9.033 \times 10^{-1}$ | 1.11          |
| Compression-<br>Tension     | 1 Hz           | $6.467 \times 10^{-2}$ | 15.46         |
|                             | 2 Hz           | $1.293 \times 10^{-1}$ | 7.73          |
|                             | 3 Hz           | $1.733 \times 10^{-1}$ | 5.77          |
| Tension-<br>Tension         | 1 Hz           | $1.464 \times 10^{-2}$ | 68.31         |
|                             | 2 Hz           | $2.928 \times 10^{-2}$ | 34.15         |
|                             | 3 Hz           | $3.918 \times 10^{-2}$ | 25.52         |

The results shows that the crack initiation life for compression-compression case is the longest compared to the others two cases for dynamic failure analysis. However, both three cases gave results that they only fail when the numbers of cycles are higher than  $5.2 \times 10^6$  cycles. These results indicate that the material and the model will not fail under the low cycle failure since that they are fail at the high strain cycles.

Though the frequency difference that applied on the analysis model, the crack initiation life cycle can be considered not affected by the frequency difference, since that the value of the cycles are very high and will never drop below the high cycle fatigue.

Meanwhile, the crack initiation life cycle for the static failure analysis shows that the tension-tension loading case has the highest life cycles compared to the others. However, because of the value of the cycles are even lower than the low cycle fatigue which is lower than  $10^4$  cycles, the model has failed immediately when the strain has applied on the analysis model. For these cases, there is no crack initiation that happen but the material has failed and breaks.

Furthermore, the frequency difference has affected the total life cycle for the static failure; however higher the frequency of the strain applied has shorten the crack initiation life of the model. Thus, the results still show that the model experience lower life cycle than low cycle fatigue and make the model fail faster than the lower frequency.

## CHAPTER 5

### CONCLUSSION AND RECOMMENDATIONS

#### 5.1 CONCLUSION

From the study, it is found that the microstrain values which initiate the fatigue failure are  $48.2 \mu\epsilon$  for compression-compression,  $38.4 \mu\epsilon$  for compression-tension and  $29.2 \mu\epsilon$  for tension-tension. The microstrain values that fail the model in static failure analysis are  $615.6 \mu\epsilon$  for compression-compression,  $300.8 \mu\epsilon$  for compression-tension and  $164.4 \mu\epsilon$  for tension-tension. From both analyses, it is conclude that the tension-tension case has the most critical fatigue failure condition for both cases which it require the smallest strain to initiate the crack, compared to the other load cases.

Meanwhile, the crack initiation life for AISI/SAE 1045 steel under dynamic failure analysis is at higher than  $5.2 \times 10^6$  cycles for every loading case where the material has high resistance on fatigue failure since it only experience high cycle fatigue before initiate the crack. However, there is no crack initiation that happens for the static failure analysis since that the study has found that the material has failed and break immediately at very low cycle.



## 5.2 RECOMMENDATIONS

For the further study, these are the recommendations that can be considered to improve the project study:

- (i) Apply microstrain cycles with random amplitudes and frequencies because most of the real applications experience with random type of cycles in their operations.
- (ii) Run the analysis with environmental considerations, such as the effect of corrosion, temperature, humidity, etc. since that most of the steel applications are exposed with the environmental effects.
- (iii) Run this project with laboratory experiments to make sure that the analysis of this project can be compared and can be validated for the results accuracy.

## REFERENCES

- Abdullah, S., Ismail, N., Nuawi, M., Nizwan, C., & Abdullah, M. (2011). Comparative study of the strain signal and the edited strain signal. *Advanced Materials Research Vols. 264-265*, 1592-1597.
- American Iron and Steel Institute. (n.d.). Steel Glossary F - J. Retrieved 19 December, 2011, from Steel Works: <http://www.steel.org/Making%20Steel/Glossary/Glossary%20F-J.aspx>
- British Broadcasting Corporation. (n.d.). 1954: 'Metal fatigue' caused Comet crashes. Retrieved 4 October, 2011, from BBC On This Day: [http://news.bbc.co.uk/onthisday/hi/dates/stories/october/19/newsid\\_3112000/3112466.stm](http://news.bbc.co.uk/onthisday/hi/dates/stories/october/19/newsid_3112000/3112466.stm)
- Budinski, K. G., & Budinski, M. K. (2010). Carbon and Alloy Steels. In *Engineering Materials: Properties and Selection - 9th Edition* (pp. 434-435). Prentice Hall.
- Budynas, R. G., & Nisbett, J. K. (2008). Characterizing Fluctuating Stresses. In *Shingley's Mechanical Engineering Design* (pp. 292-294). New York: McGraw-Hill Companies Inc.
- Budynas, R. G., & Nisbett, J. K. (2010). Mean Monotonic and Cyclic Stress-Strain Properties of Selected Steels. In *Shingley's Mechanical Engineering Design Eight Edition in SI Units* (p. 1020). Singapore: McGraw-Hill.
- Collins, J. A. (2003). Fracture Mechanics (F-M) Approach to Fatigue. In *Mechanical Design of Machine Elements and Machines* (pp. 73-74). Ohio: John Wiley & Sons.
- Das, A. K. (1997). Failure Analysis Methodology. In A. K. Das, *Metallurgy of Failure Analysis*. USA: McGraw-Hill Publishing Company Ltd.
- Hartt, W. H. (1991). A Multiple Specimen Test Technique to Determine Fatigue Crack Growth Rates for Conditions Relevant to Offshore Structures. *Fatigue of High Strength Steels for Innovative Offshore Structures*, 70-83.
- Key to Metals. (23 May, 2011). Classification of Carbon and Low-Alloy Steels. Retrieved 19 December, 2011, from Key To Metals: <http://www.keytometals.com/Articles/Art62.htm>
- National Institute of Standard and Technology. (10 May, 2012). Material Details: SRM 20g - AISI 1045 Steel. Retrieved 15 May, 2012, from Material Measurement Laboratory: Standard Reference Material: [https://www-s.nist.gov/srmors/view\\_detail.cfm?srm=20g](https://www-s.nist.gov/srmors/view_detail.cfm?srm=20g)

- Nolan, D. (13 October, 2007). Ten Plane Crashes That Changed Aviation. Retrieved 4 October, 2011, from Military.com: <http://www.military.com/NewsContent/0,13319,152543,00.html>
- Roensch, S. (2008). Finite Element Analysis: Solution. (Roensch & Associates) Retrieved 24 September, 2011, from The Finite Element Method: A Four-Article Series: <http://www.finiteelement.com/feawhite3.html>
- Roylance, D. (2011). Finite Element Analysis. Mechanics of Materials .
- Schijve, J. (2001). Fatigue as a Phenomenon in the Material. In Fatigue Structures and Materials (pp. 7-8). Dordrecht: Kluwer Academic Publishers.
- Smith, W. F., & Hashemi, J. (2006). Engineering Alloys. In Foundations of Materials Science and Engineering Fourth Edition (pp. 358-359). New York: McGraw-Hill Companies Inc.
- Widas, P. (4 August, 1997). Introduction to Finite Element Analysis. (Virginia Tech Material Science and Engineering ) Retrieved 24 September, 2011, from Numerical Approach - Finite Element Analysis: [http://www.sv.vt.edu/classes/MSE2094\\_NoteBook/97ClassProj/num/widas/history.html](http://www.sv.vt.edu/classes/MSE2094_NoteBook/97ClassProj/num/widas/history.html)